Remote Sensing **2010**, *2*, 2185-2239; doi:10.3390/rs2092185

OPEN ACCESS

Remote Sensing

ISSN 2072-4292

www.mdpi.com/journal/remotesensing

Article

Cereal Yield Modeling in Finland Using Optical and Radar Remote Sensing

Heikki Laurila [1,*], Mika Karjalainen [2], Jouko Kleemola [1] and Juha Hyyppä [2]

[1] Department of Applied Biology Section of Crop Science, University of Helsinki, P.O. Box 27, FIN-00014 University of Helsinki, Finland; E-Mail: Jouko.Kleemola@Helsinki.fi

[2] Remote Sensing and Photogrammetry Department, The Finnish Geodetic Institute, 02431 Masala, Finland; E-Mails: Mika.Karjalainen@Fgi.fi (M.K.); Juha.Hyyppa@Fgi.fi (J.H.)

* Author to whom correspondence should be addressed; E-Mail: Heikki.Laurila@Logica.com; Tel.: +358-09-191-583-57; Fax: +358-09-191-585-82.

Received: 25 July 2010; in revised form: 3 September 2010 / Accepted: 3 September 2010 / Published: 16 September 2010

Abstract: During 1996–2006, the Ministry of Agriculture and Forestry in Finland (MAFF), MTT Agrifood Research and the Finnish Geodetic Institute performed a joint remote sensing satellite research project. It evaluated the applicability of *optical* satellite (Landsat, SPOT) data for cereal yield estimations in the annual crop inventory program. Four Optical Vegetation Indices models (I: Infrared polynomial, II: NDVI, III: GEMI, IV: PAR_{ND}/FAPAR) were validated to estimate cereal baseline yield levels (y_b) using solely optical harmonized satellite data (*Optical Minimum Dataset*). The optimized Model II (NDVI) y_b level was 4,240 kg/ha (R^2 0.73, RMSE 297 kg/ha) for wheat and 4390 kg/ha (R^2 0.61, RMSE 449 kg/ha) for barley and Model I y_b was 3,480 kg/ha for oats (R^2 0.76, RMSE 258 kg/ha). Optical VGI yield estimates were validated with CropWatN crop model yield estimates using SPOT and NOAA data (mean R^2 0.71, RMSE 436 kg/ha) and with composite SAR/ASAR and NDVI models (mean R^2 0.61, RMSE 402 kg/ha) using both reflectance and backscattering data. CropWatN and Composite SAR/ASAR & NDVI model mean yields were 4,754/4,170 kg/ha for wheat, 4,192/3,848 kg/ha for barley and 4,992/2,935 kg/ha for oats.

Keywords: optical vegetation Indices models; classification; NDVI; GEMI; FAPAR; PAR_{ND}; SAR/ASAR; CropWatN; LAI-bridge; Finland; CAP; Kalman Filter; data fusion; harmonized data

1. Introduction

Remote sensing and optical satellite systems have been extensively exploited globally in national crop inventory programs. They provide valuable information especially when estimating the total cultivation areas and yield production for commercially important crops like spring and winter wheat (*Triticum aestivum* L.), durum wheat (*Triticum turgidum* L. subsp. *durum*), soybean (*Glycine max* L.) maize (*Zea mays* L.) and rice (*Oryza sativa* L). Previous studies have described attempts to apply both optical and microwave SAR (Synthetic Aperture Radar) satellite data for crop yield modeling and crop inventory monitoring, e.g., Brown *et al*. [1], Henning *et al*. [2], Maas and Dunlap [3] and Kondratyev *et al*. [4] for wheat and maize, Shibayama and Akiyama [5] and Le Toan *et al*. [6] for rice.

Optical and microwave satellite imagery data combined with cereal crop modeling and agrometeorological weather data has been extensively applied in crop yield inventory and cultivation area programs both on Pan-American and European scale. McNairn *et al.* [7] applied *composite multispectral* approach for Canadian wheat, maize and soybean classification by using both optical and SAR data with *Neural Network* and *Decision Tree* classification techniques. In USA the Lanworth Company [8,9] together with the United States Department of Agriculture (USDA) provides commercial early crop inventories for wheat, soybean and maize. In addition, Lanworth has expanded its operations to Eastern Europe countries like Russia, Kazakhstan and Ukraine for wheat and also to South America (Brazil, Argentina) for maize and soybean crop yield estimations.

The European Union (EU) has been active in agricultural remote sensing programs in order to establish Pan-European crop inventory mechanism to support EU CAP (*Common Agricultural Policy*) policies and objectives. The Directorate General for Agriculture of EU (DGA [10]) and EUROSTAT [11] provide annual estimates of the total wheat and other cereal yield production on national level. Currently EU is funding an agricultural remote sensing program 'Monitoring Agriculture with Remote Sensing' (MARS) operated by the Joint Research Centre, Institute of Remote Sensing Applications (JRC/IRSA) [12,13]. The JRC (Space Applications Institute) of the EU is monitoring agricultural production and cultivation areas for different crops by using remote sensing techniques in EU countries. In the JRC, Narciso *et al.* [14] reviewed agrometeorological aspects and requirements for common and durum wheat, barley (*Hordeum vulgare* L.), oats (*Avena sativa* L.), soybean and oil crops in Italy, Spain and Greece and, respectively, Hough [15] for UK and Ireland.

Recent research studies have applied satellite derived information combined with crop simulation models for winter, spring and durum wheat yield forecasting in EU crop inventory campaigns. Dente *et al*. [16] applied CERES-Wheat/DSSAT crop model [17,18] combined with ENVISAT Advanced Synthetic Aperture Radar (ASAR) and MERIS data for durum wheat yield potential and LAI (*Leaf Area Index*) assimilation estimations at catchment scale in southern Italy. de Wit and van Diepen [19] applied dynamic WOFOST crop model [20] combined with modified *Ensemble Kalman filter* (*EnKF*) [21] to improve winter wheat and maize regional crop yield forecast accuracy in Spain, France, Italy and Germany during the 1992–2000 period. EnKF-filter was applied to correct low resolution microwave satellite soil moisture estimates in the WOFOST water balance model. During 1995–2003 de Wit and van Diepen [22] applied WOFOST crop model for the EU regional winter wheat yield forecasting in Spain, Poland and Belgium. In their study, the applicability of MeteoSat-satellite derived weather and agrometeorological variables were tested to replace interpolated

data from weather stations (temperature, evapotranspiration and radiation). Modeling results were spatially *aggregated* to regional and national levels and results were *evaluated* by comparing the simulation results of both approaches and by assessing the relationships with EUROSTAT crop yield statistics during 1995–2003. This consolidation methodology approach was also optimal in modeling study presented by Supit [23] for Pan-European wheat forecast evaluation and for Supit and van der Goot [24] wheat yield forecast study in France. Supit [23] estimated national wheat yield *levels* and yield *volumes* for 12 European countries during a 10 year period by using *multiplicative* and *additive* prediction models in conjunction with *trend functions* for weather and nitrogen input effects.

Vegetation Indices models (VGI) derived from optical and microwave satellite data have been extensively used in recent cereal yield potential estimations. Moriondo *et al*. [25] studied wheat yield variation with CROPSYST model using NDVI (*Normalized Difference Vegetation Index*) and FAPAR Index (*Fraction of Absorbed Photosynthetically Active Radiation*) estimates. Brown *et al*. [1] and Henning *et al*. [2] studied crop canopy and microwave SAR (*Synthetic Aperture Radar*) backscattering interactions. Prasad *et al*. [26] evaluated the use of *Spectral Reflectance Indices* (SRI) similar to VGI indices applied in this study, for assessing grain yield variabil ity in winter wheat genotypes under Great Plains (USA) growing conditions. Mangiarotti *et al.* [27] applied a similar *composite* approach to the one applied by McNairn *et al.* [7]. Both studies assimilated optical SPOT/NDVI reflectance and microwave ENVISAT/ASAR backscattering data to model semi-arid herbaceous vegetation dynamics with Step and Radiative Transfer (RT) models. Serrano *et al*. [28] studied winter wheat yield and biomass variation in Spain under different nitrogen supply levels by using fIPAR Index (*fraction of Intercepted Photosynthetically Active Radiation, PAR*) in conjunction with wheat LAI canopy development and chlorophyll A content. The FAPAR Index is extensively applied by the JRC of EU in remote sensing applications (http://fapar.jrc.ec.europa.eu/Home.php). FAPAR is an indicator of the state and productivity of vegetation. It represents the fraction of the solar energy which is absorbed by vegetation during the plant photosynthetic process. The FAPAR algorithm minimizes the effects of atmospheric particle scattering, the variation of different soil covers and the changing geometry of illumination.

Research studies in *northern* high latitude agricultural production countries have focused on integrating multispectral remote sensing techniques, which combine both optical and microwave SAR imagery data. In Finland, Kuittinen *et al.* [29], Kuittinen [30] and Karvonen *et al*. [31] have reviewed spring wheat and barley yield forecasting with crop models using Landsat and SPOT data for Nordic high latitude agricultural regions. According to Kuittinen *et al.* [29], cloudiness in northern latitudes especially during growing season significantly reduces the applicability of optical spectrum satellite data. Matikainen *et al.* [32] applied microwave ERS-2 and optical SPOT data for crop species interpretation and Karjalainen *et al.* [33] applied ENVISAT ASAR data for spring cereal yield monitoring.

During 1996–2006, the Ministry of Agriculture and Forestry in Finland (MAFF), MTT Agrifood Research Finland (MTT), the Finnish Geodetic Institute (FGI) and the Technical Research Centre of Finland (VTT, Department of Space Research) performed a joint remote sensing satellite research project. It evaluated the applicability of multispectral optical and SAR satellite data for cereal yield estimations in the annual crop inventory program. Both optical and composite SAR microwave

Vegetation Indices models (VGI) were validated to estimate spring cereal yield levels using solely optical and SAR satellite data.

In Finland the applicability of *multispectral classifying techniques* for different agricultural crops (e.g., McNairn *et al.* [7] for Canadian growing conditions) is less relevant, since MAFF as part of the EU regulated CAP policy has established a national Finnish *Land Parcel Identification System* (FLPIS) with digitized parcel boundaries [34]. The FLPIS system is incorporated with the *Integrated Administration and Control System* (IACS). The IACS system controls the payments of cultivation area based agricultural subsidies for Finnish farmers. The ground based stratum sampling similar to USDA methodology [9] is currently being applied in Finland in the annual *crop inventory sampling*. MAFF together with the Finnish Agricultural Advisory and Rural Development Centres perform annually a crop yield inventory sampling.

Recent research results in EU have stated the need of integrated *Agricultural Information System* (AIS) to enable easy dissemination of *geo-referenced* data for agricultural system research on EU scale. Russell *et al.* [35] reviewed the Barley Knowledge Base and AIS system for the European Community. Janssen *et al*. [36] demonstrated the need of Integrated Database System by combining both remote sensing satellite data and ground truth data in order to establish Pan-European agricultural database system to support EU CAP objectives. The SEAMLESS database system integrates agricultural management (crop phenological calendar, cropping patterns, yield production and soil and agrometeorological climate data) and CAP policy information.

In summary, new *combined multispectral* optical and SAR VGI modeling and phenological classifying techniques, which use solely optical and SAR satellite data (*Minimum Datasets*) through data fusion, provide new integrated tools for cereal yield predictions during the MAFF annual crop inventory program. New remote sensing techniques integrated with Finnish national FLPIS and IACS systems will support Finnish national and EU CAP goals and objectives.

In a recent publication by Laurila *et al.* [37], spring cereal yield modeling results were presented for Finnish high latitude growing conditions using multispectral composite SAR backscattering and NDVI data (*Composite Minimum Dataset)*. Cereal maximum yield capacity is limited by environmental (e.g., drought periods) and vegetation stresses (e.g., nutrient deficiencies, pathogen epidemics) during growing season.

In this publication the *optical* reflectance data, obtained through *data fusion* and *harmonization* from the Landsat and SPOT satellites (*Optical Minimum Dataset*) were used as input for the *optical* VGI models (Models I-IV).

The overall goal of the present study was by integrating *optical composite* data to estimate actual non-potential grain *baseline yield levels* (y_b) for high latitude spring cereals in large area field conditions in southern Finland using *optical* vegetations indices.

The *specific objectives* of the present study were:

(i) *Calibration* of the *optical* VGI models (Models I-IV) by using phenologically classified *Optical Minimum Datasets* containing harmonized Landsat and SPOT reflectance data for spring wheat, barley and oats (*Avena Sativa* L.)

(ii) *Validation comparison of* optical VGI model baseline yield estimates (y_b) *vs.* CropWatN dynamic crop model yield estimates [29] using Landsat, SPOT, NOAA reflectance data and MAFF

inventory yield statistics and MTT Agrifood Research Finland Official Variety Trial averaged yield results (1996–2006) were used as a ground truth reference.

(iii) Validation comparison of optical VGI model baseline yield estimates (y_b) *vs.* composite multispectral VGI models with SAR/ASAR and NDVI components and using both reflectance and backscattering data from Envisat, ERS and Radarsat.

(iv) Estimation of cereal non-potential *baseline yield levels* (y_b) in growing zones (I–IV) using VGI models as *a yield inventory tool* for the annual MAFF inventory statistics.

2. Methodology and Study Area

2.1. System Analysis and Strategy

In this study, four optical *Vegetation Indices (VGI* models (VGI, Infrared polynomial, NDVI, GEMI, and PAR_{ND}/FAPAR, Table 1) were calibrated and validated with optical satellite data (Landsat and SPOT *Optical Minimum Datasets* 1996–2006) without extensive agrometeorological ground truth data required by conventional dynamic crop models [17,18]. The *System Analysis* overview is reviewed in a recent publication by Laurila *et al.* [37] and in [38-41]. Respectively, the Integrated LAI-bridge coupling mechanism applied in this publication is depicted in Figure 1 (I-Calibrated optical reflectance data, II–III phenological classification, VGI model yield estimates, IV-LAI bridge coupling, GEMI index, dynamic crop model yield estimates). *Optical minimum datasets* were measured in five different experimental locations (Mellilä, Porvoo, Kirkkonummi, Jokioinen and Lapua experimental sites) in southern Finland.

Figure 1. Integrated LAI-bridge coupling mechanism with adaptive Kalman Filter [19,21] between phenologically pre-classified optical data (GEMI model III, Table 1) and dynamic crop model (Model V, CropWatN, [29,31]).

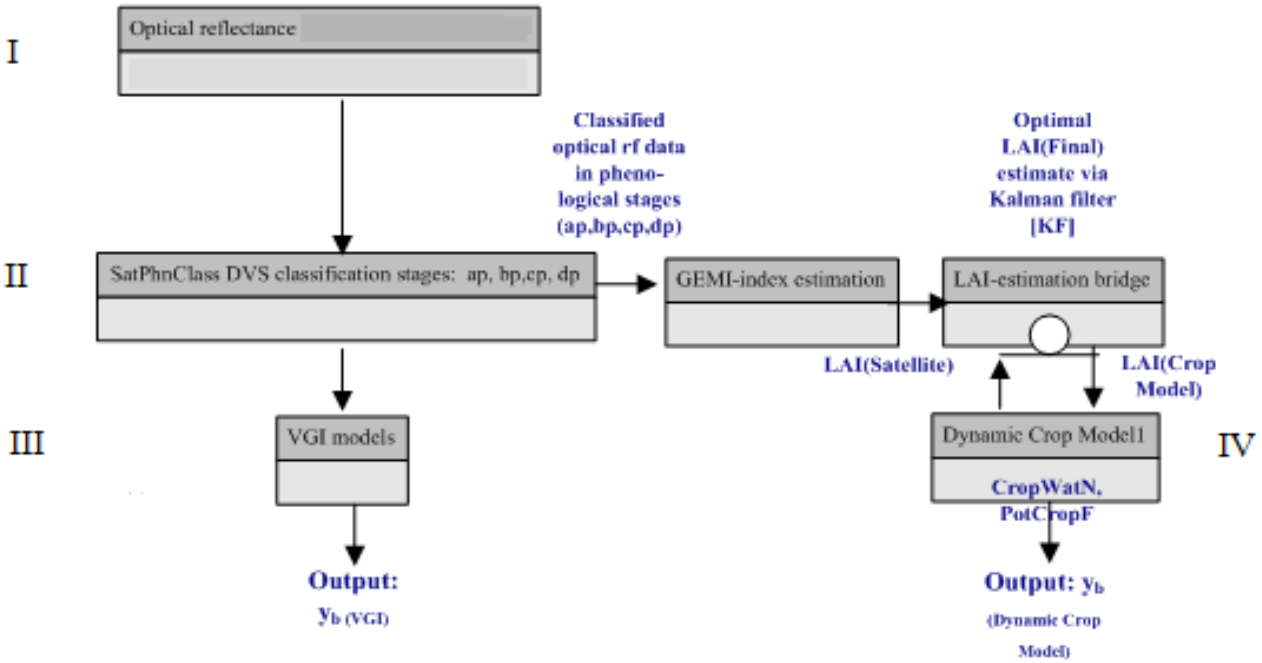

Table 1. Vegetation Indices Models (I–VI), dependent baseline yield (y_b) and independent variables [29,37,53,54]. [1), 2), 5)]

Model	Model equation [1), 2)]	Independent driving variables [2)]	Model name, description of derived satellite parameters used in regression equations
I	$y_b = \rho_{RED}(a_p, b_p, c_p) + \rho_{NIR}(a_p, b_p, c_p)$	$\rho_{RED}(a_p, b_p, c_p)$, $\rho_{NIR}(a_p, b_p, c_p)$	Polynomial infrared model Calibrated reflectance (ρ or $rf_{channel}$) values for infrared (ρ_{RED}, TM channel = 3) and near infrared (ρ_{NIR}, TM channel = 4) during growing season in different phenological stages. - a_p, b_p, c_p, d_p classes correspond on average to Zadoks crop phenological growth scale with cereals: a_p: 0-12, b_p: 12-50, c_p: 50-90, d_p:>90 [44]. [2)]
II	$y_b = NDVI(a_p, b_p, c_p)$ $NDVI = (\rho_{NIR}(a_p, b_p c_p) - \rho_{RED}(a_p, b_p, c_p))/$ $(\rho_{NIR}(a_p, b_p, c_p) + \rho_{RED}(a_p, b_p, c_p))$	$NDVI(a_p, b_p, c_p)$	Normalized Difference Vegetation Index (NDVI) model [25,53-54] [2)]. Ratio between near infrared and infrared channel surface reflectance (ρ or rf_{ch}) values - ρ_{RED} / rf_3 infrared (λ = 0.63-0.69 μm) - ρ_{NIR} / rf_4 near infrared (λ = 0.76-0.90 μm) - Landsat NDVI = $(rf_4(a_p, b_p, c_p) - rf_3(a_p, b_p, c_p))/(rf_4(a_p, b_p, c_p) + rf_3(a_p, b_p, c_p))$, - SPOT NDVI = $(rf_3(a_p, b_p, c_p) - rf_2(a_p, b_p, c_p))/(rf_3(a_p, b_p, c_p) + rf_2(a_p, b_p, c_p))$
III [3)]	$y_b = GEMI(a_p, b_p, c_p)$ $GEMI(a_p, b_p, c_p) = \eta*(1 - 0.25 * \eta) - ((\rho_{RED}(a_p, b_p, c_p) - 0.125)/$ $(1 - \rho_{RED}(a_p, b_p, c_p))$ $\eta = (2 * ((\rho_{NIR}(a_p, b_p, c_p))^2 - (\rho_{RED}(a_p, b_p, c_p))^2)$	$GEMI(a_p, b_p, c_p)$	Global Environment Monitoring Index (GEMI) [29,55]. [2)]
IV [4)]	$y_b = PAR_{ND}(a_p, b_p, c_p)$ $PAR_{ND} = (\rho_{RED}(a_p, b_p, c_p) - \rho_{PAR}(a_p, b_p, c_p))/ (\rho_{RED}(a_p, b_p, c_p) +$ $\rho_{PAR}(a_p, b_p, c_p))$	$PAR_{ND}(a_p, b_p, c_p)$	PAR_{ND}/FAPAR (Normalized Vegetation Index for Photosynthetically Active Radiation, PAR) model [2)] - ρ_{PAR} rf_1 PAR (λ = 0.45 - 0.52 μm), Landsat/TM1, SPOT/HRV/S1 - ρ_{RED} rf_3 infrared (λ = 0.63 - 0.69 μm
V [5)]	y_b = DynModel(LAI(GEMI a_p, b_p, c_p)) Equation 6 , Table 12, **Appendix B**	LAI(GEMI a_p, b_p, c_p)	LAI-bridge coupling with GEMI index [3,29] and Kalman filter [19,21] using NOAA and SPOT data. Used only in validation part with the dynamic CropWatN crop model.
VI Composite SAR/ASAR and NDVI [37][6)]	$y_b = NDVI(a_p, b_p, c_p) + \sigma^0 HH_{5GHz,}$ $(a_p, b_p, c_p, d_p) + \sigma^0 VV_{5GHz,}(a_p, b_p, c_p, d_p) + \sigma^0 HV_{5GHz,}$ $(a_p, b_p, c_p, d_p) + \sigma^0 VH_{5GHz,}(a_p, b_p, c_p, d_p)$	$NDVI(a_p, b_p, c_p)$, $\sigma^0_{5GHz}(a_p, b_p, c_p, d_p)$	Composite multispectral SAR/ASAR and NDVI model for spring cereals (swh, oats, barley) using NDVI reflectance and microwave backscattering (σ^0 , f = 5.4 GHz) data (Table 12, [37]). Used only in validation of the optical VGI models [6)]

[1)] Equations applied after REG/Stepwise for linear models (Equation 1, Table 10, **Appendix B** [51,52]) and RSREG for polynomial non-linear models (Equation 2, Table 10, **Appendix B**) [2)] Independent variables classified with *SatPhenClass*-algorithm. [3)] GEMI LAI-bridge mechanism used only in validation part. [4)] PAR_{ND} model is similar to FAPAR (Fraction of Absorbed Photosynthetically Active Radiation Index, [56-59]) and *fIPAR* (fraction of intercepted PAR, [60]). [5)] Model V used only in validation part with the dynamic CropWatN crop model (Figure 1, [29]). [6)] Model VI used only in validation of the optical VGI models [37].

More specifically detailed *analysis strategy* consisted of following specific procedures:

(a) Classification of optical data with the *SatPhenClass* phenological classifying algorithm for spring cereals is reviewed by Laurila *et al.* [37]. The *SatphenlClass* algorithm exploits BBCH [42,43] and Zadoks [44] growth scales with four phenological classes for spring cereals (a_p: BBCH 0–12, b_p: BBCH 12–50, c_p: BBCH 50–90, d_p: BBCH > 90). The phenological a_p class corresponds to development period between sowing and two leaf stage with double ridge formation. The b_p class matches with the period between two leaf stage and ear emergence with maximum Leaf Area Index (LAI_{max}) exposure and fully closed canopy structures. The c_p class corresponds to period between ear emergence and anthesis with grain filling until full maturity. Finally, the phenological d_p class relates to senescence and post-harvest phases.

(b) Calibration of four optical *Vegetation Indices (VGI)* models (I–IV, Table 1) for cereal baseline yield (y_b) estimations. VGI models were calibrated with *phenologically* classified satellite data containing solely optical satellite data (*Optical Minimum Datasets).*

(c) Landsat/TM and Spot/HRV_2 *intersensory* calibration by calculating NDVI indices from the Optical Minimum Datasets obtained from the five experimental locations in Southern Finland.

(d) NDVI *Phenological Spectral Signature Profile analysis* (SSP_{Ph}) for spring cereals in different phenological phases (a_p, b_p, c_p) derived from the TM and HRV_2 intersensory calibration.

(e) *Validation* of calibrated optical VGI models between years and locations by using separately two independent data sources: *(i)* the MTT Agrifood Research Finland Official Variety Trial data (1996–2006) *(ii)* the MAFF (Ministry of Agriculture and Forestry in Finland) annual crop yield inventory data (1996–2006).

(f) *Validation comparison of* optical VGI models *vs.* CropWatN dynamic crop model using GEMI-index and LAI-bridge coupling system developed originally by Karvonen *et al.* [31] for cereals grown in Finnish growing conditions (Model V in Table 1). LAI-bridge coupling system was later revised and applied by Kuittinen *et al.* [29] for the EU MARS program in Finland. Spring cereal non-potential yield estimates (y_b), calculated by VGI and CropWatN models, were compared by using the same optical satellite dataset in growing zones I–IV. The detailed LAI-bridge coupling system with GEMI index and adaptive Kalman filter [21] for cereal LAI development ($LAI_{Satellite,Cereal}$, $LAI_{CropModel}$) is presented in Figure 1. LAI-bridge exploits iterative *Kalman filter* [21] algorithm resembling *Ensemble Kalman Filter* (EnKF, de Wit and van Diepen [19]) to improve cereal LAI-estimates estimated from both optical satellite data and estimated by dynamic crop models [31]. Equation 6 and Table 12 (**Appendix B**) depict crop specific regression coefficients for cereal LAI estimation ($LAI_{Satellite,Cereal}$) using GEMI index [29]. Equation 7 explains the Kalman solution for the corrected, optimal LAI estimate ($LAI_{Optimal}$) corrected by standard deviations of $LAI_{Satellite,Cereal}$ and $LAI_{CropModel}$ estimates. The standard deviation of $LAI_{Optimal}$ estimate can be solved from Equation 8.

(g) *Validation comparison of* optical VGI model baseline yield estimates (y_b) *vs.* composite SAR/ASAR and NDVI models using both reflectance and backscattering data from Envisat, ERS and Radarsat in growing zones I–IV [37].

(h) Estimating *non-potential baseline* grain *yield levels* (y_b) for different spring cereals in Finnish large area field conditions by applying the validated VGI models to optical reflectance data.

2.2. Overview of Satellite and Ground Truth Sites and Measurements

A general overview of satellite and ground truth experimental sites and agrometeorological weather stations is displayed in Figure 2(a–d). Growing zones (I–V) and MTT Experimental Stations applied in cereal yield modeling are displayed in Figure 2(a). Cumulative ETS (T_b 5 °C) isolines applied in the *SatPhenClass* phenological classification [37] are depicted in Figure 2(b). Experimental sites consisted of five different locations (Mellilä, Porvoo, Kirkkonummi, Jokioinen and Lapua) in southern Finland (Figure 2(d)).

A general scheme of the measuring satellite systems and calibration parameters used in this study is displayed in Tables 9–10 (**Appendix A**). The detailed soil profile classification in the experimental areas and growing zones I-IV are explained in a recent publication by Laurila *et al.* [37]. The ground truth sampling, the phenological crop calendar observations and LAI measurements were performed according to methodology applied by Kuittinen *et al.* [29]. The abbreviations used in this study are explained in Table 7 (**Appendix A**).

Figure 2. (a) Growing zones (I–V) and MTT Experimental Station locations in Finland, **(b)** ETS (T_b 5 °C) cumulative isolines, **(c)** Meteorological Weather Stations in Finland, **(d)** satellite and ground truth measurement locations in Finland (© Original Data, MTT Agrifood Research Finland, Finnish Meteorological Institute, NASA, visibleearth.nasa.gov/).

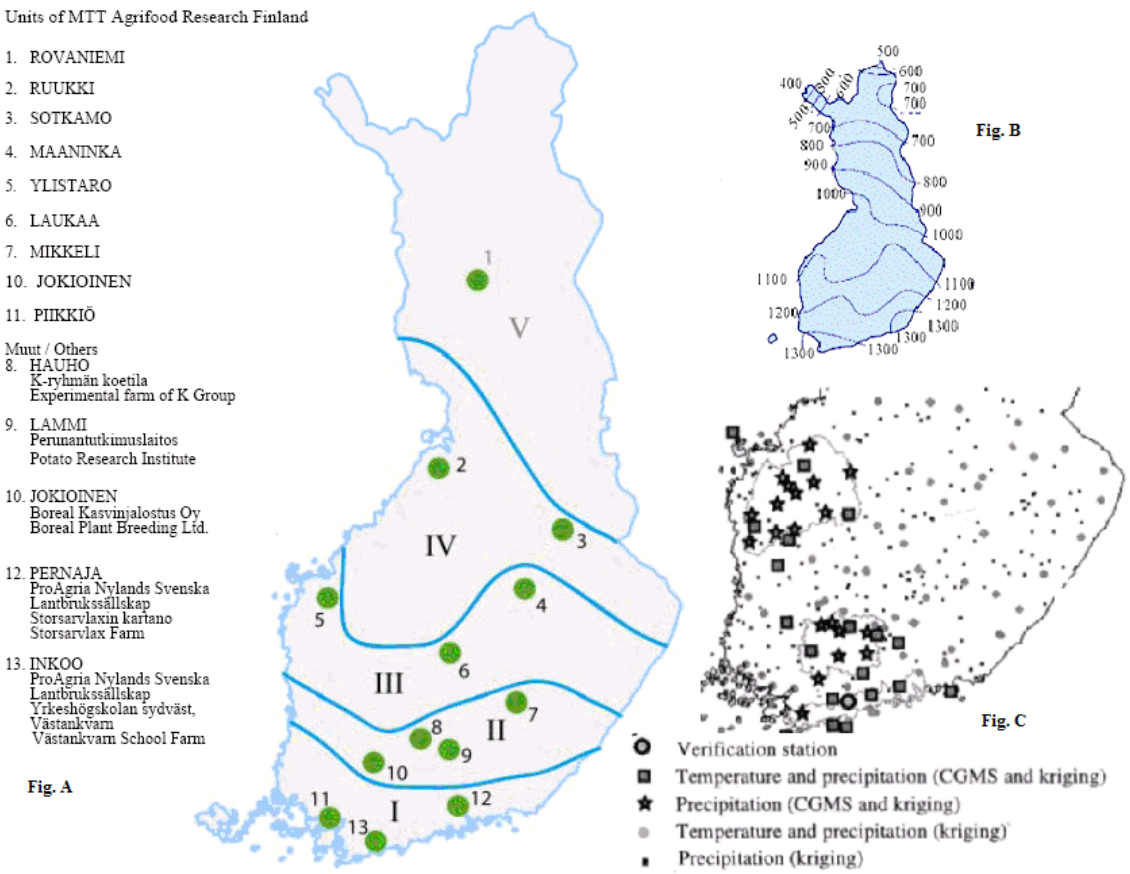

Figure 2. *Cont.*

2.2.1. Design of Ground Truth Experimental Sites

The field experimental design for satellite imagery was originally developed by Kuittinen *et al.* [29] for Finnish cereal growing conditions (Figure 3). Figure 3(a) depicts the basic experimental plot and Figure 3(b) illustrates the 2 × 2 and 2 × 3 randomized plots with replicates of the basic experimental plot growing the same cereal crop. The 2 × 2 and 2 × 3 randomized lattice design was applied in Mellilä, Porvoo, Kirkkonummi and Lapua experimental sites.

The randomized 2 × 5 plot design with two replicates for early and late wheat, barley and oat cultivars is displayed in Figure 3(c). The 2 × 5 randomized plot design was only applied in the Kuuma Experimental Site (Jokioinen, MTT Agrifood Research, Figure 3(c)).

The overlaying satellite imagery technique for Landsat/TM and Spot/HRV with different pixel sizes is depicted in Figure 3(a). Erdas/Ermapper software was used for digitization and to impose and overlay Landsat/TM (30 × 30 m pixel size) and Spot/HRV_2 (20 × 20 m) images using the central point (Point 9) as a reference (Figure 3(a), Table 11, **Appendix A**). Concurrently with satellite measurements, growing density measurements were measured in points 1,5, biomass measurements in points 1,5,9 and LAI measurements in points 1–8 (Portable Li-Cor 2000 Plant Canopy Analyzer, Li-Cor Biosciences), based on methodology suggested by Kuittinen *et al.* [29].

Figure 3. Field experimental plot design after Kuittinen *et al.* [29].

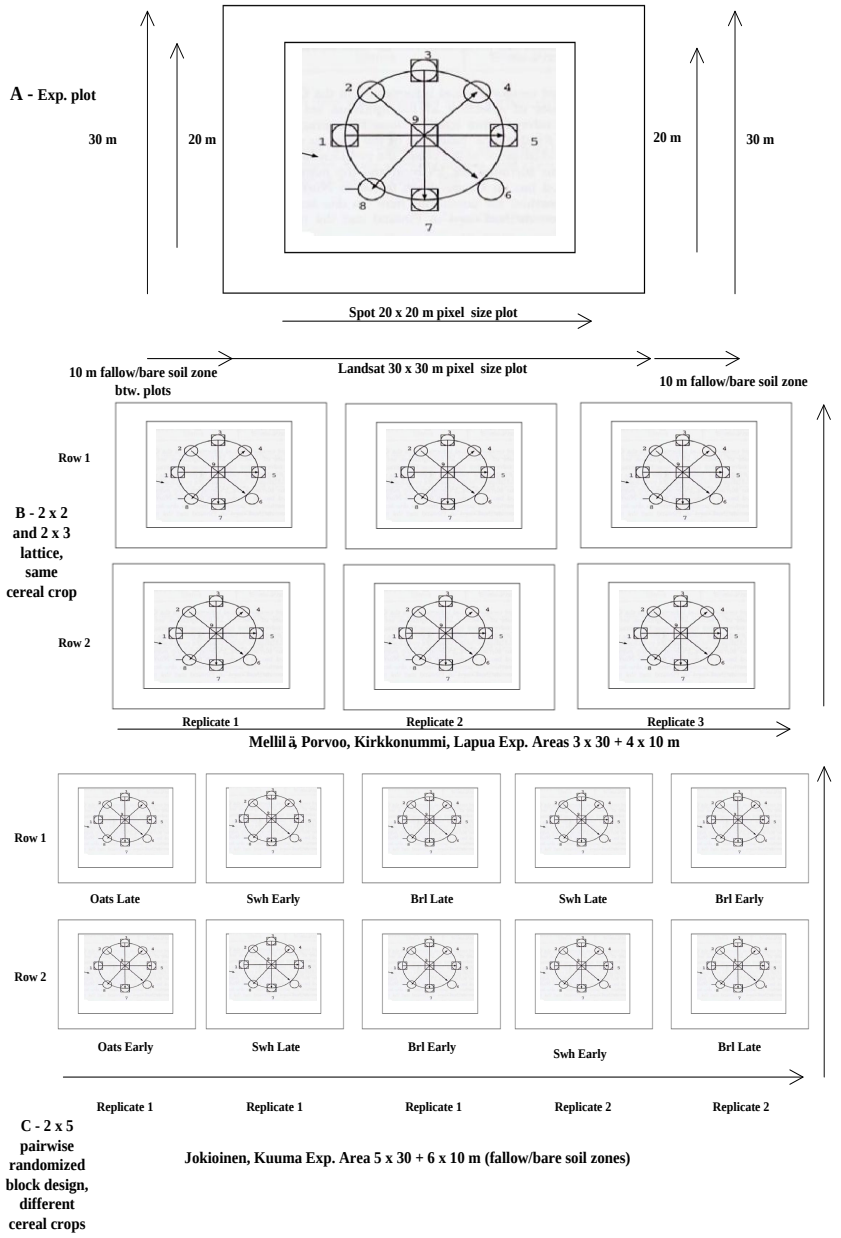

The Kuuma Experimental site in Jokioinen (60 °48'5.82"N, 23 °28'48.20"E) is illustrated in Figures 3 and 4 and the MTT Agrifood Research Centre site in Figure 4 (Growing Zone II, Häme Agric. Advisory Centre). The detailed Figures 4(a_1, f, g) in the Kuuma experimental site depict the randomized plot design with replicates for early and late wheat, barley and oat cultivars. The ground truth plot size was adjusted to Landsat 30 × 30 m pixel size (Figure 3(a)). Each cereal plot was surrounded by bare soil or fallow zone to enhance *canopy x soil* reflectance contrasts in different phenological phases (a_p, b_p, c_p, d_p). The main soil type in the Kuuma site was organic mould with mixtures of clay. During spring time, rain, flooding and excessive top soil water content close to field capacity (pF 1.5–2.0) reduced the cereal yield levels especially in replicate 1. Figure 3(b) depicts the plots in the Kuuma area affected by flooding and heavy rain (4_f), the digitized Spot image is displayed on the right hand side (4_g).

The Porvoo experimental site (60 ° 23'34" N, 25 ° 39'52" E) is depicted in Figure 4 (B_1, Kullogård Experimental Farm) and B_2 (Dräcksby Experimental Farm). Respectively the Kirkkonummi site (60 °14'13"N, 24 °23'49"E, Kylmälä Experimental Farm, Helsinki University of Technology) is depicted in Figure (C_1,C_2). Both Porvoo and Kirkkonummi sites were located in the Uusimaa Agric. Advisory Centre (Growing Zone I). The Mellilä site in Loimaa (60 °46'41"N, 22 °55'32"E, Nahi Experimental Farm) is illustrated in D_1 and D_2 (Zone I). The detailed E_1 and E_2 figures depict digitized field parcels in Lapua and Seinäjoki Experimental sites on clay type soils (62 °85'17"N, 23 °2'42"E, Zone III–IV in the Pohjanmaa Agric. Advisory Centre).

Figure 4. (A_1) Kuuma Experimental Site, (A_2) Jokioinen (MTT Agrifood Research) Jokioinen Experimental Site, (B_1) Porvoo Kullogård and Dräcksby (B_2) Exp. Farms, (C_1–C_2) Kylmälä, Kirkkonummi Experimental Site (Uusimaa Agriculture Advisory Centre, Helsinki University of Technology), (D_1–D_2) Mellilä, Loimaa Experimental site, (E_1–E_2) Lapua Experimental site (Pohjanmaa Agriculture Advisory Centre),(F–G) detailed Kuuma Experimental site [1)].

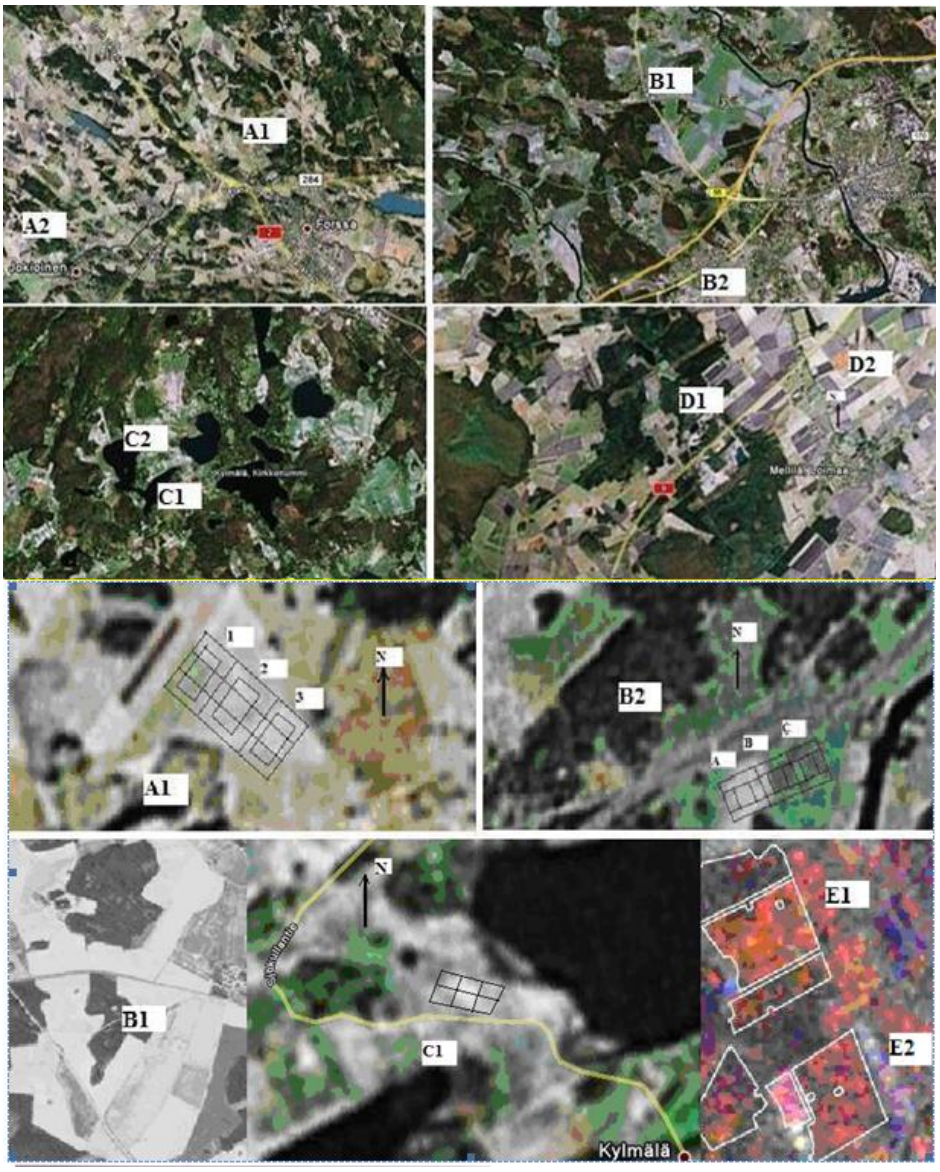

Figure 4. *Cont.*

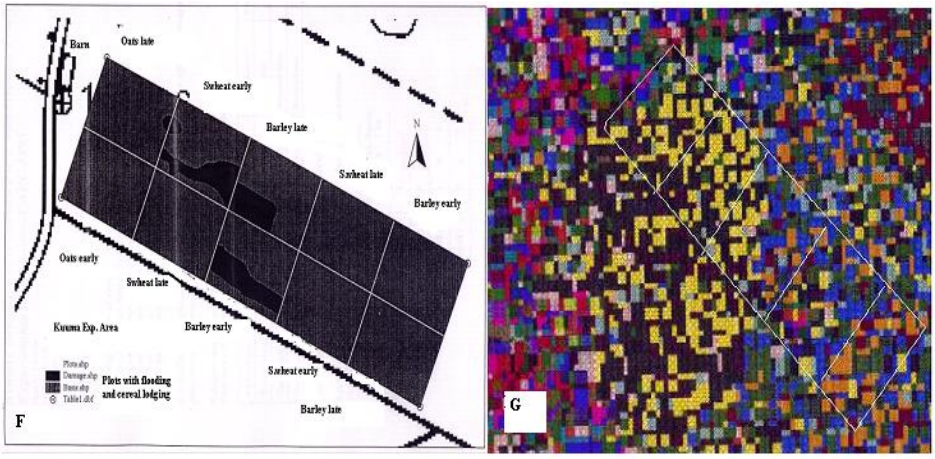

[1] A_1–D_2 , G, multitemporal Landsat, SPOT composite images, E_1–E_2 Multitemporal Envisat composite image © Original data TeleAtlas, Terrametrics 2010, European Space Agency and the Finnish Geodetic Institute 2003 [29,33].

The detailed Figures (3B and $4B_2$) in the Dräcksby experimental site in Porvoo depict the 2 × 2 and 2 × 3 randomized plot design for wheat, barley and oat cultivars. The main soil type in the Dräcksby site was clay with mixtures of organic peat. Especially both the Kuuma (Figure $4A_1$, Jokioinen) and Dräcksby (B_2, Porvoo) experimental sites with clay and organic mould and peat topsoil layers (10–15 cm) were affected by excessive water from melting snow in the beginning of the growing season (ap) causing the topsoil to reach the soil field capacity (pF 1.5–2.0). During mid-summer, drought periods in generative phases (c_p, d_p), caused the soil moisture content to recede close to wilting point (pF 4.0–4.2).

2.3. Calibration

2.3.1. Phenological Classifying Algorithm (SatPhenClass) for Satellite Data

The phenological classifying algorithm (*SatPhenClass*) [46,47] used for optical Landsat and SPOT data is presented by Laurila *et al.* [37]. The revised classifiers ETS and LAI_{max} (Li-Cor 2000 Plant Canopy Analyzer [48]) for high latitude cereals were developed based on previous studies by Kontturi [49] for Finnish long day growing conditions [47,49,50].

2.3.2. Optical Vegetation Indices (VGI) Models I–IV

Four different Optical Vegetation Indices (VGI) models (I: Infrared, II: NDVI, III: GEMI, IV: PAR_{ND}/FAPAR, Table 1) were calibrated with *linear* (SAS REG/Stepwise and *non-linear* (SAS RSREG) [51,52] polynomial regression models (Equations 1–2, Table 12 , **Appendix B**).

Figure 5 depicts typical optical *Spectral Signature Curves* (SSC) for barley (green vegetation) and bare soil in Nordic high latitude growing conditions [31]. In addition Chlorophyll A (λ 460, 680 nm), B (λ 480, 650 nm) and water (λ 1500, 2000 nm) absorption maximums and sensory bandwidths for Landsat and Spot are depicted. The measured optical reflectance data for different spring cereals were classified into *phenological classes* (a_p,b_p,c_p,d_p) *with* the *SatPhenClass* algorithm.

Figure 5. Spectral Signature Curves with scaled Reflectance Factor for barley and bare soil, Chlorophyll A, B in PAR spectrum, water absorption maximums and corresponding Landsat/TM and SPOT/HRV2 sensory bandwidths [31, Table 11, **Appendix A**] (© Original data Swedish National Environmental Board).

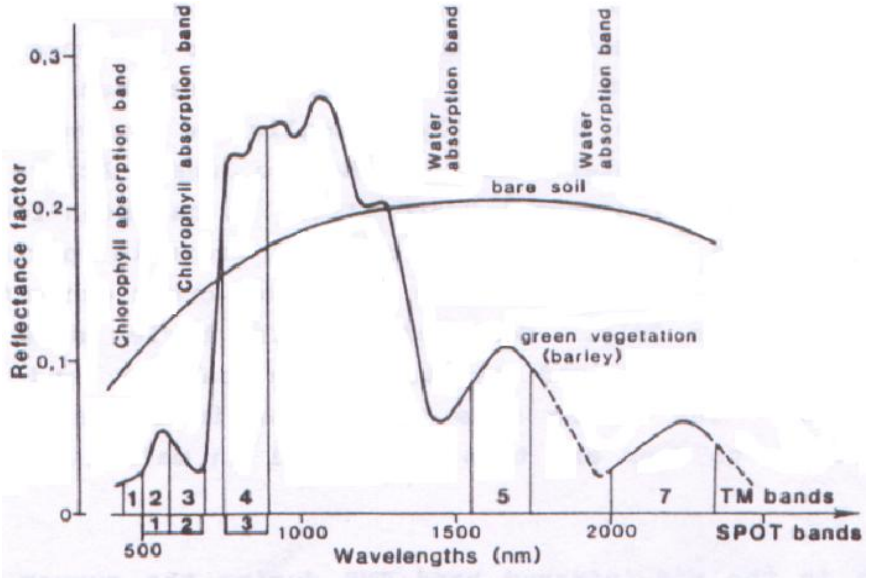

2.4. Calibration Data

2.4.1. Optical Reflectance Data

The optical Landsat 5/TM (Thematic Mapper), SPOT/HRV2 (High Resolution Visible 2) and NOAA/AVHRR (Advanced Very High Resolution Radiometer) satellite data (1996–2006) is in Tables 9–11 (**Appendix A**). Satellite measurements with optical cloud free images and ground truth observations in the experimental sites in Nylands Svenska (Zone I in Kirkkonummi), Häme (Zone II in Jokioinen) and in Pohjanmaa Agricultural Advisory Centres (Averaged III–IV zone in Lapua, Seinäjoki and Ilmajoki) were temporarily evenly dispersed along the growing season between May and August (Figure 2, [37]).

In addition, two older auxiliary optical [29,31] datasets consisting of Mellilä and Porvoo sites (Growing zone I in Nylands Svenska Agric. Advisory Centre) were used in calibration of *SatPhenClass* phenology and VGI models (I–V, Table 1). Total of 18 cloud free Landsat and Spot satellite images were obtained during the campaigns. NOAA/AVHRR data were only used for validation purposes to compare cereal yield estimations between VGI models and CropWatN crop model [29], results are reviewed in validation section.

The VTT Technical Research Centre in Finland (Department of Space Research) and the Finnish Geodetic Institute digitized and performed the *classification* of field parcels from the satellite images (Figure 2). Optical Landsat and SPOT data were calibrated with geometric and radiometric corrections in the Finnish Geodetic Institute. The *ortho-rectified* and *radiometrically corrected* satellite data after Price [53] (Equations 3–5, **Appendix B**) was classified with the SatPhenClass algorithm into cereal *phenological categories* and was applied in VGI models (I–IV). Optical calibration details with atmospheric corrections (6S software, *Second Simulation of the Satellite Signal in the Solar Spectrum*)

were reviewed by Kuittinen *et al.* [29], the optical calibration parameters are given in Table 10 (**Appendix A**). Correspondingly the SAR backscattering data calibration details were reviewed by Matikainen *et al.* [32], Karjalainen *et al.* [33] and Hyyppä *et al.* [61].

2.5. Validation

2.5.1. Validation of Optical Vegetation Indices (VGI) Models and Validation Data

After the calibration of optical VGI models (I–II, IV–V Table 1), the validation procedure was applied to test baseline grain yield (y_b, kg/ha) predictions *vs.* independent observed ground truth yield values. During the validation procedure, the modeled baseline yield estimates (y_b, kg/ha), calculated by the optical VGI models, were compared with corresponding measured yield estimates from *(i)* the 1994–2006 MAFF official inventory statistics [62,63] and *(ii)* from the 1994–2006 MTT Agrifood Research Finland Official Variety Trial results [64-66]. Yield differences were calculated as absolute values (kg/ha) and percent (%) values in corresponding growing zones (I–IV) and years.

The MAFF validation datasets consisted of yield inventory statistics from the Nylands Svenska (Growing Zone I), Häme (Growing Zone II) and Pohjanmaa (Averaged III–IV Zone) Agricultural Advisory Centres (Table 2). Figure 6 depicts scenes from the Seinäjoki, Lapua and Ilmajoki experimental areas in the Etelä-Pohjanmaa Agric. Centre. Especially in the Seinäjoki Experiment Area (62°85'17"N, 23°2'42"E) the fields were affected by severe flooding in the spring time (Figure 6(a)) and in the Lapua area heavy lodging reduced the spring cereal yield potential (Figure 6(d)). The MTT Official Variety Trial datasets consisted of yield trials from the Pernaja and Inkoo MTT Experimental Stations (Zone I), MTT Jokioinen (Zone II) and Ylistaro (Zone III) and Ruukki (Zone IV) MTT Experimental Stations Averaged to Zone III–IV. Zones III–IV were pooled together because the satellite and ground truth measurement sites in Lapua, Seinäjoki and Ilmajoki were located in the middle of 1100 $ETS_{(Tb = 5\ ^\circ C)}$ isoline (Figure 2).

Table 2. Sensors, datasets, growing zones, locations and soil classification [44].

Sensor Type [1)]	Data set	Growing Zone [2)]	MAFF Agriculture Advisory Centre (Figure 2)	Location (Figure 2)	Coarse soils (%)				Clay soils (%)			Organic (%)
					Gravel with coarse sand	Fine sand	Coarse sand	Silt	Sandy clay	Silt clay	Gyttja clay [3)]	Mould, Peat
Optical/ SAR[4)]	1.1	III (IV)	Etelä-Pohjanmaa	Lapua 23°10'E, 62°50'N		11.2	19.8		23.5			
	1.2	III (IV)	Etelä-Pohjanmaa	Seinäjoki 23°10'E, 62°50'N		15.5	10.1		20.5			25.3
	1.3	III (IV)	Etelä-Pohjanmaa	Ilmajoki 23°10'E, 62°50'N		13.2	12.0	3.9	21.4			
	2.1	I	Nylands Svenska	Porvoo 25°50'E, 60°50'N	6.2	17.8	8.5				38.0	10.9

Table 2. *Cont.*

Sensor Type [1]	Data set	Growing Zone [2]	MAFF Agriculture Advisory Centre (Figure 2)	Location (Figure 2)	Coarse soils (%)				Clay soils (%)			Organic (%)
					Gravel with coarse sand	Fine sand	Coarse sand	Silt	Sandy clay	Silt clay	Gyttja clay [3]	Mould, Peat
Optical	3.1	I	Nylands Svenska	Kirkkonummi 24°30'E, 60°10'N		9.4			27.5	8.5	41.4	5.4
Optical	3.2	II	Häme	Jokioinen 23°50'E, 60°50'N (Kuuma Exp. Area)					56.0	7.0	15.1	7.7 (Kuuma: 70–80)
	3.3	II	Häme	Mellilä 22°20'E, 60°50'N	7.4	8.3	13.2		28.6		36.0	

[1] For abbreviations refer to Table 7, Appendix B. [2] Growing zones (I–IV) are depicted in Figure 4a. [3] Gyttja clay contains peat and mud fractions [4] Composite SAR/ASAR and NDVI datasets used only in validation of optical VGI models [37].

Figure 6. Optical and SAR composite images from the Etelä-Pohjanmaa Agric. Centre Experimental Areas **(a)** Flooding areas in the Seinäjoki Experimental Area in 2003, **(b)** NOAA/AVHRR low resolution image in Lapua Exp. Area, **(c)** digitized field parcels in Seinäjoki Exp. Area, **(d)** heavy lodging in oat cultivations in Lapua Exp. Area 2003, **(e)** Lapua Exp. Area, **(f)** Seinäjoki Exp. Area [29,33]. (© Finnish Geodetic Institute, original Radarsat data © distributed by Radarsat International/TSS/Novosat Ltd. and European Space Agency).

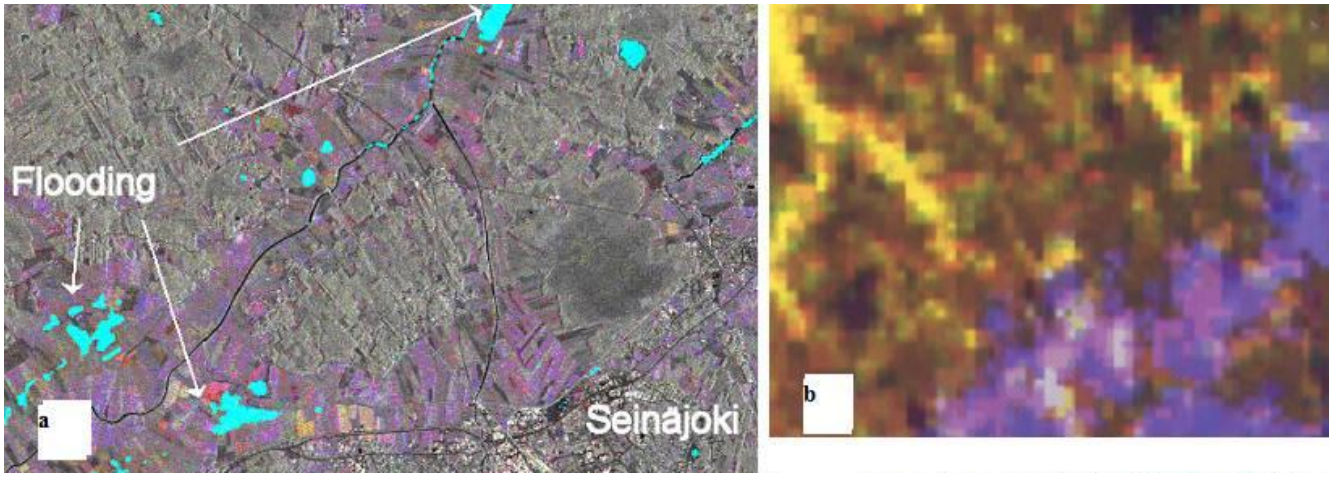

Figure 6. *Cont.*

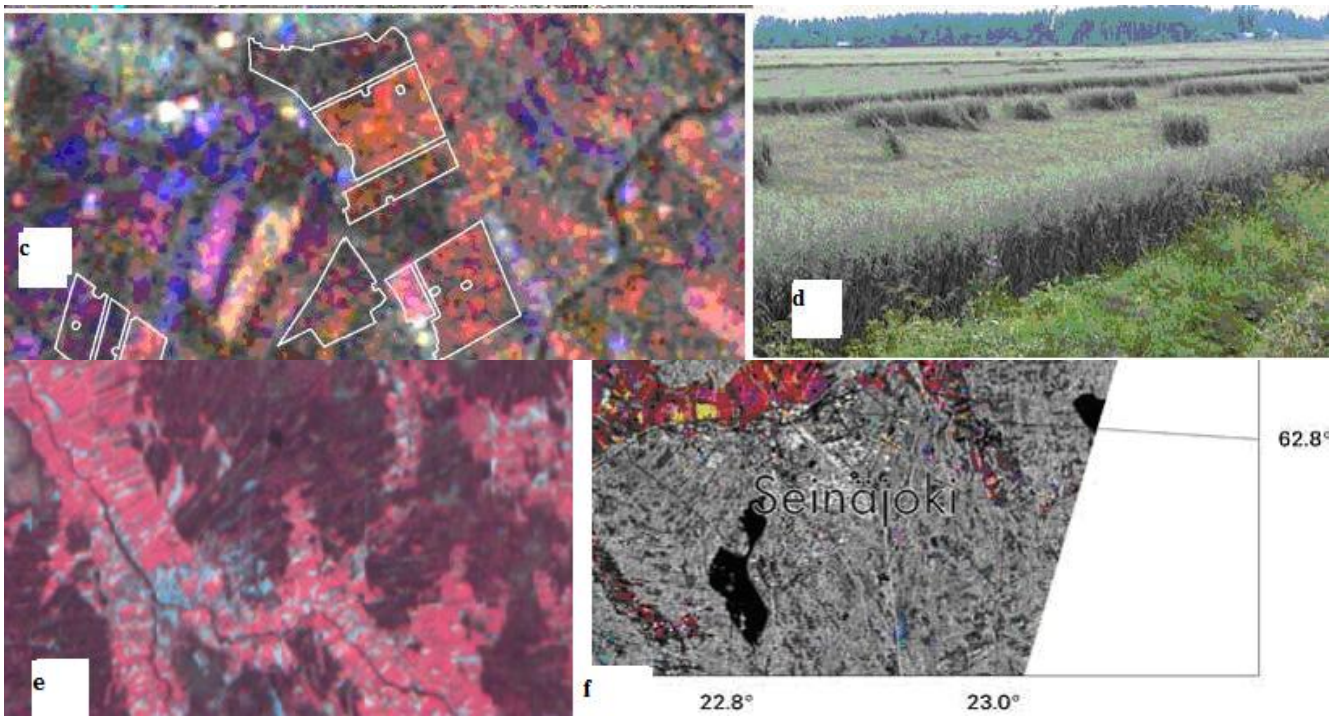

3. Results

3.1. Grain Yield, Phenological Spectral Signature Profile (SSP_{ph}) *and Vegetation Indices Variation*

Table 3 presents observed averaged grain yield variation for spring wheat, barley and oats (1996–2006) in growing zones I–IV. In addition *Phenological Spectral Signature Profile* (SSP_{ph}) variation during phenological development and crop calendar using ρ_{RED} and ρ_{NIR} reflectance values and optical VGI indices are tabulated. The averaged grain yield and SSP_{ph} variation is depicted between *(i)* species, *(ii)* cultivars and *(iii)* soil types with corresponding categories I–III. Category I depicts *crop species* variation with generic spring cereal cultivars. Category II depicts *intracultivar variance* with identified cultivars from field parcels in experimental areas, and category III *species*soil* covariance variation. Table 3 depicts averaged spring wheat, barley and oats observed grain yield levels (kg/ha), infrared (ρ_{RED}/Rf_3) and near infrared (ρ_{NIR}/Rf_4) reflectance, NDVI, GEMI and PAR_{ND}/FAPAR variation during germination and emergence after sowing (a_p, BBCH 0–12), ear emergence and maximum LAI exposure with fully closed canopy structure (b_p, BBCH 12–50) and finally during anthesis in generative phase (c_p, BBCH 50–90). The observed cereal yield, optical reflectance and Vegetation Indices varied significantly between different spring cereals, cultivars and soil types in the experimental areas in southern Finland.

Table 3. Averaged observed yields, *Phenological Spectral Signature Profiles* (SSP_{ph}) for cereals with Reflectance ($Rf_3/\rho_{RED,}$ Rf_4/ρ_{NIR}) and NDVI, GEMI, PAR_{ND}/FAPAR indices values between categories (I: crops, II: identified cultivars and III: soil types) with all data (1990–2006) pooled together[1), 2), 3), 7), 8)].

Category	**Yield (obs, X ± S_x)**[7)]		**Area**	**SSP_{ph} : NDVI, GEMI, PAR_{ND} (X ± S_x)** [1), 6)]								
I	**kg/ha**	**Cv%**	**Ha**	**a_p (May)**			**b_p (June)**			**c_p (July)**		
Crop Species [1),]				NDVI	GEMI	PAR_{ND}	NDVI	GEMI	PAR_{ND}	NDVI	GEMI	PAR_{ND}
Swh	4219 ± 290	14.5	415	0.0012 ± 004	0.257 ± 0.002	0.076 ±0.001	0.498 ± 0.007	0.411 ± 0.004	0.039 ± 0.002	0.332 ± 0.007	0.312 ±003	0.515 ±0.01
Barley	4395 ± 229	33.8	235	0.0014 ± 002	0.193 ± 0.003	0.062 ±0.001	0.898 ± 0.003	0.660 ± 0.002	0.093 ± 0.003	0.256 ± 0.01	0.347 ± 0.006	0.443 ± 0.01
Oats	3740 ± 345	27.6	47	0.0012 ± 005	0.331 ± 0.008	0.049 ± 0.002	0.766 ± 0.01	0.694 ± 0.005	0.231 ± 0.01	0.640 ± 0.02	0.678 ± 0.001	0.535 ±0.02
Mean (Area sum.)	4118 ± 338	25.3	697	0.0013 ± 001	0.2603 ±0.690	0.0623 ±0.0135	0.7207 ± 0.204	0.5883 ± 0.154	0.1210 ±0.099	0.4093 ± 0.203	0.4457 ± 0.201	0.4960 ±0.047

II		Yield (obs.)		Mean $\rho_{RED} - \rho_{NIR}$ for May. June and July [1). 2). 6)]						NDVI (mean) [1). 2)]		
Identified		Mean	C_v%	ρ_{RED}	ρ_{NIR}	ρ_{RED}	ρ_{NIR}	ρ_{RED}	ρ_{NIR}	a_p (May)	b_p(June)	c_p(July)
Cultivars [1)]		Kg/ha		a_p May	a_p May	b_p June	b_p June	c_p July	c_p July			
Swh	Kadett	3541	20.0	0.0820	0.1180	0.0012	0.2320	0.0014	0.203	0.0780	0.798	0,562
	Manu	4016	30.9	0.0011	0.0012	0.0560	0.2180	0.0940	0.259	0.0010	0.587	0.592
	Ruso	3900	11.0	0.0730	0.1040	0.0014	0.2420	0.0012	0.169	0.0730	0.887	0.679
	Satu	3181	31.9	0.0011	0.0014	0.0550	0.2550	0.0970	0.242	0.0014	0.557	0.646
	Mean swh	3659 ± 377	20.9	0.0393 ± 0.044	0.0562 ± 0.064	0.0284 ± 0.0312	0.236 ± 0.01156	0.0484 ± 0.054	0.2182 ± 0.0403	0.0383 ± 0.1001	0.707 ± 0.2474	0.619 ± 0.2211
Brl	Artturi[10)]	4656	18.5	0.0012	0.0011	0.0550	0.2020	0.0990	0.199	0.0012	0.601	0.569
MBrl	Arve[10)]	4785	34.2	~ 0.0	0.0012	0.0011	0.2011	0.0390	0.106	0.0014	0.856	0.425
FBrl [9), 10)]	Inari[10)]	4750	25.7	0.0014	0.0011	0.0490	0.1920	0.0910	0.158	0.0015	0.595	0.411
	Kymppi[10)]	3458	40.5	0.0012	0.0011	0.0012	0.2014	0.0410	0.102	0.0018	0.815	0.343
	Pokko[9)]	5473max	19.6	~ 0.0	0.0014	0.0013	0.2011	0.0560	0.219	0.0014	0.549	0.321
	Mean brl.	4624 ± 729	37.4	0.0007 ± 0.01	0.0011 ± 0.001	0.02152 ±0.0279	0.19952 ± 0.0042	0.0652 ± 0.028	0.1568 ± 0.0529	0.0015 ± 0.0002	0.6832 ±0.1412	0.4138 ± 0.318

Table 3. *Cont.*

II		Yield (obs.)		Mean $\rho_{RED} - \rho_{NIR}$ for May. June and July [1). 2). 6)]						NDVI (mean) [1). 2)]		
Identified		Mean	C_v%	ρ_{RED}	ρ_{NIR}	ρ_{RED}	ρ_{NIR}	ρ_{RED}	ρ_{NIR}	a_p (May)	b_p(June)	c_p(July)
Cultivars [1)]		Kg/ha		a_p May	a_p May	b_p June	b_p June	c_p July	c_p July			
Oats	Puhti	4565	45.4	0.0014	0.0011	0.0350	0.2310	0.0840	0.285	~ 0.0	0.547	0.437
	Salo	4680	14.7	~ 0.0	0.0013	0.0012	0.2011	0.0370	0.181	0.0012	0.822	0.428
	Veli	4129	25.7	0.0011	0.0011	0.0580	0.2802	0.0360	0.108	~ 0.0	0.867	0.655
	Mean oats	4458 ±290	28.6	0.0008	0.0011	0.0314	0.23743	0.0523	0.1913	0.0004	0.745	0.464
Cereal	Mean Tot.	4261 ±641.9	27.9	0.0133 ±0.028	0.0195 ±0.041	0.0265 ±0.0257	0.2214 ±0.0259	0.0566 ±0.034	0.1859 ±0.0581	0.0302 ±0.065	0.7327 ±0.1701	0.4830 ± 0.367

III		Yield (observed)		NDVI (mean) [5) 6)]		Mean ρ_{RED} /Rf3 and ρ_{NIR} Rf4 for b_p.June and c_p.July [4) 6) 10)]	
Soil type		(kg/ha) X ±S_x	Cv%	b_p (June)	c_p (July)	ρ_{RED} / ρ_{NIR} (June)	ρ_{RED} / ρ_{NIR} (July)
Clay[1)]	Swh	4224 ±8.9	14.3	0.497	0.330	0.006 / 0.131	0.023 / 0.088
	Brl	4363 ±30.8	34.5	0.910	0.224	0.016 / 0.256	0.023 / 0.104
	Oat	3485 ±33.8	18.3	0.786	0.569	0.037 / 0.297	0.043 / 0.255
Coarse[2)]	Swh	4224 ±8.9	14.3	0.482	0.112	0.004 / 0.214	0.029 / 0.065
	Brl	4363 ±30.8	34.5	0.720	0.356	0.024 / 0.256	0.045 / 0.121
	Oat	3485 ±33.8	18.3	0.686	0.487	0.052 / 0.316	0.064 / 0.197
Organic[3)]	Swh Erl.	3972 ±483	19.7	0.596	0.429	0.056 / 0.218	0.107 / 0.348
	Swh Lt.	4984 ±641	22.8	0.642	0.541	0.055 / 0.255	0.097 / 0.342
	Brl Erl.	4656 ±862	26.9	0.569	0.401	0.055 / 0.202	0.099 / 0.399
	Brl Lt.	4741 ±659	21.1	0.603	0.596	0.049 / 0.192	0.091 / 0.358
	Oat Erl.	3932 ±824	29.9	0.655	0.557	0.058 / 0.280	0.114 / 0.401
	Oat Lt.	3257 ±629	28.7	0.737	0.547	0.035 / 0.231	0.084 / 0.285

[1)] Includes sandy and gyttja clay soil-classes (Lapua, Mellilä, Porvoo, Kirkkonummi Exp. Areas) [2)] Includes fine and coarse sand soil-classes (Porvoo and Kirkkonummi Exp. Areas) [3)] Early (Erl.; SwH: *cv.* Manu, Brl: *cv.* Artturi, Oat: *cv.* Veli) and Late (Lt. SwH: *cv.* Satu, Brl: *cv.* Inari, Oat: *cv.* Puhti) cereal cultivars measured in the Kuuma/Jokioinen (3 x 3 randomized lattice) and Porvoo Exp. (2 x 2 randomized lattice) areas with organic mould and peat top soil profiles [4)] R_f for May excluded from the table. [5)] R_f and NVDI values for May close to ~0.0 [6)] Rf_3, Rf_4, NDVI data categorized for a_p (May, BBCH 0-12), b_p (June, BBCH 12-50) and c_p (July, BBCH 50-90) phenological classes during the growing season. [7)] Cereal averaged yields (kg/ha corrected as 15% moisture content) were measured by the farmers in the experimental areas in the autumn after the harvest, yield samples were measured from the granary silos. [8)] Averaged over years (1996-2006) and locations in growing zones I-IV. [9)] Enzyme malting barley cultivar (MBrl) [10)] Fodder barley cultivar (FBrl).

The observed spring cereal yields (kg/ha) in satellite measurement locations (Category I, Table 3) were measured by the farmers in the experimental areas in the autumn after the harvest. Yield samples were obtained from the granary silos in the experimental farms. The observed grain yield levels were 4,219 kg/ha for spring wheat, 4,395 kg/ha for barley and 3740 kg/ha for oats when averaged over years (1996–2006) and locations (Growing zones I–IV). The total cultivation area 1996–2006 interpreted from satellite images in southern Finland (growing zones I–IV) with all crops was 1,253 ha, 697 ha for spring cereals and 256 ha for winter cereals (winter wheat and rye, *Secale cereale* L.), not reviewed in this publication).

The spring cereal infrared (ρ_{RED}/Rf_3) and near infrared (ρ_{NIR}/Rf_4) reflectance values were higher in June (b_p) and July (c_p) when compared with May values (a_p, Rf_3 mean 0.0133, Rf_4 mean 0.0195). Especially fodder barley and oat cultivars presented low Rf_3 values (marked ~0.0) in May. The infrared Rf_3 signal obtained low reflectance values (b_p, Rf_3 mean 0.0265) with spring cereal cultivars in June with high PAR-radiation absorbance in fully closed canopies (LAI > 1). Especially for the highest yielding enzyme malting barley cultivar Pokko (Hankkija Plant Breeding) the Rf_3 values were low, but Rf_4 levels (Rf_4 mean 0.2214) were in average in June.

Usually in Finnish long day growing conditions the maximum LAI (LAI_{max}) and also the maximum photosynthetic capacity is observed in June (b_p [41,67]). Correspondingly maximum Rf_3 reflectance values peaked in July (c_p, 0.057). Rf_3 values were below average for wheat cultivars (0.048) but had high values with barley cultivars (0.065) in July. The near-infrared Rf_4 signal peaked with maximum reflected mean value of 0.221 in June (b_p) with lower mean reflectance in July (c_p, 0.186). Fodder barley cultivars obtained Rf_4 values higher than average in June and wheat cultivars below average in July.

The VGI indices (NDVI, GEMI, PAR_{ND}) for spring cereals in June (b_p) and July (c_p) were generally higher than the corresponding May values (a_p). Currently in southern Finland the sowing of spring cereals occurs in May, and May indices values were low denoting sparse vegetation and canopy cover. With vegetation indices (NDVI, GEMI, PAR_{ND}) a significant peak was observed between May and June values (Table 3, Category I). The NDVI ranged between 0.013 (May, a_p), 0.7207 (June b_p) and 0.4093 (July c_p), corresponding values were 0.2603, 0.5883 and 0.4457 for GEMI and 0.0623, and 0.121 and 0.4960 for PAR_{ND}.

3.1.1. Cereal Intracultivar Variance

The intracultivar variance of observed grain yield, reflectance and NDVI values are depicted in category II (Table 3). The *identified* cereal cultivars in the field parcels were reported by the farmers in the experimental areas. The averaged *observed* yield for all spring wheat cultivars was 4.3 t/ha (30.5% C_v). The maximum *observed* yield, 5.5 t/ha, was with enzyme malting barley (*cv.* Pokko, Hankkija Plant Breeding). *Cv.* Pokko optical infrared reflectance (ρ_{RED}) was below average in a_p, b_p and c_p phases (BBCH 0-90) indicating active photosynthesis in PAR-region (Figure 3) and correspondingly the near-infrared reflectance (ρ_{NIR}) was higher than average in phase c_p (BBCH 50–90). The minimum observed yield level (3.5 t/ha) was measured with fodder barley (*cv.* Kymppi). Especially in May (phenology class a_p in vegetative phase, BBCH 0–12) the cereal reflectance in *infrared* wavelength (Rf_3) was very low, close to zero (marked as ~0.0) with average of 0.0133. The fodder and malting

barley cultivars Arve and Pokko and oat cultivar Salo, especially, presented low reflectance values. The maximum infrared reflectance was observed with spring wheat *cv.* Kadett (0.082).

In May (phenology class a_p, BBCH < 12), the infrared reflectance (ρ_{RED}/Rf_3) between cultivars ranged between ~0.0 and 0.082 (*cv.* Kadett) denoting *absorbed* infrared covariance between partly covered top soil and early emergence of spring cereals with partly closed canopy structures (LAI < 1) [41,55-59,67-69]. Correspondingly in May, the near-infrared (ρ_{NIR}/Rf_4) obtained higher *emitted* reflectance. Rf_4 ranged between 0.0011 (barley *cv.* Arttu) and 0.118 (wheat *cv.* Kadett).

In June (phenology class b_p, BBCH 12–50) during generative phase with LAI_{max} and full canopy closure (LAI > 1) the mean infrared reflectance was 0.0265 and near-infrared 0.2214 suggesting high photosynthetic activity in leaf canopy during ear emergence. Notably the oat *cv.* Veli contained both maximum infrared (0.058) and near-infrared (0.282) reflectances in b_p phase.

In July (phenology class c_p, BBCH 50–90) during anthesis and initialization of grain filling the mean absorbed infrared reflectance was 0.0566 higher (0.099 max. for barley *cv.* Artturi) than the average b_p value in June concurrent with active translocation of assimilates to cereal heads from leaf canopy and especially from the flag leaf. Correspondingly the average reflected near-infrared 0.1859 in July (0.285 max. for oat *cv.* Puhti) was lower than in June.

3.1.2. Effects of Soil Type Variation on Spring Cereal Yield Formation

Category III in Table 3 illustrates the spring cereal yield, reflectance and NDVI variation between different soil types containing all averaged 1996–2006 data. Category III includes sandy and gyttja clays for clay type soils and coarse type soils with gravel and coarse sand fractions and finally organic type soils with peat or mould top-layer (10–15 cm) with clay sub-soil profile (depth > 15 cm). The main soil type in the experimental areas was clay with mixtures of coarse elements and minor fraction of organic compounds. Soil types consisted of sandy and gyttja clays for clay soil types (Cla.) and coarse soil types (Crs.) with gravel and coarse sand fractions and also organic soil type (Org.). The Kuuma experimental area in Jokioinen (1995) was the only field with organic mould top layer (Figure $4A_1$) and correspondingly the Dräcksby site in Porvoo contained peat top-soil layer (Figure $4B_2$).

The observed average yield levels (kg/ha) and C_v (%) in clay type soils under suboptimal growing conditions were highest for barley (4,363 kg/ha, 34%), intermediate for spring wheat (4,224 kg/ha, 14%) and lowest for oats (3,485 kg/ha, 18%). Correspondingly in coarse type soils, the observed yield levels were highest for barley (4,803 kg/ha, 26%), intermediate for spring wheat (4,233 kg/ha, 16%), and lowest for oats (4,146 kg/ha, 32%). In organic type soils containing mixtures of peat and mould in the top soil layer (10–15 cm), the highest yield were recorded for oats (5,978 kg/ha, 28%), intermediate for barley (4,727 kg/ha, 26%) and lowest for spring wheat (3,390 kg/ha, 38%). Especially spring wheat yield levels were significantly reduced by the drought stress in mid-summer (b_p, c_p) in the Kuuma (Figure $4A_1$), and Dräcksby (Figure $4B_2$) experimental sites.

Respectively, in the soil covariance category (III, Table 3) a significant NDVI peak was observed for June and July values when compared with May values (Category I). The NDVI ranged on different soil types between 0.582 (Crs.) and 0.848 (Cla.) and in June and between 0.3743 (Cla.) and 0.8103 in July.

Infrared (ρ_{RED} /Rf_3) and near-infrared (ρ_{NIR}/Rf_4) covariances on clay, coarse and organic soil types were consistent on cultivar level (Category II, Table 3) in different phenological stages (a_p, $b_{p,}$ $c_{p,}$). Especially infrared signal presented high absorbance in June (b_p) on clay type soils.

3.2. Calibration Results

The optical VGI model calibration results for spring cereals containing all optical Landsat and SPOT data are presented in Table 4. The optical data were phenologically pre-classified with the SatPhenClass-algorithm. Table 4 depicts cereal baseline yield (y_b) estimates for Polynomial Infrared (I), NDVI (II, [25,53,54]), GEMI (III, [55]) and PAR_{ND}/FAPAR (IV, [56-60]) models. In addition, Table 4 presents corresponding R^2 and RMSE, coefficient of variation (C_v, %) and Anova F-test significance level estimates for *linear*, *quadratic*, *cross product* and finally for the total model [51,52]. Statistical significance levels are given in Table 7 (**Appendix A**).

The optical baseline yield (y_b) calibration results indicate that the R^2 of the VGI models varied significantly between spring sown cereals over years and locations in growing zones I-IV in southern Finland. The overall optical R^2 for baseline yield (kg/ha) was 0.630 for spring sown cereals (mean response yield 3958 kg/ha, RMSE 360 kg/ha) ranging between 0.056 and 0.794. The R^2 varied with spring wheat cultivars between 0.510 (PAR_{ND}-model (IV), RMSE 406 kg/ha) and 0.790 (Infrared model (I), RMSE 42 kg/ha), with barley cultivars between 0.587 (IV, RMSE 463 kg/ha) and 0.615 (I, RMSE 449 kg/ha) and with oats between 0.06 (IV, RMSE 998 kg/ha) and 0.760 (I, RMSE 55 kg/ha).

The average VGI modeled baseline yield response (y_b) varied between 3.5 t/ha and 4.2 t/ha with spring wheat, between 4.1 t/ha and 4.4 t/ha with barley and between 3.4 t/ha and 3.7 t/ha with oats. The coefficient of variation (C_v, %) varied between 1.6% and 28.7% with spring sown cereals, respectively with F-test all the VGI model (I-IV) subcomponents (*linear*, *quadratic* and *cross products*) were significant on 0.1% error level.

Table 4. VGI optical linear and non-linear model (I-V) non-potential baseline yield estimates (y_b, kg/ha) [51,52] [1) 2) 3) 4)].

Crop	Model (Table1) [1)]	Grow.zone[1)]	Main soil type[1)]	Dataset /Model Equation (Table 11) [1)]	R^2 lin[a)]/non-lin.polyn. [b)]	RMSElin[.c)]/non-lin polyn.[d)] (kg/ha)	Response mean baseline yield (y_b, kg/ha) [2)]	Cv (%)	Pr > F linear	Pr > F quad ratic	Pr > F cross product	Pr > F total model
Swh	I [7)] IR	I-IV	Gyttja and Sandy clay	1.1,2.1, 3.1-3.3 [1.1)] 1.1,2.1, 3.1-3.3 [1.2)]	0.764[a)] 0.794[a)]	282.3[.c)] 42.46[c)]	4219.0 3768.6	6.66 5.89	<.0001 *** 	<.0001 *** 	<.0001 *** 	<.0001 ***
	II [7)] NDVI	I-IV	Gyttja Sandy clay	1.1,2.1, 3.1-3.3 [1.3)] 1.1,2.1, 3.1-3.3 [1.4)]	0.737[b)] 0.732 [a)]	297.6[d)] 300.1 [c)]	4219.0 3556.7	7.02 7.88	<.0001 *** 	<.0001 *** 	<.0001 *** 	<.0001 ***
	IV[5)] GEMI	I-IV	Gyttja and Sandy clay	1.1,2.1, 3.1-3.3 [1.5)] 1.1,2.1, 3.1-3.3 [1.6)]	0.704[b)] 0.570 [a)]	316.1[d)] 536.8 [c)]	4219.0 3556.7	7.45 8.11	<.0001 *** 	<.0001 *** 	<.0001 *** 	<.0001 ***
	V[6)] PARND	I-IV	Gyttja and Sandy clay	1.1,2.1, 3.1-3.3 [1.7)] 1.1,2.1, 3.1-3.3 [1.8)]	0.712 [b)] 0.509 [a)]	311.6[d)] 406.3 [c)]	4219.0 3768.6	7.34 7.34	<.0001 *** 	<.0001 *** 	<.0001 *** 	<.0001
Brl	I [7)] IR	I-II,IV	Gyttja and Sandy clay	1.1-1.3, 2.1,3.3 [2.1)]	0.615[.a)]	449.3[.c)]	4395.0	10.3	<.0001 *** 	<.0001 *** 	N.S.	<.0001
	II [7)] NDVI	I-II,IV	Gyttja and Sandy clay	1.1-1.3, 2.1,3.3 [2.2)]	0.611[b)]	449.6[d)]	4298.0	10.3	<.0001 *** 	<.0001 *** 	0.0014 * 	***
	IV[5)] GEMI	I-II,IV	Gyttja and Sandy clay	1.1-1.3, 2.1,3.3 [2.3)]	0.614[b)]	448.6[d)]	4310.0	10.3	<.0001 *** 	<.0001 *** 	0.0081 * 	<.0001
	V[6)] PARND	I-II,IV	Gyttja and Sandy clay	1.1-1.3, 2.1,3.3 [2.4)]	0.587[b)]	463.7[d)]	4150.0	10.6	<.0001 *** 	<.0001 *** 	<.0001 *** 	***
Oats	I [7)] IR	I-II, IV	Sandy clay	1.1-1.3, 2.1, 3.1 - 3.3 [2.5)]	0.760[.a)]	55.0[.c)]	3740.0	1.58	<.0001 *** 	<.0001 *** 	<.0001 *** 	<.0001
	I [e)]	I-II, IV	Sandy clay	[e)]	0.756	55.1	3488.7	1.58	<.0001 *** 	N.S.	N.S.	***
	II [7)] NDVI [e)]	I-II, IV	Sandy clay	[e)]	0.056	994.8	3462.0	28.7	<.0001 *** 	<.0001 *** 	N.S.	<.0001
Cereal mean					0.630	360.6	3958.0	8.16				

[1)] Model equations 1.1 – 2.5 (Table 11, **Appendix B**) applied after SAS REG/Stepwise for linear models (Equation 1, **Appendix B**, [51,52]) and SAS RSREG for polynomial models (Equation 2, **Appendix B**), experimental datasets used, soil types and Growing Zones are listed in [37]. [2)] Grain baseline yields (y_b, kg/ha) estimated by the corresponding VGI model. [3)] Optical data classified with SatPhenClass-algorithm (Figure 3a,b [37]) [4)] The Composite NDVI and SAR modeling results are reviewed in [37] [5)] GEMI VGI model (Table 1, [55]) [6)] PAR_{ND} VGI model (Table 1, [56-60]) [7)] Presented also in Part I [a)] R^2 linear [b)] R^2 non-linear polynomial equation [c)] RMSE linear [d)] RMSE (kg/ha) non-linear polynomial equation [sc)] Spring cereal (spring wheat, barley, oats) [e)] Equation not shown.

3.3. Intersensory Calibration Results with NDVI Phenological Spectral Profiles (SSP_{ph})

Figure 7 displays NDVI based intersensory calibration results between Landsat/TM and Spot/HRV_2 sensors using *Phenological Spectral Profiles (SSP_{Ph})* in different phenological phases (P_a, P_b, P_c) on clay, coarse and organic soil types. The original radiometrically and geometrically calibrated and harmonized TM and HRV_2 reflectance data were classified with the *SatPhenClass* algorithm [37] using BBCH and Zadoks phenological classes [43,44]. The NDVI values used in the VGI model II (Table 1, Table 12, **Appendix B**) were calculated from the calibrated ρ_{NIR} (a_p, b_p, c_p) and ρ_{RED} (a_p, b_p, c_p) reflectance values.

Figure 7. Landsat/TM and Spot/HRV_2 sensory calibration with NDVI Phenological Spectral Profiles (SSP_{ph}) in different phenological phases (P_a, P_b, P_c) and soil types. **(A)** depicts unadjusted Landsat/TM and Spot/HRV2 NDVI values for spring cereals in major phenological phases (Pa, Pb, Pc) and soil types. **(B)** displays transformed and enhanced NDVI values in early Pa phase after spring cereal germination and emergence on logarithmic scale.

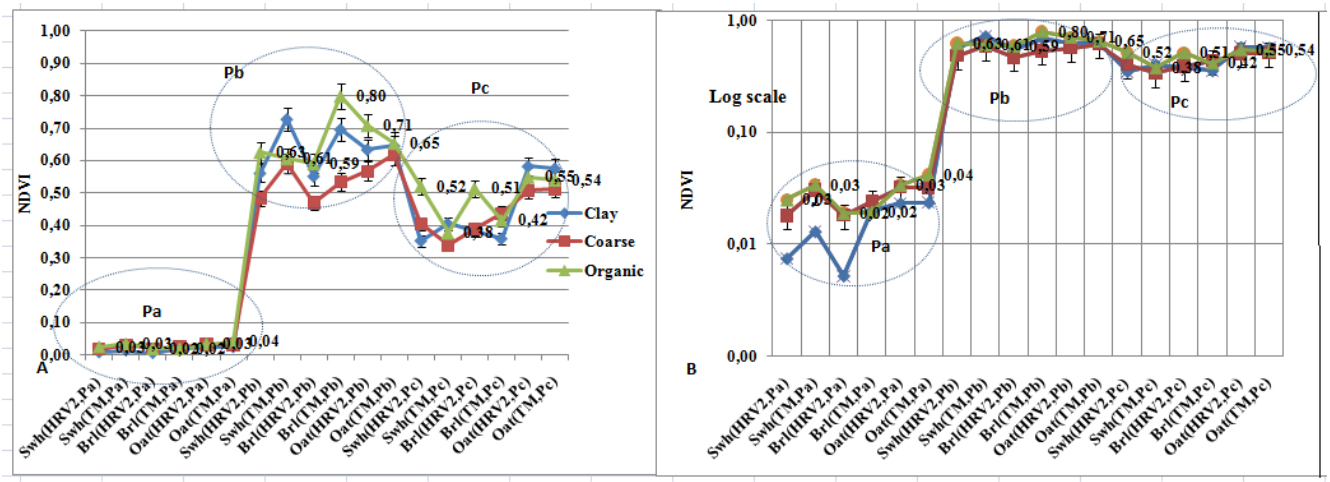

The NDVI values in early P_a phase in May (Figure 7(B)) after germination and emergency is displayed on logarithmic scale to enhance NDVI values. In general, the NDVI with HRV_2 and TM sensors ranged between 0.01 and 0.1 in the initial P_a phase during the cereal germination and emergence on all soil types, the maximum level of 0.03 was obtained with HRV_2 on barley cultivars grown on organic type soils (Figure 7(B)). In phase P_b during the maximum LAI exposure (LAI_{Max}), the NDVI increased on 0.60–0.80 level and was decreased on 0.4-0.50 level in phase Pc after anthesis and grain filling (Figure 7(A)). In phase P_b the maximum NDVI level of 0.80 was obtained using HRV_2 sensor on oat cultivars grown on organic soils and respectively in phase P_c the maximum level of 0.55 with TM on oat cultivars grown on clay type soils.

Figure 8(A,I) displays digitized TM and HRV_2 pairwised images from the Porvoo Experimental site (Kiiala, Dråksby, Kullogård and Bosgård Experimental Farms) in June with LAI maximum (P_b) and in July after cereal anthesis (P_c). Pairwised composite images were composed of $\rho_{RED(bp,cp)}/\rho_{NIR(bp,cp)}$ reflectance data, which were used in calculating corresponding NDVI values (Figure 7). The pairwised Figure 8(A,B) illustrates the Kiiala experimental farm with digitized and classified cereal experimental

plots used for ground truth sampling (Figure 3(b)). More specifically, Figure 8(A) image was composed of Landsat TM reflectance data (channels $\rho_{RED}(b_p)/\rho_{NIR}(b_p)$ and correspondingly Figure 8(B) of Spot HRV_2 data ($\rho_{RED}(c_p)/\rho_{NIR}(c_p)$). Respectively, Figure 8(C,D) illustrates Dräcsby Farm, Figure 8(F,G) Kullogrd Farm and Figure 8(H,I) Bosgård Farm. Figure 8(J) depicts a Spot HRV_2 composite image ($\rho_{RED}(c_p)/\rho_{NIR}(c_p)$ from the Jokioinen site in July, Kuuma Experimental area in the middle.

Figure 8. Landsat/TM and Spot/HRV_2 pairwised ρ_{RED} (b_p, c_p)/ρ_{NIR} (b_p,c_p) composite images from the Porvoo Experimental site in June (P_b, Figures 8(A,C,F,H)) and July (P_c, Figures 8(B,D,G,I)) (© Original Data Finnish Geodetic Institute).

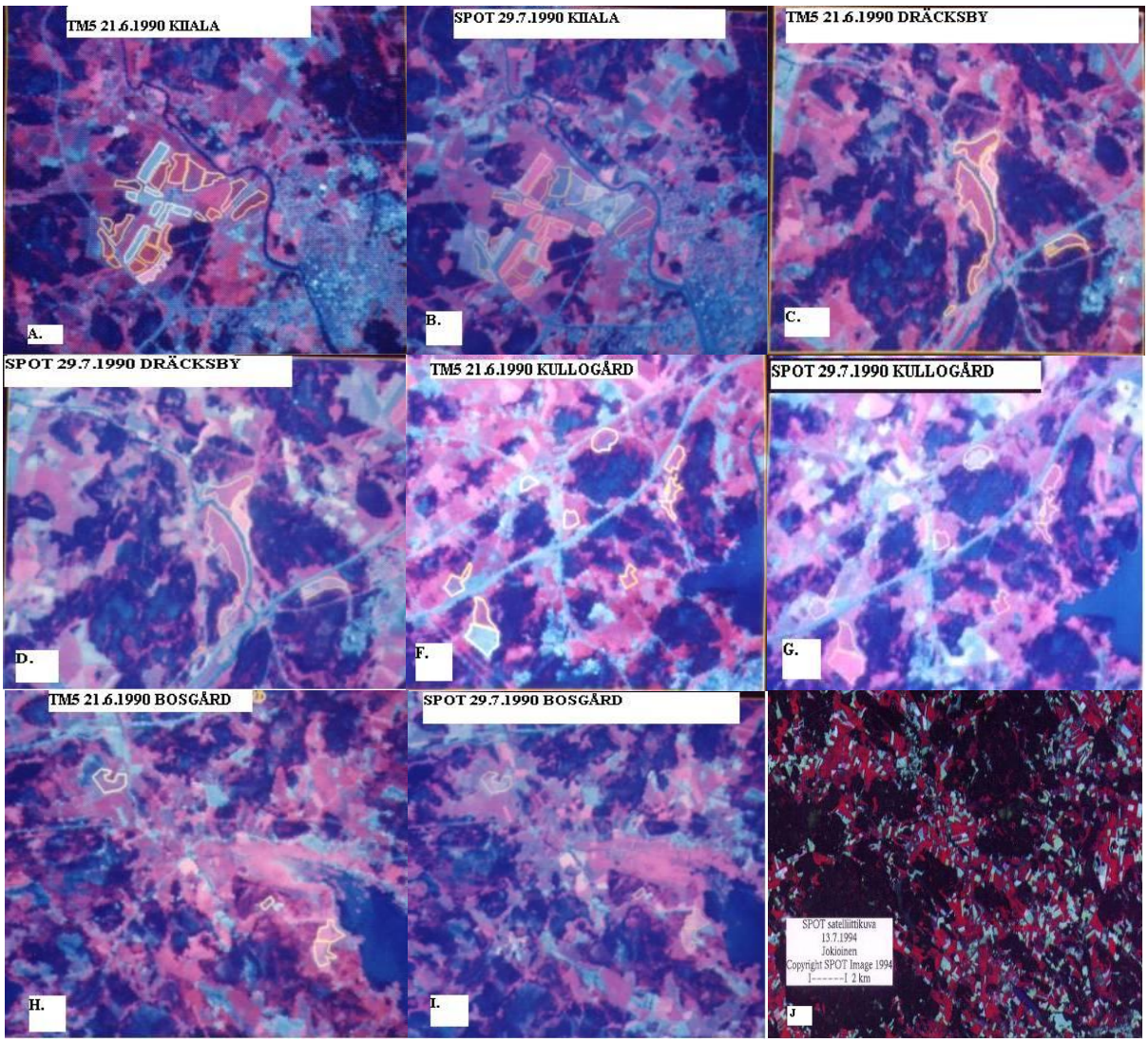

Figure 9 displays combined *phenologically clustered* Landsat/TM *vs.* Spot/HRV_2 NDVI values averaged over different experimental locations (Me: Mellilä, Po: Porvoo, Kn: Kirkkonummi, Lp: Lapua, Ku: Kuuma, Jk: Jokioinen, Figure 2(d)) and soil types (Clay, Crs: Coarse, Org: organic) and clustered into different phenological classes (P_a, P_b, P_c). In addition a logarithmic scale adjustment for the initial P_a phase after germination is displayed to enhance calibrated TM *vs.* HRV_2 NDVI values (swh: Figure 9(A,B), brl: Figure 9(C,D), oat: Figure 9(E,F). Clustering analysis results indicate that cereal NDVI values ranged between 0.01 and 0.1 in the initial P_a phase after germination and

emergence. The NDVI values reached maximum values in class P_b on all soil types ranging between 0.60 and 0.90 during the maximum LAI exposure (LAI_{Max}). In class P_c after the cereal anthesis the NDVI ranged between 0.30 and 0.60.

With spring wheat (Figure 9(A,B)) the TM had the maximum NDVI value (0.865) on clay types soils and HRV_2 NDVI (0.648) on organic soils (peat, mould) in class P_b. Respectively, with barley (P_b, Figure 9(C,D)) the TM had the maximum NDVI value (0.710) on organic soils and HRV_2 NDVI (0.760) on coarse soils. With oat cultivars (P_b, Figure 9(E,F)) the TM had the maximum NDVI value (0.701) on clay soils and HRV_2 NDVI (0.760) on organic soils in class P_b.

Figure 9. Phenologically clustered Landsat/TM *vs.* Spot/HRV_2 NDVI values averaged over different experimental locations and soil types [1]. **(A, C, E)** depict spring cereal (A-wheat, C-barley, E-oats) unadjusted Landsat/TM *vs.* Spot/HRV2 NDVI values in major phenological phases (Pa, Pb, Pc), soil types and experimental locations. **(B, D, F)** display spring cereal (B-wheat, D-barley, F-oats) transformed NDVI values on logarithmic scale in early Pa phase [29,37].

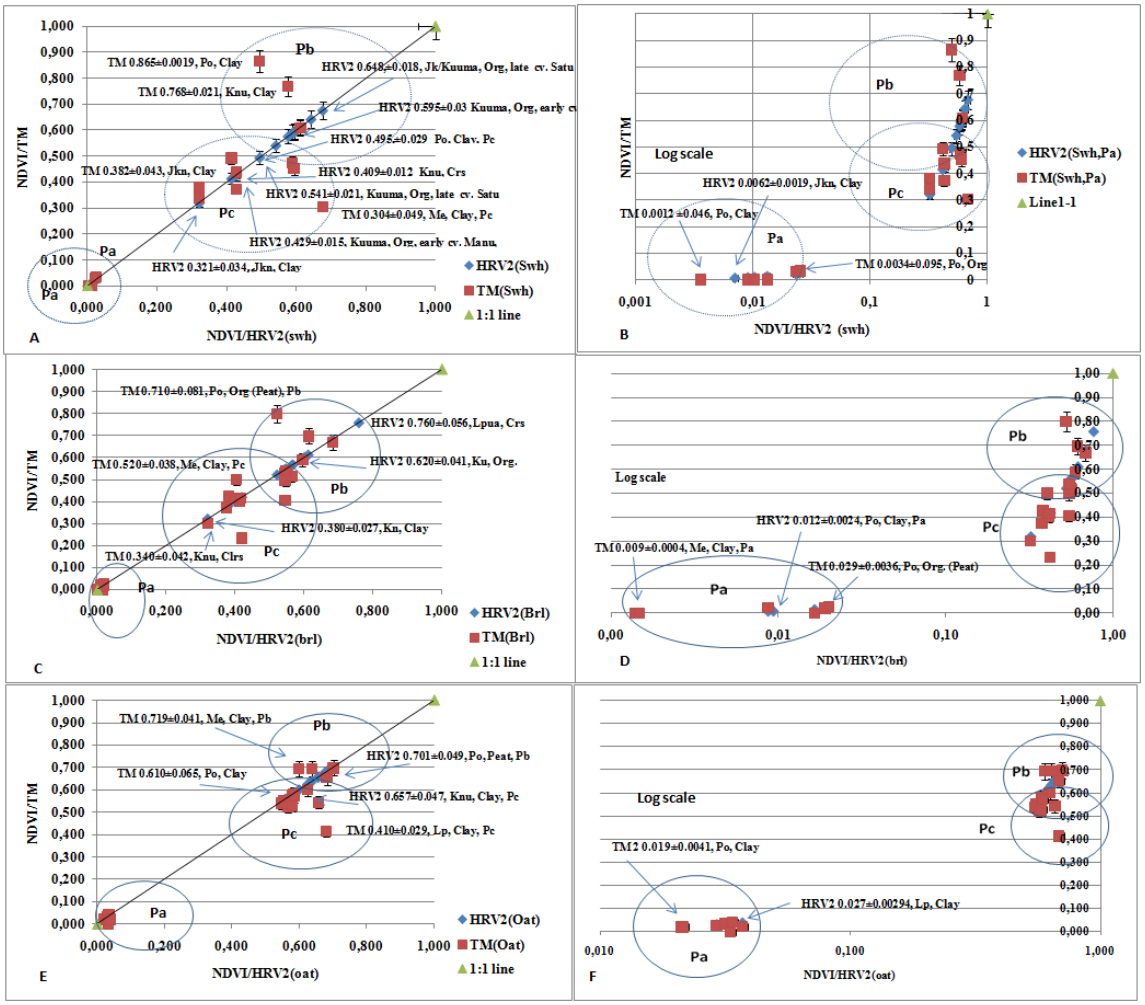

3.2.1. Soil*Species and soil*Cultivar Covariance Calibration Results

The *soil*species* and *soil$_{(clay)}$* cultivar* covariance interactions on clay type soils with Infrared Model I are depicted in Table 5 with spring wheat (*cv.* Manu and Satu) and barley (*cv.* Inari) cultivars

currently cultivated in Finland. Different soil types have significant effect on cereal yield potential: The Infrared and NDVI models (I, II) *calibration* results with *soil*species covariances* indicated that the R^2 was considerably higher for spring wheat (R^2 0.764) than for barley (R^2 0.166). In addition, the *soil*cultivar* covariance calibration results with spring cereal cultivars on clay type soils indicated a low R^2, varying between 0.089 and 0.144.

Table 5. Spring wheat and barley non-potential yield estimates (kg/ha) for soil*species and soil $_{(clay)}$ * cultivar covariance categories (VGI Model I)[1)].

Cereal, VGI Model Equation 1)	Soil type/Cultivar	R^2 lin.[a)]/non-lin. polyn.[b)]	RMSE lin.[a)]/non-lin polyn.[b)] (kg/ha)	Yield response mean (kg/ha)	Cv (%)	Pr > F (Linear)	Pr > F (Quad-ratic)	Pr > F (Cross-prod.)	Pr > F (Tot. model)
Soil*species covariance category									
Swh (2.6)	Clay	0.764 [a)]	282.3 [a)]	4240.9	6.66	<.0001 ***	<.0001 ***	<.0001 ***	<.0001 ***
Brl (2.7)	Clay	0.166 [a)]	1382.3 [a)]	4428.0	31.22	<.0001 ***	N.S.	N.S.	<.0001 ***
Soil $_{(clay)}$ * cultivar covariance category									
Swh (3.1)	Clay*Manu	0.089 [b)]	1292.1 [b)]	4015.5	32.18	N.S.	N.S.	N.S.	N.S.
Swh (3.2)	Clay*Satu	0.046 [b)]	1031.7 [b)]	3181.1	32.43	N.S.	N.S.	N.S.	N.S.
Brl (3.3)	Clay*Inari	0.144 [b)]	1220.9 [b)]	4749.8	25.70	0.02013 *	N.S.	N.S.	N.S.

[1)] Data classified with SatPhenClass-algorithm, model equations 2.6–3.3 (Table 11, **Appendix B**) [a)] R^2 for linear model (Tables 1, 3, **Appendix B**: Equation 1, Table 11) [b)] R^2 for non-linear polynomial model (Tables 1,3, **Appendix B**: Equation 2, Table 11) with corresponding RMSE linear and non-linear error estimates (kg/ha).

More specifically, the yield and soil interactions were estimated on two category levels by estimating the *(i) soil*species* and *(ii) soil*cultivar* covariances: *(i)* The soil*species covariance on clay type soils was higher for spring wheat (R^2 0.764, RMSE 282 kg/ha) than for barley (R^2 0.166, RMSE 1,382 kg/ha), denoting a statistically more significant fit for spring wheat cultivars. The corresponding average baseline response levels for yield (y_b) were 4,240 and 4,428 kg/ha respectively and the Coefficient of Variation (C_v, %) ranged between 6 and 31 percent including both species. Both *linear*, *quadratic*, *cross product* and the *total model* terms were statistically significant for wheat. Correspondingly with barley only the linear component was significant. The R^2 for barley model, especially on clay type soils, was significantly lower than for wheat.

(ii) The *soil*cultivar* covariance interaction (Table 5) with clay type soils was further tested on *cultivar level* with *cv.* Manu and *cv.* Satu for spring wheat and *cv.* Inari for barley. With the *soil*cultivar* as category variable, the number of observations in each class remained low thus decreasing the R^2 varying between 0.089 and 0.144 and respectively increasing the RMSE value. For *cv.* Manu the R^2 was 0.089 (RMSE 1,292.1 kg/ha, the model response for yield was 4,015 kg/ha), for *cv.* Satu 0.046 (RMSE 1,031.7 kg/ha, response yield 3,181 kg/ha) and for *cv.* Inari 0.144 (RMSE 1,221 kg/ha, response yield 4,749 kg/ha), respectively. The Coefficient of Variation (C_v) ranged between 25 and 32

percent with different cultivars; the linear component was statistically significant only with barley (*cv.* Inari) grown on clay type soils.

3.3. Validation Results

3.3.1. Optical VGI Model and CropWatN Crop Model Validation Results for Baseline Yield Levels (yb)

The optical VGI model *validation results* using two independent datasets *(i)* MAFF inventory statistics [62,74] and *(ii)* MTT Agrifood Research Finland Official Variety Trial results [64-66] are presented in Table 6 to assess the VGI baseline yield estimates (y_b, kg/ha) for different spring cereals.

Yield estimates are depicted using four categories: (I) *Crop* category, (II) *Crop*Growing Zone* (I–IV) covariance category, (III) the *soil cultivar* covariance *validation* results using Models I and II [37] and (IV) the SAR/ASAR and NDVI Composite Model (VI, Table 1) validation results using Envisat, ERS and Radarsat backscattering data (σ^0) [37]. Both MAFF and MTT observed yield values averaged over years and locations were compared with corresponding simulated VGI baseline yield estimates (y_b) using absolute (DY_{MAFF}, DY_{MTT}, kg/ha) and percent differences (%, DP_{MAFF}, DP_{MTT}).

The optical VGI models (I–II) used solely phenologically pre-classified optical reflectance data (*Optical Minimum Dataset*). The dynamic CropWatN crop model exploited both optical reflectance and extensive ground truth agrometeorological data. The CropWatN model was linked through LAI-bridge [29] and GEMI index [55] coupling system to use both Spot/HRV_2 (zones III–IV) and NOAA/AVHRR (zones I–IV) sensory data (Tables 9 and 10, **Appendix A**). The adaptive Kalman filter ([19,21], Figure 1) was applied in the LAI-bridge coupling system to obtain the optimal LAI estimate ($LAI_{Optimal}$) from the optical satellite data ($LAI_{Satellite,Cereal}$) and from the initial crop model LAI estimate ($LAI_{CropModel}$) in different phenological phases (Equations 6–8). The corrected LAI estimate was used for the final grain yield estimation in the CropWatN crop model [29].

The *soil*species* and *soil*cultivar covariance* validation results are depicted in Table 6 (Category III, [37]). Two spring wheat (*cv.* Manu, Satu) and one malting barley (*cv.* Inari) cultivars grown on heavy clay type soils were analyzed by using optical VGI Infrared and NDVI models. The response mean yields (kg/ha) were compared with the MTT Official Variety Trial mean yield results correspondingly grown on clay type soils in cultivation zone I (Pernaja and Inkoo Exp. Stations), II (Jokioinen Exp. Station) and III–IV (Ylistaro and Ruukki Exp. Station, Figure 2a). The validation results indicated with the optical Model I and II using MTT Agrifood Finland Official Variety Trial validation data, that both observed wheat and barley yield levels from the MTT official variety trials (kg/ha) exceeded corresponding modeled spring wheat and barley yield levels. In both categories (soil*species, soil*cultivar) the VGI models underestimated the baseline yield levels (y_b) when compared with the corresponding observed MTT yield levels. The modeled results for spring wheat and barley baseline yield levels (y_b) in both categories were lower than the corresponding yield levels in MTT Official Variety trials. The model I (Infrared) and Model II (optical NDVI) indicated an underestimated *yield difference* (DP_{MTT},%) by −10% in *soil*species* category and between −31% and −14% in *soil*cultivar category*. Spring wheat and barley cereals in MTT field trials were grown on more optimal, *non-limiting* growing conditions.

Table 6. Averaged VGI optical and CropWatN dynamic crop model validation estimates for baseline yields (y_b) *vs.* observed MAFF yield inventory and MTT Official Variety Trials [29,65,66,74].

		VGI model (y_b) yield estimate		**MAFF Inventory estimate**				
Category and Crop [1)]		**Model**	**Model mean response kg/ha, X ± S_d**	**MAFF mean inventory yield kg/ha, X ± S_d**	**DP_{MAFF} (%,100 ref.)** [8)]	**DY_{MAFF} (kg/ha)** [9)]		
Category I Crop								
Swheat		I-II	4240 ± 228	3783 ± 212	112[oe)]	458 ± 97[oe)]		
Barley		I-II	4394 ± 279	3520 ± 108	125[oe)]	874 ± 112[oe)]		
Oats		I	3488 ± 352	3458 ± 131	101[oe)]	31 ± 22 [oe)]		
Category II Growing Zone (I-IV)		VGI model estimate		MAFF Inventory yield estimate [62,74]		MTT Official Variety trial yield result [64-66]	CropWatN Dynamic Model yield estimate with GEMI [55] and LAI-bridge [29] [12,13)]	
		Model	y_b, kg/ha, X ± S_d	kg/ha, X ± S_d	$DP_{MAFF,VGI}$ 100% ref. [8)] ($DY_{MAFF,VGI,}$ kg/ha) [9)]	kg/ha, X ± S_d($DP_{MTT,VGI\%}$,100 ref.) [10)]	NOAA data[12)] $DP_{MAFF,NOAA,}$ kg/ha, X ± S_d	Spot data[13)] $DP_{MAFF,Spot}$Kg/ha, X ± S_d
Zone I-II Mean [2), 3)]	Swh	I-II	4218 ± 579	3530 ± 339	120%[oe)](+710 kg/ha)	3789 ± 318(112%)[oe)]	3620 ± 908 (115%)[oe)]	-
	Brl [5)]	I-II	4428 ± 719	3570 ± 297	124%[oe)](+858 kg/ha)	4867 ± 107(91%)[ue)]	3490 ± 539 (91%)[ue)]	-
	Oat	I	3488 ± 105	3605 ± 431	97%[ue)] (−116 kg/ha)	4634 ± 226 (75%)[ue)]	3315 ± 877 (93%)[ue)]	-
Zone III-IV Mean [4), 5)]	Swh	I-II	3768 ± 1042	3556 ± 160	106%[oe)](+200 kg/ha)	4522 ± 271(83%) [ue)]	4605 ± 518(146%)[oe)]	4609 ± 227 (146%)[oe)]
	Brl [7)]	I-II	4470 ± 1339	3430 ± 458	130%[oe)](+1040 kg/ha)	4250 ± 432(105%)[oe)]	4022 ± 99 (120%)[oe)]	3984 ± 182(119%)[oe)]
	Oat	I	3462 ± 1046	3370 ± 279	103%[oe)](+92 kg/ha)	4913 ± 217(71%)[ue)]	3811 ± 75(112%)[oe)]	3752 ± 167 (110%) [oe)]

Table 6. *Cont.*

Category III [37]	Species	Model	Category	Soil type/Cultivar[1)]	Averaged Model (I,II) yield (y_b, $X \pm S_d$)	MTT mean ($X \pm S_d$ kg/ha) [3)]	DY_{MTT} Difference (kg/ha) from MTT obs [7)]	DP_{MTT}, Difference (%) from MTT obs (100 ref.) [6)]
Optical Infrared (I), NDVI (II)	Swheat	I+II	Soil*Species	Sandy clay	4240 ±52	4645 ±546	−404[*ue)]	91.3[*ue)]
	Barley	I+II		Sandy clay	4428 ±48	4791 ±29	−363[*ue)]	92.4[*ue)]
	Swheat	I+II	Soil*Cultivar	Sand clay*Manu	4015 ±62	4423 ±72	−408[*ue)]	90.8[*ue)]
	Swheat	I+II		Sandy clay*Satu	3181 ±31	4608 ±92	−1427[*ue)]	69.0[*ue)]
	Barley	I+II		Sandy clay*Inari	4749 ±89	5483 ±44	−733[*ue)]	86.6[*ue)]
Category IV [37]	Crop	SAR and NDVI Model (Table 12)	Category Soil type (Table 2)	SAR Sensor	Mean y_b, kg/ha, $X \pm S_d$	MAFF estimate ($X \pm S_d$) [2)]	DY_{MAFF} Difference (kg/ha) from MAFF obs. [1) 5)]	DP_{MAFF} Difference (%) from MAFF obs.(100 ref.) [4)]
Composite SAR/ASAR and NDVI (Model VI [37])	Swh	VI/6.1	Fine coarse sandy clay	Envisat ASAR	4127 ±68	3950 ±72	−177.0 [oe]	104.4
		VI/5.1		Radarsat SAR	4213 ±41	3840 ±86	−373.0 [oe]	109.7
		Swh ave.			4170 ±54	3895 ±78	−275.0 [oe]	107.1
	Brl general	VI/6.2	Fine coarse sandy clay	Envisat ASAR	3750 ±91	3880 ±47	130.0 [ue]	96.6
		VI/4.1		ERS2 SAR	3835 ±98	3 420 ±82	−415.0 [oe]	112.1
	Brl malt	VI/5.2		Radarsat SAR	3909 ±24	4050 ±76	141.0 [ue]	96.5
	Brl feed and	VI/5.2		Radarsat SAR	3899 ±32	3820 ±82	−79.0 [oe]	102.7
		Brl ave.			3848 ±74	3792 ±72	−55.7 [oe]	101.8
	Oats	VI/6.3	Fine coarse sandy clay	Envisat ASAR	2826 ±85	3310 ±54	484.0 [ue]	85.4
		VI/4.2		ERS2 SAR	2942 ±49	3330 ±54	388.0 [ue]	88.4
		VI/5.3		Radarsat SAR	3038 ±23	3520 ±81	482.0 [ue]	86.3
		Oats ave.			2935 ±28	3386 ±48	451.3 [ue]	86.7
		Mean tot.			3615 ±12	3680 ±49	64.5 [ue]	98.2

[1)] MAFF average yield statistics in the Nylands Svenska and Etelä-Pohjanmaa Agricultural Advisory Centres [74] [2)] Averaged zone I-II, Nylands Svenska and Häme Agricultural Advisory Centres [66] [3.)] Pernaja and Inkoo MTT Experimental Stations [4)] Averaged III-IV Zone, Etelä-Pohjanmaa Agricultural Advisory Centre [66] [5)] Ylistaro (Zone III) and Ruukki (Zone IV) MTT Experimental Stations [6)] MTT Official Variety Trial results averaged yield levels over the years and different soil types in MTT experimental locations. [7)] Contains both malting and fodder barley [8)] $DP_{MAFF,VGI}$ - difference (%) VGI modeled *vs.* MAFF average inventory result (100%) [9)] $DY_{MAFF,VGI}$ - difference (kg/ha) VGI modeled *vs.* MAFF average inventory result. [10)] $DP_{MTT,VGI}$ - difference (%) VGI modeled *vs.* MTT Official Variety Trial result (100%) [11)] $DY_{MTT,VGI}$ - difference (kg/ha) VGI modeled *vs.* MTT Official Variety Trial result. [12)] $DP_{MAFF,NOAA}$ - difference (%) modeled (CropWatN) *vs.* MAFF average inventory result (100%), model CropWatN with GEMI LAI-bridge, NOAA data [29] [13)] $DP_{MAFF,Spot}$ - difference (%) modeled (CropWatN) *vs.* MAFF average inventory result (100%), model CropWatN with GEMI LAI-bridge, Spot data [29] [ue)] - underestimated by the corresponding model *vs.* observed [oe)] - overestimated by the corresponding model *vs.* observed.

Table 6 (Category IV) illustrates the ASAR/SAR and NDVI Composite Model (VI, Table 1, [37]) validation results from the MAFF Etelä-Pohjanmaa Agricultural Advisory Centre (Table 2, [29]). The SAR and NDVI modeling results, using phenologically classified backscattering data from the Envisat, ERS and Radarsat ASAR/SAR sensors with different polarization levels (HH, VV, VH, HV), depict detailed *soil*canopy* interactions between cereal canopies and soil top cover (5–10 cm) with fine and coarse sand soil *textures*. The ASAR/SAR and NDVI *composite model* validation results take into account both the *pre-anthesis* a_p and b_p phenological phases using the NDVI component and *post-anthesis and senescence* phases (c_p and d_p) using the SAR component with HH and VV levels. The Model VI *soil*species validation* results using MAFF validation data, indicated with spring wheat an overestimation (DP_{MAFF}, %) between +104% (Envisat) and 107% (Radarsat) from the observed MAFF inventory reference (100% [29]). With oat cereals, the underestimation was between 85% (Envisat) and 88% (ERS2). Respectively with barley between 97% (Envisat) and 112% (ERS) and more precisely with malt barley 96% underestimation (Radarsat) *vs.* fodder barley 102%. Respectively, the yield difference calculated as kg/ha (DY_{MAFF}) ranged between 177 kg/ha (swh, Envisat ASAR) and 484 kg/ha (Oats, Envisat ASAR).

The VGI *validation results* (Table 6, Categories I–IV) with spring cereals indicate, that in general the average baseline yield (y_b) estimates tend to stabilize between the observed non-potential yield levels and potential maximum *yielding capacity* levels at non limiting environmental factors (e.g., vegetation water stress, nutrient deficiencies). Results suggest that *optical* VGI models tend to overestimate the baseline yield levels (modeled/observed ratio, $DP_{MAFF,VGI}$) ranging between 101 (oats) and 125 (barley) percent *vs.* annual MAFF *non-potential* yield inventory estimations (ref. 100%). The optical VGI mean baseline yield response (y_b) for spring wheat was 4,240 kg/ha (Zone I: 4,218, III–IV: 3,768), for barley 4,394 kg/ha (Zone I: 4,428, III–IV: 4,470) and for oats 3,488 kg/ha (Zone I: 3,488, III–IV: 3,462). Respectively the mean ASAR/SAR and NDVI composite model (VI) baseline yield (**y_b**, kg/ha) was 4,170 kg/ha for wheat, 3848 kg/ha for barley (3,909 for malting barley and 3,899 kg/ha for fodder barley) and 3,386 kg/ha for oats [37].

Figure 10(A–D) illustrates the combined validation results for spring cereals using VGI models and for CropWatN crop model on clay, coarse and organic soil types in growing zones I–IV [29]. In addition, the corresponding observed MAFF stratum sampling estimates from the farm level and the averaged MTT Agrifood Official Variety Trial results during the 1990–1997 period are plotted.

With spring wheat (VGI Model II/NDVI, 1.3, Table 12), the simulated yield was 4,218 kg/ha (R^2 0.729) in Zone I–II and correspondingly in Zone III–IV 3,768 kg/ha (R^2 0.742, Figure 10(A)). The simulated CropWatN/Spot yield for wheat was 4609 kg/ha and CropWatN/NOAA 4605 kg/ha in Zones (III–IV) [29]. Corresponding averaged MAFF estimate for wheat was 3,556 kg/ha and MTT trial result 4,522 kg/ha in Zones (III–IV).

With barley (VGI Model II/NDVI, 2.2, Table 12), the simulated yield was 4,428 kg/ha in Zone I–II (R^2 0.609) and in Zone III–IV 4470 kg/ha (R^2 0.615, Figure 10(B)). The simulated CropWatN/Spot yield for barley was 3,984 kg/ha and CropWatN/NOAA 4,022 kg/ha in Zones (III–IV) [29]. Corresponding averaged MAFF estimate for barley was 3,430 kg/ha and MTT trial result 4,250 kg/ha in Zones (III–IV).

With oat (VGI Model I, 2.5, Table 12), the simulated yield was 3488 kg/ha in Zone I–II (R^2 0.762) and in Zone III–IV 3460 kg/ha (R^2 0.748, Figure 10(C)). The simulated CropWatN/Spot yield for oats was 3,752 kg/ha and CropWatN/NOAA 3,811 kg/ha in Zones (III–IV) [29]. Corresponding averaged MAFF estimate for oats was 3,370 kg/ha and MTT trial result 4,910 kg/ha in Zones (III–IV).

Figure 10(D) depicts the simulated CropWatN/CGMSF model spring cereal yield levels *vs.* MAFF Information Centre (IC) averaged statistics in the 1990–1997 period in Zones I–IV (R^2 0.740, RMSE 391 kg/ha, [29]).

Figure 10. Validation results for spring cereal VGI models using NDVI VGI models in growing zones I–IV. (© Original data Finnish Geodetic Institute,[29]).

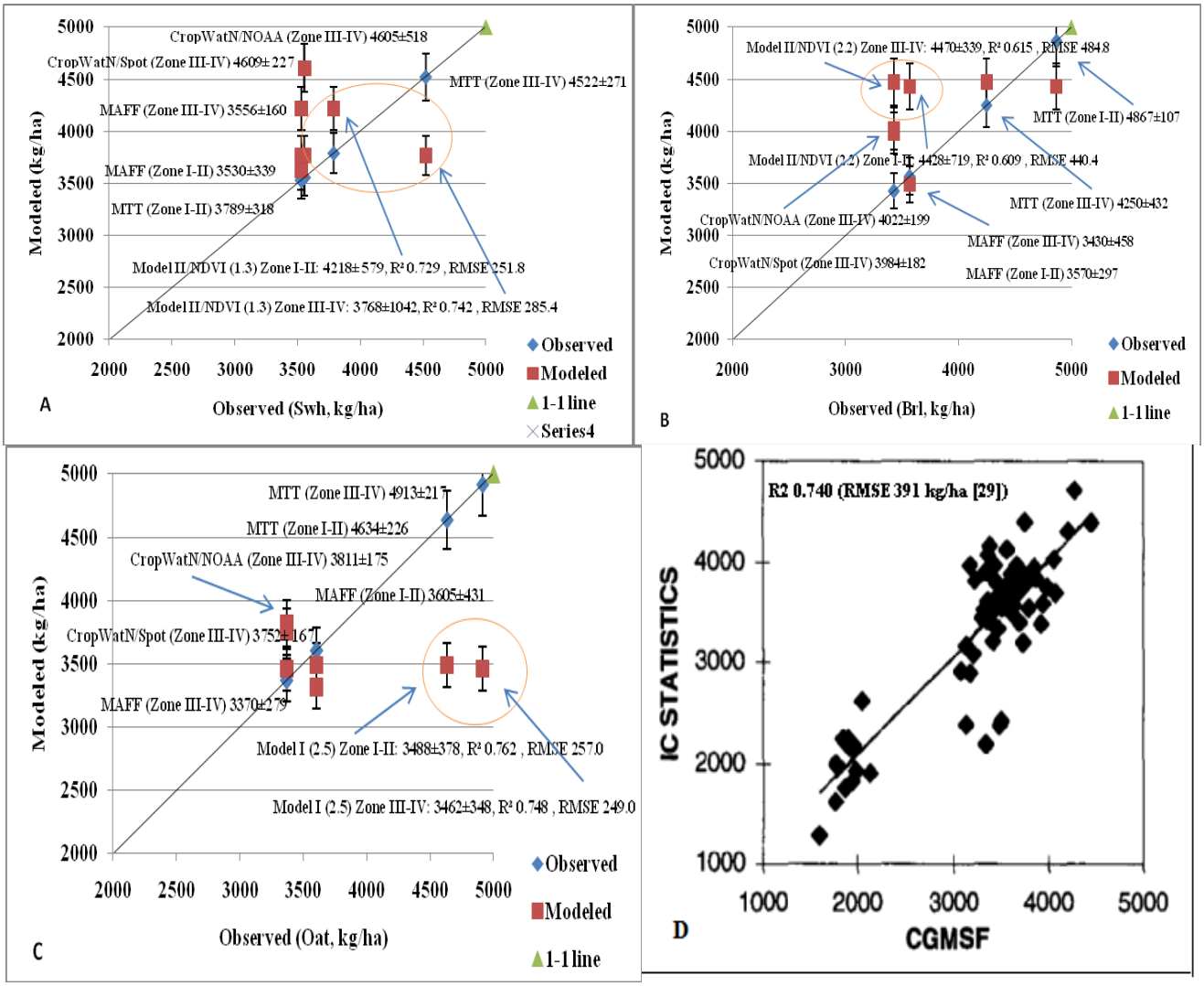

3.3.2. Time Series Validation Analysis for Baseline Yield Levels (y_b)

Figure 11 displays simulated spring cereal yield trends (y_b, kg/ha) in the 1990–1997 period modeled with different VGI models for spring wheat and barley (Model II/NDVI, Table 12, **Appendix B**) and for oats (Model I) in growing zones I–IV. Simulation time series input data were extracted from Spot and Landsat optical *minimum datasets* measured in the experimental locations (Me: Mellilä, Po: Porvoo, Kn: Kirkkonummi, Lp: Lapua, Ku: Kuuma, Jk: Jokioinen, Figure 2(d)). In addition, simulated

CropWatN crop model estimates [29] and MAFF stratum sampling estimates from the sampling farms in Zone I, II and in the averaged Zone III/IV (Figure 11(A–I)) are displayed. In general, the CropWatN model simulated yield levels were below the MAFF estimates in Zones I–IV [29].

In Zone I (Uusimaa Agric. Advisory Centre, Figure 11(A–C)) the VGI simulated spring wheat baseline yield levels (y_b) were below the MAFF stratum sampling levels in 1990 but above in 1994, with barley above MAFF estimates in 1990 but below in 1994 and with oats below MAFF estimates both in 1990 and 1994.

In Zone II (Häme Agric. Advisory Centre, Figure 11(D–F)) the VGI simulated wheat, barley and oat baseline yield levels (y_b) were above the MAFF levels in 1994 and 1995.

In the averaged Zone III/IV (Pohjanmaa Agric. Advisory Centre, Figure 11(G–I)) the VGI wheat and oat baseline yield levels (y_b) were below the MAFF level but above with barley in 1996.

Figure 11. Simulated baseline (y_b, kg/ha) and observed spring cereal yields in the 1990-1997 period in Zone I (Uusimaa Agric. Advisory Centre), Zone II (Häme Agric. Advisory Centre), Zone III/IV (Pohjanmaa Agric. Advisory Centre, © Original data Finnish Geodetic Institute [29]).

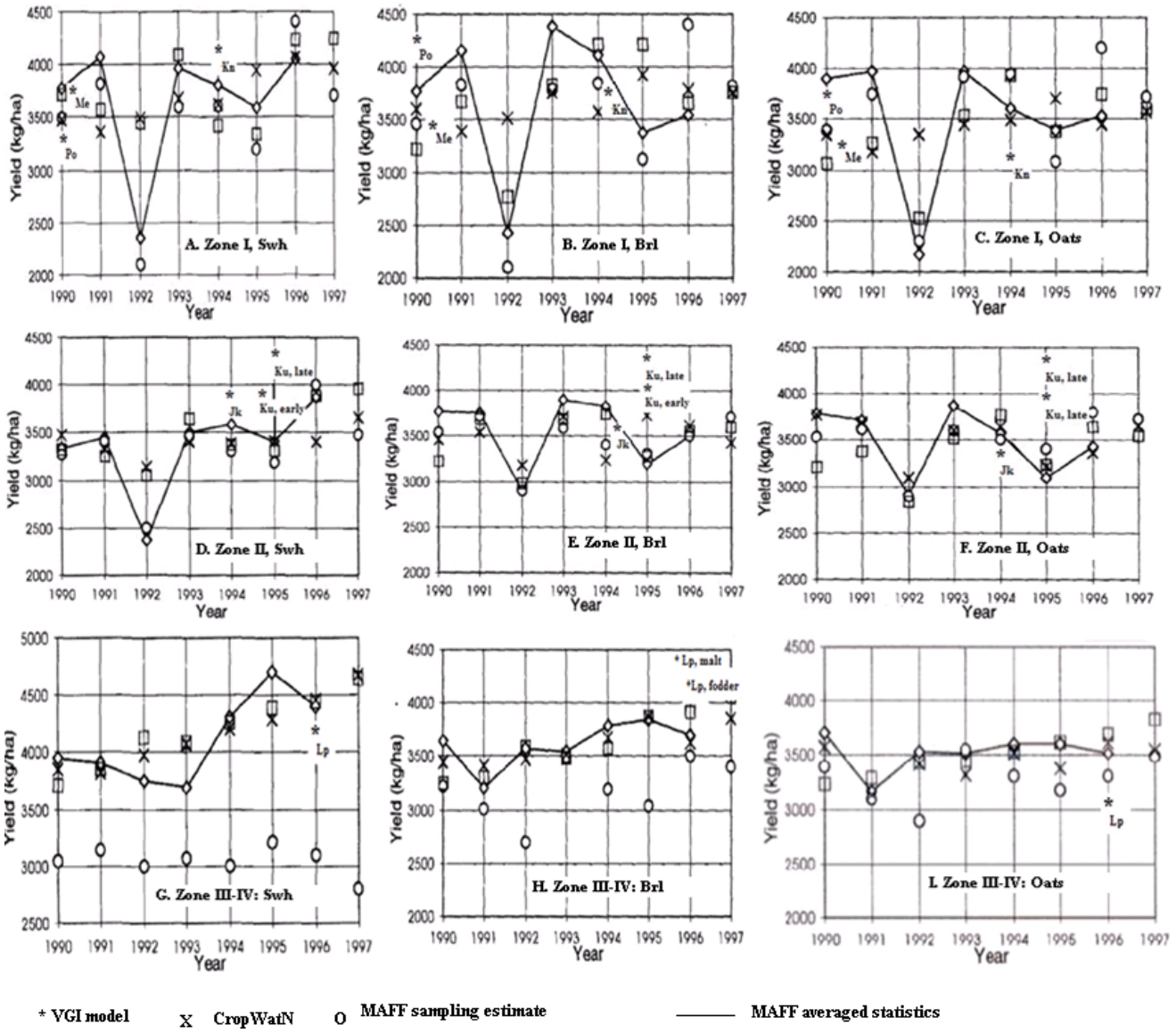

When comparing the averaged optical *VGI validation results* in *growing zones* I-IV (Category II, Table 6), the modeled yield estimates were between MAFF sub-optimal inventory statistics (DP_{MAFF}) derived from actual field conditions and MTT variety trial results ($DP_{MTT,VGI}$) grown on experimental fields with more *optimal* growing conditions. This baseline yield trend (y_b, kg/ha) is outlined in simulation results illustrated in Figure 11 with time series analysis using 1990–1997 optical minimum datasets.

When combining validation and time series analysis results (Table 6, Figure 11), in growing zone I (Jokioinen and Kirkkonummi), the overestimation (*oe*) was 124% for barley and underestimation (*ue*) 96% for oats *vs.* MAFF inventory statistics (Nylands Svenska Agric. Advisory Centre). Respectively the overestimation was 112% for wheat and underestimation (75%) for oats *vs.* MTT Official Variety Trial results (Pernaja and Inkoo MTT Experimental Stations).

In growing zones III–IV in Lapua (Table 5, category II) the overestimation was 130% for barley and 102% for oats *vs.* MAFF inventory statistics (Etelä-Pohjanmaa Agric. Advisory Centre). Respectively the overestimation was 105% for barley and 70% for oats *vs.* MTT Official Variety Trial results in Ylistaro (Zone III) and Ruukki (Zone IV) MTT Experimental Stations.

When comparing CropWatN model *validation results* (Model V in Table 1, category II in Table 5) *vs.* MAFF Inventory mean estimates, the $DP_{MAFF,NOAA}$ difference ratio (%) calculated as modeled (CropWatN) *vs.* MAFF average inventory reference (100%) varied between 93% (oats, growing zones I–II) and 146% (wheat, zone III–IV) using NOAA/AVHRR data. With Spot/HRV_2 data, the difference ratio ($DP_{MAFF,Spot}$) varied between 110% (oats, zone III–IV) and 146% (wheat, zone III–IV). LAI-bridge linked CropWatN average yield levels were 4,754 kg/ha for spring wheat, 4,192 kg/ha for barley and 4,992 kg/ha for oats in growing zones I–IV [29]. The average R^2 was 0.57 (RMSE 561 kg/ha) for spring cereals with NOAA/AVHRR data and 0.85 (RMSE 310 kg/ha) with Spot data. The VGI modeled baseline yield levels (y_b, kg/ha) varied between 3,315 (oats, zone I–II) and 4,609 kg/ha (wheat, zone III–IV).

When comparing averaged optical VGI baseline yield level estimates (y_b) *vs.* CropWatN dynamic crop model results using Spot/HRV_2 data in growing zones III–IV in the Pohjanmaa Agricultural Advisory Centre, the comparison *Difference Ratio* (%) ($DR_{MAFF,VGI}/DR_{MAFF,CropWatN,Spot}$) indicated a slightly higher accuracy with VGI models for oat and spring wheat cultivars. With malting and fodder barley cultivars the CropWatN results indicated a higher accuracy. The averaged MAFF inventory grain yield data were used as a reference (100%). The $DR_{MAFF,VGI}/DR_{MAFF,CropWatN,Spot}$ ratio was 106/14 for spring wheat,130/119 for malting and fodder barley and 103/110 for oats in growing zones III–IV mainly on clay type soils (Table 5, Category II).

Correspondingly, in growing zones I–II (Nylands Svenska and Häme Agric. Advisory Centres) on sandy and clay type soils the comparison *Difference Ratio* ($DR_{MAFF,VGI}/DR_{MAFF,CropWatN,NOAA}$,%) indicated underestimation (91%) with CropWatN using NOAA data and overestimation (124%) with VGI models. With oat cultivars both models ($DR_{MAFF,VGI}/DR_{MAFF,CropWatN,NOAA}$) underestimated yield levels (97/93%). In growing zones I–II the comparison ratio was 120/115 for spring wheat, 124/91 for malting and fodder barley and 97/93 for oats. On clay type soils in zones III–IV both models overestimated yield levels, the DR ratio was 106/146 for spring wheat, 130/120 for barley and 103/112 for oats.

4. Discussion

4.1. Implications from the Optical Infrared Reflectance Data for Baseline Yield (y_b) Estimations

The optical reflectance is a combination of *reflected, transmitted* and *absorbed* radiant fluxes from cereal canopies and soil cover varying during growing season. During cereal germination and emergence in spring time, optical vegetation indices are low in May (a_p phenology class, BBCH 0–12) countries with only partly covered soil surfaces (LAI < 1). In June (b_p, BBCH 12–50, LAI > 1**)** and July (c_p BBCH 50–90, LAI > 3**)** the cereal vegetation indices are higher due to increased photosynthetic activity with maximum LAI values usually observed in June [41]. The PAR_{ND} Index (Model IV) is similar to JRC-FAPAR algorithm (Fraction of Absorbed Photosynthetically Active Radiation [68]). Green vegetation with completely closed canopies (LAI > 1) strongly absorbs solar radiation in the red spectral region (ρ_{RED}) and, respectively, emits and scatters in near-infrared (ρ_{NIR}). The reflectance in the blue band is sensitive to the optical thickness of aerosols in the atmosphere. The blue band has been applied in the JRC-FAPAR algorithm to decontaminate the red and the near-infrared bands from atmospheric effects [56-59]. The JRC-FAPAR algorithm simulates with Radiative Transfer Models (RT, [55]) bidirectional radiant fluxes both inside the vegetation canopy and in the soil beneath.

When interpreting the optical *Infrared* (I) and *NDVI* (II) modeling results for spring cereals in this study, a significant change in NDVI, GEMI, PAR_{ND}/FAPAR values was observed between May (phenological class a_p) and June (b_p) with maximum peaks. Correspondingly in July (c_p) the values were reduced from those in June. In this study, the VGI model I (Table 1) independent variable, *infrared* reflectance in PAR/RED region (ρ_{RED}/Rf_3, λ = 630–690 nm for Landsat/TM and λ = 610–680 nm for SPOT/HRV2, Table 10), was low especially in June (b_p) coinciding with high photosynthetic and translocation activity (Figure 7). The low infrared reflectance values also indicated high *absorbance* of incoming radiation in cereal leaf chlorophyll A and B pigments in generative phase during heading and anthesis initialization. Respectively, the infrared reflectance ($\boldsymbol{\rho_{RED}}/Rf_3$) reached maximum values in July (c_p) and near-infrared reflectance ($\boldsymbol{\rho_{NIR}}/Rf_4$) in June ($b_p$). Previous crop physiological studies (Ledent [75], Reynolds *et al.* [76]) and in Finland Laurila [41] and Peltonen-Sainio *et al.* [77,78] have emphasized the role of cereal flag leaf and the 2nd uppermost leaf below the cereal head for final baseline (y_b) yield determination. According to Reynolds *et al*. [76] the flag leaf area through LAI and flag leaf dry-weight through *Harvest Index* (HI) were significant *yield component* factors, when setting the final yield levels for wheat ideotypes grown under actual non-potential field conditions. Yield components affected through photosynthetic capacity and translocation in SS-metabolism (*Source-Sink*) mechanism. Cereal *flag leaf* and the 2nd uppermost leaf below head contain Chlorophyll A with *absorption maximums* at 460 and 680 nm and Chlorophyll B at 480 and 650 nm, respectively (Figure 3, [79]).

The other independent variable in VGI model I (Table 1), the *near infrared* reflectance values (ρ_{NIR}/Rf_4, λ = 760–900 nm for Landsat/TM and λ = 790–890 nm for SPOT/HRV2/S_3, Table 10) were relatively high in June (b_p) between heading and anthesis near to LAI_{max} proximity compared with corresponding lower ρ_{NIR} / Rf_4 values in May (a_p) and July (c_p). According to Price [53], Maas [73], Flowers *et al.* [80] and Hadria *et al*. [81] the reflectance signal measured by the optical satellite sensors is a combined interacting signal reflected from both soil cover and vegetation canopies. The *soil/canopy*

reflectance ratio (SCR) similar to *Spectral Reflectance Indices* applied by Prasad *et al.* [26] for winter wheat grain yield estimations is varying along with spring cereal phenological development during growing season. In spring time before cereal sowing and emergence, the bare soil reflectance is prevailing in optical SCR reflectance ratio [53,73,80]. The SCR is reduced by germinating cereal tillers, which develop gradually into full canopy coverage and closure between heading and anthesis with maximum LAI exposure. With spring cereals the maximum LAI values are commonly observed between July and August in Finland corresponding to Phase III with SatPhenClass (c_p, BBCH 50–90) [42-44,47,49].

The VGI modeling results indicate, that during the *generative grain filling phase* (d_p-class, BBCH > 90) after the cereal *anthesis* the reflectance data from the infrared and near-infrared channels was *less significant* for the final yield prediction [47,49]. The leaf and other organs with high chlorophyll concentration begin to disintegrate. They become senescent as cereals translocate assimilates from source organs (e.g., flag leaf) to sinks (head) using SS-translocation mechanism [76].

4.2. Intersensory Calibration Results

Intersensory calibration results using *Phenological Spectral Signature Profile (SSP_{Ph}) Analysis* for cereals indicate that both the TM and HRV_2 sensors measured NDVI maximum values especially during the vegetative P_b phase with cereal maximum LAI exposure (LAI_{Max}). The *Spectral Signature Profile Analysis* suggests that the averaged NDVI values from both HRV_2 and TM sensors in the early P_a vegetative phase in May after germination and emergency had very low values ranging between 0.01 and 0.1 on all soil types. In the vegetative phase P_b during the maximum LAI, the NDVI increased on average on 0.60–0.80 level. The averaged NDVI was decreased on 0.4–0.50 level in generative phase P_c after anthesis and grain filling. In P_b phase, the maximum NDVI level of 0.80 was obtained using HRV_2 sensor with oat cultivars grown on organic soils and respectively in phase P_c the maximum level was 0.55 with TM sensor with oat cultivars grown on clay type soils.

*4.3. The soil*Species, Soil*Cultivar and Cultivar*Canopy Interactions*

*Soil*canopy* and soil*crop yield covariances including total *evapotranspiration*, canopy *transpiration* through stomatal cavity and *evaporation* from soil surfaces with remote sensing techniques have been reviewed by Kondratyev *et al.* [70], Ulaby [71] and Henderson and Lewis [72].

The optical reflectance and microwave backscattering measured by satellite sensors contain combined interacting signal reflected from soil cover and vegetation canopies, varying with spring cereal phenological development during growing season. In spring time before cereal sowing in May, the bare soil reflectance dominates the reflectance signal. Soil *reflectance fraction* is reduced by germinating cereal tillers developing gradually into full canopy coverage and closure between heading and anthesis with maximum LAI values [33,53,72,73].

Currently spring cereal sowing in southern Finland generally occurs in the beginning of May. In May most of the soil on spring cereal cultivations is still a mixture of bare soil combined with germinating and emerging spring cereals. Thus the soil component absorbance is high compared to combined reflectance and albedo.

The optical Infrared modeling results in southern Finland are especially affected by the *soil*canopy* interactions in the beginning of growing season (a_p, May, BBCH 0–12) when the soil is only partly covered with emerging spring cereal canopies. Because of this *infrared, near infrared* and also Landsat Thermal Infrared (λ = 10.4–12.5 μm) reflectance values are close to zero ranging between 0.010 and 0.020 on *species* and *cultivar* level.

The optical Infrared VGI *calibration* results in the soil $_{(clay)}$*species covariance category indicated that the *non-potential baseline yield* (y_b) response was 4,240 kg/ha for spring wheat with high R^2 (0.764) and 4,420 kg/ha for barley with low R^2 (0.166) on cultivars grown on clay type soils. In general, the results indicated a significantly better polynomial fit for spring wheat cultivars on clay type soils. The more detailed *soil*cultivar* covariance calibration for spring cereals with clay type soils indicated a low R^2 varying between 0.089 and 0.144.

The optical *covariance validation* results with non-potential VGI Infrared models indicated an underestimated yield difference between −8.2% and −9.5% in soil*species category and between −10.1 and −44.9% in soil*cultivar category. In both categories the Infrared models underestimated the spring wheat and barley yield levels compared with corresponding MTT Agrifood Official Variety trial yield levels grown on more optimal non-limiting growing conditions. On more detailed *soil*species* and *soil*cultivar* level the Infrared models underestimated the baseline yield levels compared with the corresponding observed MTT yield levels. Especially the spring wheat *cv.* Satu yield level on clay type soils was clearly underestimated (−44.9%). Respectively the yield difference calculated as kg/ha varied between −363 kg/ha (barley*clay) and −1,427 kg/ha (Satu*clay).

The *enzyme malting barley cv.* Pokko (breeder Hankkija Kasvinjalostus) with maximum yielding capacity had optical infrared reflectances below average in a_p b_p c_p phases (BBCH 0–90) indicating active photosynthesis in PAR-region and near-infrared reflectance above average in phase c_p (BBCH 50–90). In Finland, the minimum protein content of 10.5% for malting barley genotypes is generally required. Typically the protein content is controlled by nitrogen fertilization. The nitrogen requirement for *cv.* Pokko grown on clay type soils is 90 kg N/ha and 70–80 kg/ha on coarse type soils in growing zones I–IV [82]. Especially fodder and malting barley experimental plots with clay topsoil layer in Porvoo experimental area were affected by severe drought with low water table and water deficiency stress periods especially in generative phases (c_p, d_p). This affected the translocation of assimilates to cereal heads and a reduction in final grain filling.

The combined *cultivar*canopy* covariance results from both VGI optical modeling results (stages a_p–c_p) from this study and SAR backscattering analysis and VGI *Composite* modeling results (stages c_p–d_p [37]), indicate specific morphological differences in canopy structure between different spring cereal species. Oat cultivars with more *planophile* leaf and canopy structure (*i.e.*, leaves aligned perpendicular to the plane of incident light and PAR-radiation) and *panicle* inflorescence differ both in optical PAR spectrum and also with SAR polarization properties from those of wheat and barley with more *erectophile* head and canopy structures [6,72,83].

With *planophile* crops, flag leaf and upper canopy structure are more perpendicular to incoming PAR-radiation. The planophile canopy structure is affected by mutual shading attenuating lower canopy photosynthesis. Frantz *et al.* [83] reported significant changes in *Photosynthetic Photon Flux* (PPF) and in PAR radiation conditions especially in lower canopy layers with planophile species.

In this study, oat cultivars in June (b_p) had infrared reflectance (ρ_{RED} 0.031) above average and in July (c_p) near infrared reflectance (ρ_{NIR} 0.191) above average. Notably the *cv.* Veli oat reflectance data contained both maximum infrared (ρ_{RED} 0.058) and near-infrared reflectance values (ρ_{NIR} 0.282) in b_p phase in June indicating lower photosynthetic absorbance compared to wheat and barley cultivars. In general, oat cultivars yielded lower final grain yield levels under actual field conditions compared to wheat and barley cultivars (Table 3). In addition, the SAR modeling results with oat cultivars presented in a recent publication by Laurila *et al.* [37] indicated, that during later phenological stages especially after the anthesis (c_p) and grain filling and canopy senescence (d_p, BBCH > 90) the SAR VH cross-polarization (σ^0) amplitude was higher when compared with VV vertical levels both in anthesis (c_p) and full maturity (d_p) on clay and sandy type soils. Both the horizontal and vertical (HH, VV) signal amplitudes were higher in anthesis stage (c_p, BBCH 50–90) compared to full maturity stage (d_p).

4.4. The optimal VGI Modeling Results for Baseline Yield Estimations

The optical *VGI Composite modeling* results for spring cereals obtained from this study suggest that the best VGI models for both spring wheat and barley cultivars were NDVI based VGI models (Model II) using phenologically classified and harmonized Landsat/TM and SPOT/HRV_2 data. With spring wheat cultivars the Model II overall accuracy was 0.737 (R^2) for spring wheat cultivars (mean baseline yield y_b 4,240 kg/ha, RMSE 297 kg/ha) and for barley cultivars R^2 was 0.611 (mean y_b 4,390 kg/ha, RMSE 449 kg/ha) grown on different soil types in growing zones I–IV. With oat cultivars the best VGI model was the Polynomial Infrared VGI model (Model I, y_b 3,480 kg/ha, R^2 0.70, RMSE 258 kg/ha).

The *Time Series Validation Analysis* results for cereal yields indicated varying baseline yield levels between years with optimized VGI models when compared with annual MAFF stratum yield estimates in growing zones I–IV. The *Time Series Analysis* suggests using 1990–1997 optical validation data [29] from growing zones I–IV that the VGI simulated spring wheat baseline yield levels (y_b) in Zone I were below the MAFF stratum sampling levels in 1990 but above in 1994, with barley above MAFF estimates in 1990 but below in 1994 and with oats below MAFF estimate both in 1990 and 1994. In Zone II the VGI simulated wheat, barley and oat baseline yield levels (y_b) were above the MAFF levels in 1994 and 1995. In the averaged Zone III/IV the VGI wheat and oat baseline yield levels (y_b) were below the MAFF level but above with barley in 1996. In general, the CropWatN model simulated yield levels were below the MAFF estimates in Zones I–IV [29].

4.5. Validation of Optical VGI Composite Models vs. Dynamic Crop Models

The *VGI Composite modeling* results for spring cereals seem to be in line with previous optical and SAR measurement campaigns and modeling results for winter wheat and maize on EU scale. The mean R^2 was 0.630 when both optical and SAR [37] were integrated. The modeling results obtained in this study seem to be in accordance with EUROSTAT crop inventory statistics reported from Spain, France, Belgium, Italy, Poland and Germany [19,20,85].

Previous *optical crop modeling* results in Finland reported by Kuittinen *et al.* [29] and Karvonen *et al.* [31] indicated that the R^2 range varied between 0.57 and 0.78 for spring cereal yield estimations in southern Finland when optical SPOT/HRV2 and NOAA/AVHRR data were combined with CropWatN [31,84] and WOFOST [20] dynamic crop models.

More specifically, a cereal specific *LAI-bridge* (Figure1, Phase XI(c) scheme) using GEMI index (*Global Environment Monitoring Index* [55]) was established between optical reflectance data and dynamic crop models. LAI estimates $LAI_{(Satellite,\ Cereal)}$ using red and near infrared GEMI index were derived from SPOT and NOAA optical data in the Nylands Svenska, Häme and Etelä-Pohjanmaa Agricultural Advisory Centres in growing zones I–IV [29].

Crop specific LAI values $LAI_{(Optimal)}$ estimated by the LAI-bridge were used as input data for CropWatN [29,84] and WOFOST [20] dynamic crop models combined with CGMS GIS system (*Crop Growth Monitoring System* managed by JRC/IRSA [85]). The CropWatN dynamic crop model is analogous to CERES-Wheat [17,18], CROPSYST [25] and AFRCWHEAT2 [40] dynamic crop models. It uses cumulative ETS temperature sum as a *phenological driving variable* with cumulative biomass and yield integrations during growing season.

According to Kuittinen *et al.* [29] the mean R^2 and RMSE results using CropWatN model were in Etelä-Pohjanmaa (R^2 0.57, RMSE 561 kg/ha), Nylands Svenska (R^2 0.85, RMSE 310 kg/ha) Agriculture Advisory Centres when compared with the corresponding MAFF annual inventory statistics [62,74]. The CROPWATN modeled mean yield levels (y_b) combined with optical SPOT reflectance data were 4,754 kg/ha for spring wheat, 4,192 kg/ha for barley and 4,992 kg/ha for oats [29].

Correspondingly the VGI modeling results, obtained in this study, indicated that the mean *non-potential baseline yield level* (y_b) were 3,960 kg/ha for spring cereals (R^2 0.63, RMSE 360 kg/ha) averaged over the years and locations in growing zones I–IV.

4.6. Validation of optical VGI models vs. Composite ASAR/SAR and NDVI models

The optical VGI model *vs.* ASAR/SAR and NDVI Composite Model (VI) validation results in the Etelä-Pohjanmaa Agricultural Advisory Centre indicated varying results between the modeled *vs.* observed MAFF inventory statistics. The Composite model (VI) validation results indicated that the R^2 accuracy tends to stabilize on the 60–70% level similar to optical VGI models (I–II).

The *Composite Multispectral models* combined with the SatPhenClass phenological classification algorithm for spring cereals provides a promising integrating technique for combining both microwave SAR/ASAR and optical reflectance data. The Composite Multispectral model takes into account both the pre-anthesis phenological phases (a_p, b_p) using the NDVI component and post-anthesis and senescence phases (c_p, d_p) using the SAR component with backscattering polarization levels. In addition, the Composite multispectral model can be used in assessing the *soil*canopy* covariances between cereal canopies and soil top layers on different soil types [37].

With ENVISAT/ASAR sensory data, the Model VI overestimated the MAFF averaged stratum estimate for spring wheat and feed barley, but underestimated it for malting barley and oats in Zones III-IV. Respectively the Model VI overestimated the SAR/Radarsat and SAR/ERS spring wheat and oat averaged yield levels, but overestimated SAR/ERS barley yield levels when compared with the MAFF averaged inventory estimates.

The ASAR/SAR and NDVI composite model VI mean yield accuracy was 0.61 (R^2) and RMSE 402 kg/ha using both phenologically classified reflectance and backscattering data. However with Envisat and Radarsat composite models, the inclusion of ASAR/SAR in conjunction with the NDVI component increased the overall accuracy from 60% to 70% level.

The Composite model (VI) validation results indicated that the use of the Envisat ASAR additional cross-polarization component (VH) did not increase the R^2 level compared to ERS (VV) and Radarsat (HH) with only one polarization level in the 5.3 GHz measurement spectrum.

The mean ASAR/SAR and NDVI model baseline yield (y_b**,** kg/ha) was 4,170 kg/ha for spring wheat, 3,848 kg/ha for barley (3,909 for malting barley and 3,899 kg/ha for fodder barley) and 3,386 kg/ha for oats [37].

The NDVI optical model II overall accuracy with spring wheat yield was 0.73 using R^2 (RMSE 297 kg/ha) and with barley (R^2 0.61, RMSE 449 kg/ha). Respectively with the Composite ASAR/Envisat and NDVI model VI, the overall accuracy with spring wheat yield was 0.72 (RMSE 302 kg/ha) and with barley (R^2 0.69, RMSE 349 kg/ha) and with oats (R^2 0.62, RMSE 389 kg/ha). With the Composite SAR/Radarsat and NDVI model, the overall accuracy with spring wheat yield was 0.73 (RMSE 300 kg/ha) and with barley (R^2 0.70, RMSE 322 kg/ha) and with oats (R^2 0.62, RMSE 483 kg/ha).

Contrary to Envisat and Radarsat model estimates, the ERS yield accuracy was significantly lower, with the Composite SAR/ERS and NDVI model, the overall accuracy with barley yield was R^2 0.45 (RMSE 480 kg/ha) and with oats (R^2 0.42, RMSE 584 kg/ha). This lower accuracy with ERS model can be partly explained by the missing horizontal (HH, available in Envisat and Radarsat) and cross-polarization components (VH, only in Envisat). The ERS model (VI) contains only the vertical (VV) polarization component in conjunction with the optical NDVI component modeling the spring cereal yield in different phenological phases (a_p, b_p, c_p).

In summary, the Envisat and Radarsat validation results suggest the inclusion of the horizontal polarization component (HH) in the SAR/ASAR composite models, thus increasing the overall accuracy of the composite VGI models. The VH cross-polarization component, available only in the Envisat data, did not significantly increase the Model VI overall accuracy. The oat canopy and head morphological structures differ from those of wheat and barley potentially changing the backscattering polarization properties [37].

4.7. Synthesis for cereal baseline grain yield estimation using VGI models and Minimum Datasets

The recent SAR modeling results by Laurila *et al.* [37] for Finnish growing conditions and optical VGI modeling results obtained from this study for cereal baseline yields (y_b) indicate that the R^2 tends to stabilize on the 0.60–0.70 level in southern Finland (growing zones I–IV). The VGI modeling results indicate that the average R^2 for yield (kg/ha) varied significantly during growing season. The overall R^2 average for spring sown cereals in growing zones I–IV in Southern Finland was 0.63. Results indicate that with relatively few observations ($n < 500$) the R^2 tends to increase above 0.80, whereas with larger datasets ($n > 1{,}000$) the R^2 stabilizes between 0.50-0.60. One possible explanation to this extensive R^2 variance lies in the algorithm itself, with large datasets, the *Least-Square* Estimation-algorithm (LSE) applied in linear and non-linear regression models is unable to fit all the variables into a linear or polynomial model. In addition, when simulating spring cereal non-potential yield levels, soil component with different soil types, affects significantly on final grain yield level.

The Vegetation Indices models using solely *Minimum datasets* using only optical and SAR data lack the *plasticity* of dynamic crop models, which can adapt to adverse climatic conditions by using extensive

ground truth agrometeorological and crop phenological data [29,31]. However, the *SatPhenClass* submodel, combined with VGI models and using dynamic ETS and LAI classifiers, increases the *adaptability* of VGI models during cereal phenological development both in vegetative phase before anthesis and also in generative phase during the head ripening stage. In northern latitudes the cloudiness and rain during the growing season seriously reduce the applicability of optical Landsat and SPOT satellite data. Based on Finnish field experiment results it should be possible to obtain two or three cloud-free optical satellite images during growing season in southern Finland. It was known *a priori* that the probability of obtaining a cloud-free image in Finland in June is *ca.* 50%, the corresponding probability in southern France lies between 15 and 31% [29,30]. Previous studies have critically reviewed problems with atmospheric modeling and radiometric correction of satellite signal, especially the complicated correction of reflectance signal interacting with atmospheric aerosols and clouds has been reviewed by Kondratyev *et al.* [70].

On other hand, remote sensing satellites provide a well calibrated multitemporal and multispatial data source for crop monitoring and input data for yield estimation models. In addition, new microwave based satellite systems can map images through cloud coverage and during the night-time. Scurlock and Prince [79] suggested that in order to obtain statistically significant yield estimations one should concentrate on obtaining cloud free optical satellite images especially in the beginning of growing season during the vegetative growth. Dynamic crop models would improve the accuracy of final yield estimations specifically in generative grain filling phase after the cereal anthesis.

4.8. Rationale and Implications for the Finnish CAP Policy

Recently McNairn *et al.* [7] applied *multispectral Decision Tree and Neural Network classification techniques* with integration of SAR and optical satellite data for Canadian crop inventory monitoring. In Canadian growing conditions *Decision Tree Classifier (DTC)* with composite optical and dual polarization mode SAR (VV–VH) data produced highest classification accuracy over 85% overall accuracy (Kappa κ 0.47–0.89) for wheat, maize and soybean. In comparison, the SatPhenClass phenological classification results for Finnish spring cereals, indicated a general classification accuracy exceeding 74% in different vegetative phenological (a_p, b_p) and generative classes (c_p, d_p). The Canadian growing conditions with latitudal variation between 45 °N and 60 °N resemble those of Scandinavia and southern Finland. However, in Finland, the applicability of multispectral classifying techniques for different crops is less relevant, since MAFF as part of the Pan-European effort and EU regulated CAP policy (*Common Agricultural Policy*) has established a national Finnish Land Parcel Identification System (FLPIS [34]) with digitized parcel boundaries. The FLPIS system is incorporated with the Integrated Administration and Control System (*IACS*). The IACS system controls the payments of cultivation area based agricultural subsidies for Finnish farmers. The USDA ground based stratum sampling methodology [8] is currently applied in Finland in the annual crop inventory sampling. MAFF and the Finnish Rural Development Centres perform annual crop yield inventory sampling. Inventory program is based on farm level interviews three times every growing season in June, July for *intermediate* yield estimates and in August for the *final* yield level estimations after the harvest [62,74].

According to recent MAFF official inventory statistics [74] for spring cereals the averaged 2006–2007 Finnish total cultivation area (ha), the total grain yield production (Mkg) and average yield

levels (kg/ha) were 172,000 ha, 684 Mkg, 3,560 kg/ha for spring wheat, 563,000 ha, 1,972 Mkg, 3,500 kg/ha for barley containing both *malt* (129,800, 515, 3,970) and *feed* barley (403,500, 1,469, 3,640) and for oats 352,000, 1,082 Mkg, 2,920 kg/ha, respectively.

The calibrated VGI models, using phenologically pre-classified satellite data and applied in this study, would significantly reduce the operating costs and time compared to traditional ground based crop inventory and monitoring systems applied currently in Finland.

The optical *VGI Composite modeling* results for spring cereals obtained from this study suggest that the best VGI models for both spring wheat, barley and oat cultivars were NDVI and Polynomial Infrared based VGI models. With spring wheat cultivars the VGI Model overall accuracy R^2 was 0.737 (mean baseline yield y_b 4,240 kg/ha, RMSE 297 kg/ha), for barley cultivars (y_b 4,390 kg/ha, R^2 0.611, RMSE 449 kg/ha), and for oat cultivars (y_b 3,480 kg/ha, R^2 0.70, RMSE 258 kg/ha) grown on different soil types in growing zones I–IV.

The calibrated *optical* VGI models using Optical Minimum Datasets in cereal vegetative growth phase (a_p and b_p) before anthesis and grain filling could be applied as a supplementary method for farm level sampling interviews in June and July in the annual MAFF cereal yield inventory estimations. Optical VGI models could be also applied in cultivation areas where extensive crop phenological and agrometeorological data is missing during vegetative growth, if traditional dynamic crop models are applied in crop inventory programs [29].

The calibrated optical VGI models evaluated in this study and *composite multispectral ASAR/SAR VGI models*, reviewed by Laurila *et al.* [37], using SAR and NDVI Minimum datasets, could be applied especially in cereal generative phase (c_p, d_p) as a supplementary method for estimating inventory final yield levels in August. The Composite Multispectral VGI model takes into account both the pre-anthesis phenological phases using the NDVI component and post-anthesis and senescence phases using the SAR component [72].

The optical VGI models evaluated in this study resemble *Rapid Monitoring Estimates* (RME) applied by EU MARS program [12,13,85] for crop inventory programs on EU scale and also simple regression based predictive models with *trend functions* for weather and nitrogen input effects applied by Supit [23] and Supit and van der Goot [24]. According to Supit [23] the optimum prediction accuracy for wheat yield levels may be obtained by first modeling regional wheat levels, e.g., on Agriculture Advisory Centre level and subsequently upscaling and *consolidating* yield estimates on national level.

The validated VGI models obtained in this study could also be applied for cereal yield consolidation estimations on Finnish national level, when the total cultivation area for spring cereals is available from the MAFF FLPIS/IACS Administration and Control System [34].

5. Conclusions

The *optical* VGI modelling results obtained from this study, indicate that the overall R^2 accuracy tends to stabilize on the 60%–70% level with different spring cereal *baseline yield* predictions. The accuracy level is similar to results obtained from the previous SAR/ASAR and NDVI composite modelling results in southern Finland and also with the results obtained on large area crop inventory estimations on the EU scale. The validation results indicated with the best optimized VGI models, that especially the combined

inclusion of NDVI and SAR/ASAR components with different polarization levels in the VGI models yielded highest baseline yield accuracy for the spring cereals over the years, different soil types and varying climatic growing conditions. Especially the NDVI component supported the cereal vegetative development estimation during maximum LAI exposure before anthesis and SAR/ASAR component supported yield accumulation, grain filling and senescence estimation during generative phase.

Optical VGI models, validated in this study and combined with *phenologically classified* satellite data would significantly reduce the operational costs and time required compared to traditional ground based crop inventory surveys. Alternatively, optical VGI models using Minimum Datasets could be applied as a supplementary method for dynamic crops models in the MAFF crop yield inventory estimations in areas where extensive crop phenological and agrometeorological data required by the dynamic crop models is missing.

In conclusion, both methodology approaches could be applied as a *yield inventory tool* supporting the annual crop inventory program and Finnish IACS/FLPIS system. In addition, these new inventory tools could also be applied for the construction of EU scale *Agricultural Information System* (AIS) integrating all national AIS Systems.

Acknowledgements

We wish to express our sincere gratitude to the following persons: Director General, Risto Kuittinen (satellite data, general management), Eero Ahokas (calibration of datasets, GIS and coordinate systems, satellite data calibration) from The Finnish Geodetic Institute contributed significantly to this publication during the field experiments, modeling work and preparation of the manuscript. Also the support of Pirjo Mäkelä (University of Helsinki), Timo Mela and Pirjo Peltonen-Sainio, Kaija Hakala, Riitta Saarikko, Markku Kontturi, Olli Rantanen (MTT Agrifood Research of Finland) is gratefully acknowledged for their advises and support during the field experiments, modeling work and preparation of the manuscript. This project was funded by the Finnish National Board of Agriculture from the Maatilatalouden kehittämisrahasto fund and by the European Union AO (Announce of Opportunity) contract AOE-488 for ENVISAT.

References and Notes

1. Brown, S.C.M.; Quegan, S.; Morrison, K.; Bennett, J.C.; Cookmartin, G. High-resolution measurements of scattering in wheat canopies-Implications for crop parameter retrieval. *IEEE Trans. Geosci. Remote Sens*. **2003**, *41*, 1602-1610.
2. Henning, S.; Svendsen, M.; Thomsen, A. Multitemporal C- and L-band polarimetric signatures of crops. *IEEE Trans. Geosci. Remote Sens.* **1999**, *37*, 2413-2429.
3. Maas, S.; Dunlap, J. Reflectance, transmittance and absorptance of light by normal, etiolated, and albino corn leaves. *Agron. J.* **1989**, *81*, 11-19.
4. Kondratyev, K.; Kozoderov, V.; Fedchenko, P. Remote sensing of the state of crops and soils. *Int. J. Remote Sens*. **1986**, *7*, 10-22.
5. Shibayama, M.; Akiyama, T. Seasonal visible, near-infrared and mid-infrared spectra of rice canopies (*Oryza sativa* L.) in relation to LAI and above-ground dry phytomass. *Remote Sens. Environ.* **1989**, *27*, 119-127.

6. Le Toan, T.; Ribbes, F.; Wang, L.; Floury, N.; Ding, K.; Kong, J.A.; Fujita, M.; Kurosu, T. Rice crop mapping and monitoring using ERS-1 data based on experiment and modeling results. *IEEE Trans. Geosci. Remote Sens*. **1997**, *35*, 41-56.
7. McNairn, H.; Champagnea, C.; Shanga, J.; Holmstromb, D.; Reichert, G. Integration of optical and Synthetic Aperture Radar (SAR) imagery for delivering operational annual crop inventories. *ISPRS J. Photogramm. Remote Sens.* **2008**, *64*, 434-449.
8. *Lanworth Agriculture Satellite Imagery and Modeling*; Lanworth: Itasca, IL, USA, 2009. Available online: http://www.lanworth.com/agriculture/ (accessed on 12 February 2009).
9. Paynter, B. Feeding the masses: Data in, crop predictions out. *Wired Magazine* 16 July 2008.
10. *Directorate General for Agriculture of EU Website*; DGA: Brussel, Belgium, 2009. Available online: http://ec.europa.eu/dgs/agriculture/index_en.htm (accessed on 14 September 2009).
11. *EUROSTAT*; EUROSTAT : Luxembourg, Luxembourg, 2009. Available online: http://epp.eurostat.ec.europa.eu/portal/page/portal/eurostat/home/ (accessed on 14 September 2009).
12. *Monitoring Agriculture with Remote Sensing (MARS)*; MARS: Ispra, Italy, 2008. Available online: http://mars.jrc.it (accessed on 19 August 2008).
13. Meyer-Roux, J. Crop yield forecasting methods. In *Proceedings of the EUROSTAT Seminar*, Villefranche-Sur-Mer, France, 1994; pp. 24-27.
14. Narciso, G.; Ragmo, P.; Venturi, A. *Agrometeorological Aspects of Crops in Italy, Spain and Greece. A Summary Review for Common and Durum Wheat, Barley, Maize, Rice, Sugar Beet, Sunflower, Soya Bean, Rape, Potato, Tobacco, Cotton, Olive and Grape Crops. An Agricultural Information System for the European Community*; Joint Research Centre Publication (EUR-14124-EN): Brussel, Belgium, 1992.
15. Hough, M. *Agrometeorological Aspects of Crops in the UK and Ireland. A Review for Sugar Beet, Oilseed Rape, Peas, Wheat, Barley, Oats, Potatoes, Apples and Pears. An Agricultural Information System for the European Community*; Joint Research Centre Publication (EUR-13039-EN): Brussel, Belgium, 1990.
16. Dente, L.; Satalino, G.; Francesco, M.; Rinaldi, M. Assimilation of leaf area index derived from ASAR and MERIS data into CERES-Wheat model to map wheat yield. *Remote Sens. Environ*. **2008**, *112*, 1395-1407.
17. Jones, J.; Hoogenboomb, G.; Porter, C.; Boote, K.; Batchelorc, W.; Hunt, L.; Wilkense, P.; Singhe, P.; Gijsmana, A.; Ritchie, J. The DSSAT cropping system model. *Eur. J. Agron.* **2003**, *18*, 235-265.
18. Hodges, T. *Predicting Crop Phenology*; CRC Press: London, UK, 1991.
19. de Wit, A.J.W.; van Diepen, C.A. Crop model data assimilation with the Ensemble Kalman filter for improving regional crop yield forecasts. *Agric. Forest Meteorol.* **2007**, *146*, 38-56.
20. Supit, I.; Hooijer, A.; van Diepen, C. *System Description of the Wofost Crop Simulation Model Implemented in CGMS. Volume I: Theory and Algorithms*; SC-DLO: Wageningen, The Netherlands, 1994.
21. Kalman, R.E. A new approach to linear filtering and prediction problems. *Trans. ASME. J. Basic Eng.* **1960**, *82*, 35-45.

22. de Wit, A.J.W.; van Diepen, C.A. Crop growth modelling and crop yield forecasting using satellite-derived meteorological inputs. Modern methods in crop yield forecasting and crop area estimation. *Int. J. Appl. Earth Obs. Geoinf.* **2008**, *10*, 414-425.
23. Supit, I. Predicting national wheat yields using a crop simulation and trend models. *Agric. Forest Meteorol.* **1997**, *88*, 199-214.
24. Supit, I.; van der Goot, E. National wheat yield prediction of France as affected by the prediction level. *Ecol. Model.* **1999**, *116*, 203-223.
25. Moriondo, M.; Masellib, F.; Bindi, M. A simple model of regional wheat yield based on NDVI data. *Eur. J. Agron.* **2007**, *26*, 266-274.
26. Prasad, B.; Carver, B.; Stone, M.; Babar, M.; Raun, W.; Klatt, A. Potential use of spectral reflectance indices as a selection tool for grain yield in winter wheat under great plains conditions. *Crop Sci.* **2007**, *47*, 1426-1440.
27. Mangiarotti, S.; Mazzegab, P.; Jarlana, L.; Mougina, E.; Baupa, F.; Demartye, J. Evolutionary bi-objective optimization of a semi-arid vegetation dynamics model with NDVI and σ^0 satellite data. *Remote Sens. Environ.* **2008**, *112*, 1365-1380.
28. Serrano, L.; Filella, I.; Peñuelas, J. Remote Sensing of biomass and yield of winter wheat under different nitrogen supplies. *Crop Sci.* **2000**, *40*, 723-731.
29. Kuittinen, R.; Ahokas, E.; Granqvist, M.; Ikäheimo, E.; Heikinheimo, M.; Venäläinen, A.; Jänne, S.; Keskisarja, V.; Parmes, E.; Perdiago, V.; van der Goot, E. *An Early Crop Yield Estimation for Finnish Conditions. The Crop Growth Monitoring System of the Joint Research Centre with and without Remotely Sensed and Other Additional Input Data*; Reports of the Finnish Geodetic Institute; Finnish Geodetic Institute: Masala, Finland, 1998.
30. Kuittinen, R. *Remote Sensing in Agriculture*; Reports of the Finnish Geodetic Institute; Finnish Geodetic Institute: Masala, Finland, 1996.
31. Karvonen, T.; Laurila, H.; Kleemola, J.; Varis, E. *Estimation of Agricultural Crop Production Using Satellite (Landsat and SPOT) Information*; Publication 26; Department of Plant Production, University of Helsinki: Helsinki, Finland, 1991.
32. Matikainen, L.; Karjalainen, M.; Kuittinen, R. *SAR Images and Ancillary Data in Crop Species Interpretation*; Reports of the Finnish Geodetic Institute 98:1; Finnish Geodetic Institute: Masala, Finland, 1998.
33. Karjalainen, M.; Kaartinen, H.; Hyyppä J. Agricultural monitoring using Envisat alternating polarization SAR images. *Photogramm. Eng. Remote Sens*. **2008**, *74*, 117-126.
34. *The Finnish Land Parcel Identification System (FLPIS) and Finnish Administration and Control System (IACS)*; Ministry of Agriculture and Forestry in Finland: Helsinki, Finland, 2009.
35. Russell, G.; Muetzelfeldta, R. I.; Taylor, K.; Terres, J.M. Development of a crop knowledge base for Europe. *Eur. J. Agron.* **1999**, *11*, 187-206.
36. Janssen, S.; Andersen, E.; Athanasiadis, I. N.; van Ittersum, M. K. A database for integrated assessment of European agricultural systems. *Environ. Sci. Policy* **2009**, *12*, 573-587.
37. Laurila, H.; Karjalainen, M.; Hyyppä, J.; Kleemola, J. Integrating vegetation indices models and phenological classification with composite sar and optical data for cereal yield estimation in Finland (Part I). *Remote Sens.* **2010**, *2*, 76-114.

38. Ritchey, R. Analysis and synthesis on scientific method—Based on a study by Bernhard Riemann. *Systems Res.* **1996**, *8*, 21-41.
39. IIASA. *The International Institute for Applied Systems Analysis (IIASA)*; Laxenburg, Austria, 2008. Available online: www.iiasa.ac.at (accessed on 9 September 2008).
40. Harrison, P.A.; Porter; J.R., Downing, T.E. Scaling-up the AFRCWHEAT2 model to assess phenological development for wheat in Europe. *Agric. Forest Meteorol.* **2000**, *101*, 167-186.
41. Laurila, H. Simulation of spring wheat responses to elevated CO_2 and temperature by using CERES-wheat crop model. *Agric. Food Sci. Fin.* **2001**, *10*, 175-196.
42. Lancashire, P.D.; H. Bleiholder, P.; Langeluddecke, R.; Stauss, T.; van den Boom, E.; Weber, A. Witzen-Berger. A uniform decimal code for growth stages of crops and weeds. *Ann. Appl. Biol.* **1991**, *119*, 561-601.
43. Witzenberger, A.; Hack, H.; van den Boom, T. Erläuterungen zum BBCH-Dezimal-Code für die Entwicklungsstadien des Getreides - mit Abbildungen. *Gesunde Pflanzen* **1989**, *41*, 384-388.
44. Zadoks, J.C.;Chang, T.T.; Konzak, C.F. A decimal code for the growth stages of cereals. *Weed Res.* **1974**, *14*, 415-421.
45. Yli-Halla, M.; Mokma, D.; Peltovuori, T.; Sippola, J. *Agricultural Soil Profiles in Finland and Their Classification*; Publications of Agricultural Research Centre of Finland Serie A 78.; Agricultural Research Centre of Finland: Jokioinen, Finland, 2000.
46. Åfors, M.; Ohlander, L.; Stendahl, F. *Stråsädens utveckling I. En litterastudie och beskrivning av en skala för bestämmning av stråsädens axrespektive vippanlag*; Inst. för Växodlinglära Sveriges Lantbruks-universitet: Uppsala, Sweden, 1988; (In Swedish).
47. Peltonen-Sainio, P.; Rajala, A.; Seppälä, T. *ABC of Cereal Development and Growth*; Elintarviketalous No. 67; MTT Agrifood Research Finland: Maaja, Jokioinen, Finland, 2005; (In Finnnish).
48. *Li-Cor LAI-2000 Plant Canopy Analyzer*; Li-Cor Biosciences: Lincoln , NE, USA, 2009. Available online: http://www.licor.com/env/Products/AreaMeters/lai2000/2000_intro.jsp (accessed on 11 October 2008).
49. Kontturi, M. the effects of weather on yield and development of spring wheat in Finland. *Ann. Agric. Fenniae* **1979**, *18*, 263-274.
50. Saarikko, R.A. Climate Change and Crop Potential in Finland: Regional Assessment of Spring Wheat. Ph.D. Thesis, Publication No. 55; Department of Plant Production, University of Helsinki: Helsinki, Finland, 1999.
51. SAS Publishing. *SAS/Stat User's Guide Version 6*, 3rd ed.; SAS Inst. Inc.: Cary, NC, USA, 1990. Available online: http://www.sas.com/ (accessed on 14 September 2009).
52. SAS Publishing. *SAS Procedures Guide, Version 6*. 3rd ed.; SAS Inst. Inc.: Cary, NC, USA, 1990. Available online: http://www.sas.com/ (accessed on 14 September 2009).
53. Price, J. Calibration of satellite radiometers and the comparison of vegetation indices. *Remote Sens. Environ.* **1987**, *21*, 15-27.
54. Jackson, P.L.; Gaston, G.G. Digital enhancement as an aid to detecting patterns of vegetation stress using medium-scale aerial photography. *Int. J. Remote Sens*. **1994**, *15*, 1009-1018.

55. Pinty, B.; Verstraete, M. GEMI. A non-linear index to monitor global vegetation from satellite. *J. Veg.* **1992**, *101*, 10-15.
56. Gobron, N.; Pinty, B.; Verstraete, M.; Govaerts, Y. The MERIS Global Vegetation Index (MGVI): Description and preliminary application. *Int. J. Remote Sens*. **1999**, *20*, 1917-1927.
57. Gobron, N.; Pinty B.; Mélin, F.; Taberner, M.; Verstraete, M.; Belward, A.; Lavergne, T.; Widlowski, J. The state of vegetation in Europe following the 2003 drought. *Int. J. Remote Sens*. **2005**, *26*, 2013-2020.
58. Gobron, N.; Pinty, B.; Taberner, M.; Mélin, F.; Verstraete, M.; Widlowski, J. Monitoring the photosynthetic activity of vegetation from remote sensing data. *Adv. Space Res*. **2006**, *38*, 2196-2202.
59. Gobron, N.; Pinty, B.; Mélin, F.; Taberner, M.; Verstraete, M.; Robustellia, M.; Widlowski, J. Evaluation of the MERIS/ENVISAT FAPAR product. *Adv. Space Res*. **2007**, *39*, 105-115.
60. Serrano, L.; Filella, I.; Peñuelas, J. Remote sensing of biomass and yield of winter wheat under different nitrogen supplies. *Crop Sci.* **2000**, *40*, 723-731.
61. Hyyppä, J.; Mäkynen, M.; Hallikainen, M.T. Calibration accuracy of the HUTSCAT airborne scatterometer. *IEEE Trans. Geosci. Remote Sens.* **1999**, *37*, 1450-1454.
62. MAFF/TIKE. *Report of the Agricultural Land Use in the Rural Development Centers in 2003*; The Information Centre of the Ministry of Agriculture and Forestry in Finland: Helsinki, Finland, 2003; In Finnish.
63. MAFF/TIKE. *The Finnish Land Parcel Identification System (FLPIS)*; Ministry of Agriculture and Forestry in Finland: Helsinki, Finland, 2009. Available online: www.mmmtike.fi/fi/index/tilastojatietopalvelut/tietopalvelu/rekistereiden_tietosisalto/peltolohkorekisteri.html (accessed on 17 January 2009).
64. Kangas, A.; Laine, A.; Niskanen, M.; Salo, Y.; Vuorinen, M.; Jauhiainen, L.; Nikander, H. *Results of Official Variety Trials 1998–2005*; No. 105; MTT Agrifood Research Finland: Jokioinen, Finland, 2006.
65. Kangas, A.; Laine, A.; Niskanen, M.; Salo, Y.; Vuorinen, M.; Jauhiainen, L.; Nikander, H. *Results of Official Variety Trials 2000–2007*; No. 150; MTT Agrifood Research Finland: Jokioinen, Finland, 2008.
66. Järvi, A.; Kangas, A.; Rahkonen, H. *Results of Official Variety Trials 1989–1996*; Serie A. No. 19; MTT Agrifood Research Finland: Jokioinen, Finland, 1997.
67. Hakala, K. Growth and yield potential of spring wheat in a simulated changed climate with increased CO_2 and higher temperature. *Eur. J. Agron.* **1998**, *9*, 41-52.
68. Verstraete, M.; Gobron, N.; Aussedat, O.; Robustelli, M.; Pinty, B.; Widlowski, J.; Taberner, M. An automatic procedure to identify key vegetation phenology events using the JRC-FAPAR products. *Adv. Space Res*. **2008**, *41*, 1773-1783.
69. Pinty B.; Lavergne T.; Widlowski J.-L.; Gobron N.; Verstraete M.M. On the need to observe vegetation canopies in the near-infrared to estimate visible light absorption. *Remote Sens. Environ.* **2008**, *113*, 10-23.
70. Kondratyev, K.; Kozoderov V.; Smokty, O. *Remote Sensing of the Earth from Space: Atmospheric Correction*; Springer-Verlag: Berlin, Germany, 1992.

71. Ulaby, F.T. SAR biophysical retrievals: Lessons learned and challenges to overcome. In *Proceedings of the 2nd International Workshop on Retrieval of Bio- and Geo-Physical Parameters from SAR Data for Land Applications*; Noordwijk, The Netherlands, 21–23 October 1998. Available online: http://conferences.esa.int/98c07/index.html (accessed on 05 November 2007).
72. Henderson, F.M.; Lewis, A.J. *Principles and Applications of Imaging Radar. Manual of Remote Sensing*, 3rd ed.; John Wiley & Sons, Inc.: New York, NY, USA, 1997.
73. Maas, S.J. Use of remotely sensed information in plant growth simulation models. *Adv. Agron.* **1991**, *1*, 17-26.
74. National Board of Agriculture in Finland. *Yearbook of Farm Statistics 1989–2006*; Ministry of Agric. & Forestry in Finland: Helsinki, Finland, 2007. Available online: http://www.matilda.fi/servlet/page?_pageid=501,193&_dad=portal30&_schema=PORTAL30 (accessed on 17 January 2009).
75. Ledenet, J.F. Relationships between grain yield and morphological characters in the winter wheat genotypes of the Belgian national list. *Biol. Plantarum* **1979**, *21*, 161-169.
76. Reynolds, M.; Calderini, D.; Condon, A.; Vargas, M. Association of source/sink traits with yield, biomass and radiation use efficiency among random sister lines from three wheat crosses in a high-yield environment. *J. Agr. Sci*. **2007**, *145*, 3-16.
77. Peltonen-Sainio, P.; Kangas, A.; Salo, Y.; Jauhiainen. L. Grain number dominates grain weight in temperate cereal yield determination: Evidence based on 30 years of multi-location trials. *Field Crops Res.* **2007**, *100*, 179-188.
78. Peltonen-Sainio, P.; Muurinen, S.; Rajala, A.; Jauhiainen, S. Variation in harvest index of modern spring barley, oat and wheat cultivars adapted to northern growing conditions. *J. Agr. Sci.* **2008**, *146*, 35-47.
79. Scurlock, J.; Prince, D. Remote sensing of biomass and productivity. In *Photosynthesis and Production in a Changing Environment. A Field and Laboratory Manual*, 2nd ed.; Hall, D., Scurlock, J., Bolhar-Nordenkampf, R., Leegood, R., Long, S., Eds.; Chapman and Hall: London, UK, 1993.
80. Flowers, M.; Randall-Weisz, R.; Heiniger, R. Remote sensing of winter wheat tiller density for early nitrogen application decisions. *Agron. J.* **2001**, *93*, 783-789.
81. Hadria, R.; Duchemin, B.; Baup, F.; Le Toan, T.; Bouvet, A.; Dedieu, G.; Le Page; M. Combined use of optical and radar satellite data for the detection of tillage and irrigation operations: Case study in Central Morocco. *Agr. Water Manag.* **2009**, *96*, 1120-1127.
82. *Pokko Malting Barley Cultivation in Finland*; Farmit.net: Helsinki, Finland, 2009; In Finnish.
83. Frantz, J.; Chun, C.; Joly, R.; Mitchell, C. Intracanopy lightning as a sole source of irradiation for planophile crop canopies in controlled environments. *Life Support Biosphere Sci*. **1998**, *5*, 183-189.
84. Kleemola, J. Modelling Nitrogen and Water Limited Crop Growth. PhD Thesis, Department of Plant Production, University of Helsinki: Helsinki, Finland, 1997.
85. Vossen, G.; Rijks, D. *Early Crop Yield Assessment of the EU Countries: The System Implements by the Joint Research Centre*; Office for the Official Publications of the EU (ISBN-92-827-5107-4); JRC: Roma, Italy, 1995.

Appendix 1. Electronic Supplementary Information (ESI) and Additional Figures and Tables

Appendix A–D, figures and tables can be downloaded from the link:
http://koti.armas.fi/~hlaurila/download/Pb4
Alternative mirror-site is http://cid-c669a6f402aa3b2b.skydrive.live.com/self.aspx/.Public

The SatPhenClass algorithm can be downloaded from the link:
http://koti.armas.fi/~hlaurila/download/Pb4
file: SatPhenClass-Appendix.pdf

Appendix A. Abbreviations, significance levels and tables, satellite systems and locations.

Table 7. Abbreviations used.

Definition, abbreviation	Unit, (range)	Description
X		Mean of sample
S_d		Standard deviation of sample (n)
C_v		Coefficient of variation (%) = S_d/X
S_x		Standard error of mean $\frac{Sd}{\sqrt{n}}$ =
MSE		Mean squared error $\mathrm{MSE}(\overline{X}) = \mathrm{E}((\overline{X} - \mu)^2) = (\frac{\sigma}{\sqrt{n}})^2$
RMSE		Root Mean Square Error , square root of MSE
R^2		Coefficient of determination
LSE		Least-Square Estimation-algorithm
VGI with submodels (I-III)		Vegetation Indices submodels (I-III: I—Infrared polynomial, II—NDVI, III—composite NDVI and backscattering model (Table 6)
a_p, b_p, c_p, d_p (SatPhenClass Phenology classes P_a, P_b, P_c, P_d)		DVS (Phenological Development stage, [37, 43]) four classification values in *SatphenlClass* algorithm. Used in VGI models: a_p—vegetation stage class from emergence until 2 leaf and *double ridge* stages, b_p—generative stage class until *heading*, c_p—grain filling stage in generative phase between anthesis and full maturity, d_p—senescence phase (Used only in microwave polynomial model III) *SatphenlClass* algorithm contains corresponding phonological classification classes (P_a, P_b, P_c, P_d)
SSP_{Ph}	Phenological Spectral Signature Profile	Phenologicallly classified NDVI values for a specific cereal crop in a phenlogical class P_a, P_b, P_c, P_d .Classfication with the SatPhenClass algorithm [37].
DY_{MTT}		Yield Difference (kg/ha) modeled (VGI)—observed MTT average (Table 11,14)
DRT_{MTT}		Yield Difference Ratio, Modeled (VGI)/MTT Observed; over/underestimation (%) from the reference (100%) (Table 11, 14)
DY_{MAFF}		Yield Difference (kg/ha) modeled (VGI)—obs. MAFF average (Table 10, 13).
DRT_{MAFF}		Yield Difference Ratio, modeled (VGI)/MAFF Observed; over/underestimation (%) from the reference (100%) (Table 10,13)

Table 7. *Cont.*

Oe / ue		Overestimated / Underestimated by the corresponding VGI model *vs.* observed (Tables 12–14).
spc., *Cv.*		species, cultivar
spc.		Spring sown cereal species (spring wheat, barley, oats)
Swh		Spring wheat (*Triticum aestivum* L.) including *cv.* Heta, Kadett, Manu, Reno, Ruso, Satu, Tjalve
Brl		Barley (*Hordeum vulgare L.*) including *cv.* Arra, Arttu, Artturi, Arve, Eero, Ida, Inari, Kustaa, Kymppi, Loviisa, Mette, Pohto, Pokko
Oats		Oats (*Avena Sativa* L.) including *cv.* Aarre, Salo
loc.		Loc—Location: J-Jokioinen, K—Kirkkonummi, M-Mellilä, P—Porvoo, L—Lapua
T_b	degree (℃)	Threshold temperature
DD	Degree Days	
ETS(T_b)	dd—degree days	Cumulative temperature sum over threshold temperature (T_b = 5 ℃)
PAR	MJ/d/m^2 (10–20)	Photosynthetically Active Radiation (λ = 400–700 nm)
IR NIR—Near IR Mid IR Thermal IR	MJ/d/m^2	infrared radiation (IR), λ = 630–690 nm near infra, λ = 760–900 nm mid infra, λ = 1.55–1.75 μm thermal IR, λ = 10.4–12.5 μm
Rf (Ch, a_p,b_p,c_p)	(0.0– 1.0) Optical (λ = 400–700 nm) and infrared sensors (λ = 630–12.5 μm).	Reflectance; reflected radiation from soil and vegetation canopies and measured by optical satellites [22-23,57-58,68-69]. Landsat or SPOT calibrated reflectance values with index denoting channel and phenlogical stage with correspondingaverage month for spring cereals (a_p–May, b_p–June, c_p–July); used in VGI Infrared model (I) as independent variables for crop*cultivar*soil covariance interaction and yield estimations (Table 3, Models. 1.1–7.3, Table 12 Appendix C), * - general notation for covariance effects
ρ_{RED} (a_p,b_p,c_p) ρ_{NIR} (a_p,b_p,c_p) ρ_{PAR} (a_p,b_p,c_p)		ρ_{RED} , $\rho_{NIR,}$ ρ_{PAR} specific Landsat or SPOT infrared, near infrared and PAR calibrated reflectance values with index denoting phenological stage for spring cereals (a_p–May, b_p–June, c_p–July), see also Rf-value.
σ^0 (sigma zero) σ^0_{HH} σ^0_{HV} σ^0_{VH} σ^0_{VV}	(–20–10 dB). Calibrated SAR (Synthetic Aperture radar) backscattering signal with microwave 5.4 GHz (C-band, λ = 5.7 cm) and 9.8 GHz (X-band) and polarization levels (HH, VV, VH, HV).	Backscatter coefficient (sigma zero) for microwave backscattering signal, which is a combined signal reflected from soil and vegetation canopies [60-63,26-28].
Potential, non-limited yield, yield potential	kg/ha	Modeled maximum yield capacity (kg/ha) for a specific cultivar without limiting environmental stress factors during growing season (vegetation water stress, nutrient deficiencies, pathogen epidemics etc.)
Non-potential, limited yield	kg/ha	VGI modeled yield level (kg/ha) for a specific cultivar with limiting environmental stress factors during growing season reducing maximum yield capacity, see potential yield.

Table 7. *Cont.*

$y_{b(spc, cv, soil type.)}$ spc=swh,brl,oats	kg/ha, 15% moisture content	*Baseline yield* for spring cereal species (swh, brl, oats).VGI (I-III) modeled cereal yield level (kg/ha) using time series for a specific cultivar under field conditions, see non-potential yield. Index denotes crop, cultivar and soil type; used as dependent variable in VGI models (Models. 1.1–7.3, Table 12, Appendix C).
NDVI	%	Normalized Difference Vegetation Index
SatphenlClass	BBCH and Zadok's scaling	Satellite data classification algorithm based on cereal phenology
Minimum dataset		Experimental dataset without ground truth or meteorological data, containing only optical or microwave satellite data
VGI with submodels (I-II)		Vegetation Indices submodels (I-IIII: I—Infrared polynomial, II—NDVI, III—composite NDVI and backscattering model.
MAFF		Ministry of Agriculture and Forestry in Finland
IIASA		The International Institute for Applied Systems Analysis [32]

Table 8. Statistical significance levels.

Significance levels (α = reference probability) [(1)]	
N.S.	Statistically non-significant
0	Moderately significant on 10% error level, α(0.10)
*	Significant on 5% error level, α(0.05)
**	Highly significant on 1% error level, α(0.01)
***	Highly significant on 0.1% error level, α (0.001)

[(1)] Used in testing the p-value (Pr) in F-test

Table 9. Satellite measurements in Finnish experimental locations [23,26,28,37] [6)].

Location	**Date (Satellite measurement)**	**Satellite type, sensor and Image no.**	**Incidence angle (φ)** [–1)]	**Major soil types**[4)]
Lapua, Seinäjoki , Ilmajoki 23 °10'E, 62 °50'N	1994:6.7 , 1995: 24.6 1996: 21.5., 3.7.	Optical: SPOT XS 65 220	–21.3, –4.3, 10, 0.2	Clay (Sandy clay 56%), coarse (Coarse sand 33.5%)
	1997: 17.5.,7.6.,1.7	Optical: SPOT XS 65 220–221	9.3,5.9,–23.8	
	1996: 17.6, 30.7, 25.8, 25.9	Microwave SAR: ERS1 SAR[5)], f = 5.3 GHz, C band, (λ = 5.7 cm), VV polarization		
	2001: 6.5,16.5, 30.5, 6.6, 16.6, 23.6.,10.7, 17.7, 24.7, 3.8, 17.8, 27.8, 10.9, 17.9, 20.9, 27.9, 28.10.	Microwave SAR: Radarsat1 SAR, f = 5.3 GHz, C band, HH polarization		
	2003–2004: 15.6,18.6,21.6,28.6,4.7,7.7,14.7,23.7,02.8,11.8,24.8,15.9 2005–2006: Only ground truth observations [5)]	Microwave ASAR: ENVISAT ASAR , f = 5.3 GHz, C-band), VV, HH, VV/HH, HV/HH, or VH/VV polarizations		

Table 9. *Cont.*

Kirkkonummi 24 °30' E, 60° 10' N	1994:25.7,1995:3.6 1994: 6.6., 7.7 1995:15.6.	LANDSAT TM 189 18 SPOT XS 73 227	23.0, - 24.5, –21.6	Clay [(2)] (gyttja clay 41.4%)
Jokioinen 23 °50' E, 60° 50' N	1994: 25.7 1994: 13.7 1995: 25.6, 15.7 1996: 25.7	LANDSAT TM 189 18 SPOT/HRV2/XS 69 225 SPOT/HRV2/XS 69 225 SPOT/HRV2/XS 69 225	– -2.2 +23.4, -1.6 -197.7	Clay (Sandy clay 56%), Kuuma exp. area (70–80% organic top layer, Table 3)
Mellilä 22 °20' E, 60°, 50' N	1989:24.5, 25.6, 27.7	LANDSAT 5/TM	48.28, 50.39, 46.05	Clay (Sandy clay 29%, gyttja clay 36%)[(2)]
Porvoo 25 °50 ' E, 60 °50' N	1990: 13.5, 21.6 1990: 13.5, 29.7 1994: 14.6 1995: 25.6, 15.7 1996:25.7	LANDSAT 5/TM SPOT/HRV2/XS SPOT XS 65 220 SPOT XS 69 225 SPOT XS 69 225	50.01 48.1 5.2 -1.6 -	Clay [(2)] (gyttja clay 38%, organic peat, 11%)
	1990: 25.7, 24.8	Microwave SAR: HUTSCAT Scatterometer (f = 5.4 GHz, C-band, 9.8 GHz, X-band), VV, HH, VH, HV [polarizations(3)]		

[1)] Used in Equation 2 (Appendix C) [2)] Gyttja clay contains peat and mud fractions) [3)] Helicopter mounted [61-63] [4)] Main soil type classification with soil sub fractions [5)] No Envisat data obtained in 2005–2006 because of re-programming of ASAR sensors and technical problems in ESA. Only ground truth phenological and LAI measurements measured in experimental areas. [6)] SAR/ASAR sensory data applied only in the [37].

Table 10. SAR and optical satellite systems used in remote sensing campaigns [29,37][7)].

Satellite type	**Name**	**Sensor**	**Experimental locations and years**	**Reference**
Microwave ASAR	ENVISAT [(3)]	ASAR[(6)], f = 5.3 GHz, C-band), VV, HH, VV/HH, HV/HH, or VH/VV polarizations	Seinäjoki, Lapua (2002–2004, Table 11).	http://earth.esa.int, http://envisat.esa.int/object/index.cfm?fobjectid=3772, [27,28]
Microwave Scatterometer	HUTSCAT [(1),(6)]	Scatterometer (f = 5.4 GHz, C-band, 9.8 GHz, X-band), VV, HH, VH, HV polarizations	Porvoo, calibration data (1990, Table 11).	www.space.hut.fi/research/equipment/ hutscat.html. [61-63]
Microwave SAR	ERS1[2)]	SAR [(5)], f = 5.3 GHz, C band, (λ = 5.7 cm), VV polarization	Seinäjoki, Lapua (1995–1996, Table 11).	http://earth.esa.int/ers, earth.esa.int/ers/sar, [26,62]
Microwave SAR	Radarsat1	SAR[(5)], f = 5.3 GHz, C band, HH polarization	Seinäjoki, Lapua (2001, Table 11).	Reference [27], Canadian Space Agency (CSA). ccrs.nrcan.gc.ca/, radar/spaceborne/radarsat1/index_e.php
Optical	Landsat 5	Thematic Mapper (TM) (λ = 450 nm–2.35 μm)	Porvoo, Mellilä, Kirkkonummi, Jokioinen, Lapua (1989–1997, Table 11).	www.landsat.org, [76,22-23]

Table 10. *Cont.*

Optical	SPOT 2	HRV2/XS (λ = 450 nm–890 nm)	Porvoo, Mellilä, Kirkkonummi, Jokioinen, Lapua (1989–1997, Table 11).	www.spot.com, www.spotimage.fr, [77,22,23]
Multi-sensor	ADEOS1 Advanced Earth Observing Satellite[4)]	AVNIR, ILAS, RIS, IMG,TOMS: atmospheric greenhouse gas (CO_2, O_3, CH_4) columns [(4)]	(1996-1997, non-operational) Collaboration with Prof. Hiroshi Koizumi, NIAES/ Tsukuba, Japan	NASDA/ JAXA, http//home.gna.org/adeos/ http://kuroshio.eorc.jaxa.jp/ADEOS,http://msl.jpl.nasa.gov/QuickLooks/ adeosQL.html

[1)] HUTSCAT is helicopter mounted, see space.hut.fi/research/equipment/hutscat.html [63]

[2)] European Remote Sensing satellite (ESA, European Space Agency)

[3)] ENVISAT (Environmental satellite, ESA) AOS (Announce of Opportunity) contract: AOE-488 for ENVISAT

[4)] ADEOS1 AOS contract: NASDA Contract 1062/Vegetation and Biology, MAFF, 5118/416/94

[5)] SAR, Synthetic Aperture Radar [(6)] Advanced Synthetic Aperture Radar

[6)] HUTSCAT used for calibration verification purposes only (helicopter mounted)

[7)] SAR/ASAR sensory data applied only in the [37].

Table 11. Optical calibration parameters of Landsat and SPOT satellites [53].

Satellite/ sensor [(1),(2)]	**Sensor channel/λ (wave length)/type**	**Date**	**Sun elevation Angle (deg.)**	**S[(6)]**	**α[(7)]**	**β[(8)]**
TM_1[(1)]	450–520 nm/PAR[(3)]	24.5.1989	48.28	620	0.602	–1.5
TM_2[(1)]	520–600 nm/PAR[(3)]	25.6.1989	50.39	577	1.17	–2.8
TM_3[(1)]	630-690 nm/infrared[(3)]	27.7.1989	46.05	493	0.806	–1.2
TM_4[(1)]	760–900 nm/ near infra	21.6.1990	50.01	332	0.815	–1.5
TM_5[(1)]	1.55–1.75 μm / mid infra			67.1	0.108	–0.37
TM_6[(1)]	10.4–12.5 μm/ thermal IR[(4)]			n.a.[(3)]	-	-
TM_7[(1)]	2.08–2.35 μm / mid infra			24.5	0.057	–0.15
HRV_2/S_1[(2)]	500–590 nm / PAR[(3)]	13.5.1990	n.a.[(5)]	587.0	1.22181	0
HRV_2/S_2[(2)]	610–680 nm / infrared[(3)]	29.7.1990	48.1	502.0	1.22545	0
HRV_2/S_3[(2)]	790–890 nm/near infrared			331.0	1.29753	0

[(1)] Landsat5 / TM: Landsat (1987). Sensor: Thematic Mapper (λ = 450 nm–2.35 μm, resolution 30 × 30 m^2 [(2)] SPOT / HRV2/XS: SPOT (1986). High Resolution Visible 2 (λ=500 nm–890 nm, resolution 20 × 20 m^2). [(3)] PAR – Photosynthetically Active Radiation (λ = 400–700 nm) [(4)] Thermal infrared channel with ground resolution of 120 m. [(5)] n.a.—parameter not available

[(6)] S—Equivalent solar radiance [(7)] α—Calibration gain coefficient [(8)] β—Calibration offset coefficient.

Appendix B. Equations

Statistical Analysis Equations

Equation (1) $y_{(i)} = \beta_0+\beta_i*x_{(i)}+...\beta_{(i+1)}*x_{(i+1)}+\varepsilon$ (linear REG/Stepwise [51])

Equation (2) $y_{(i)} = \beta_0+\beta_1*x_{(1)}+ \beta_2*x_{(2)+} \beta_3*x_{(1)}^2+\beta_4*x_{(2)}^2+\beta_5* x_{(1)*}x_{(2)} +\varepsilon$ (non-linear RSREG [52])

$y_{(i)}$ = dependent grain yield for spring cereals (wheat, barley, oats, kg/ha, 15% moisture content)

x(i)= independent ground truth and satellite variables in Vegetation Indices regression models

β_0= model intercept, β_i= coefficient for independent variable $x_{(i),}$

ε = error residual variation,

$\beta_1*x_{(1)}+ \beta_2*x_{(2)}$ - the linear term,

$\beta_3*x_{(1)}^2+\beta_4*x_{(2)}^2$ - the squared effect term,

$\beta_5* x_{(1)*}x_{(2)}$ - the cross product effect.

Optical Satellite Data Calibration Equations

Equation (3) $R = \alpha * dc + \beta$ [57]

R = Spectral radiance ($W*m^{-2}*sr^{-1}*\mu m^{-1}$)

dc = digital count value from the satellite sensor (0-255)

α = calibration gain coefficient ($W*m^{-2}*sr^{-1}*\mu m^{-1}*count^{-1}$)

β = calibration offset coefficient ($W*m^{-2}*sr^{-1}*\mu m^{-1}$), sr = angle expressed as steradians

Equation (4) $rf = R/(S*\cos(\varphi)$

rf = surface reflectance value (%-ratio between the radiation reflected from the soil cover and the incoming solar radiation)

R = spectral radiance ($W^*m^{-2}*sr^{-1}*\mu m^{-1}$)

S = equivalent solar radiance ($W*m^{-2}*sr^{-1}*\mu m^{-1}$)

cos (φ) = Solar zenith-angle correction, calculated from the measuring time and the corresponding elevation or incidence angle (el) : φ =(90-el), φ expressed in radians,

sr = angle expressed as steradians

Equation (5) $S = [1/w]*\int d\{\Omega*(eqv.solarradiance)*[\Omega]*\Phi[\Omega]\}$

Ω = satellite channel wavelength (μm)

w = satellite channel spectral bandwidth (μm)

$\Phi(\Omega)$ = normalized wavelength response function of specific satellite channel

Cereal LAI estimation using LAI-bridge [29,31], GEMI-index [55] and Kalman Filter [21]

Equation (6) $LAI(Satellite,Cereal) = \alpha_c + \beta_c * GEMI_n$

LAI(Satellite,Cereal) = Leaf area index for specific cereal estimated from satellite data on pixel level

GEMI(Cereal) = Global Environment Monitoring Index (GEMI) [55].

α_c, β_c= crop specific linear regression coefficients (Table 12)

Equation (7) $LAI_{Optimal} = (\sigma_{CropModel}*LAI_{Satellite,Cereal} + \sigma_{Satellite,Cereal}*LAI_{CropModel})/((\sigma_{Satellite,Cereal})^2 + (\sigma_{CropModel})^2)$ [21,29,84]

LAI(Optimal) = Optimal, corrected Leaf Area Index estimated by the Kalman filter for cereals

LAI(Satellite,Cereal) = Leaf Area Index estimated by the GEMI VGI model (Equation 6)

LAI(CropModel) = Initial Leaf Area Index estimated by the CropWatN dynamic crop model

$\sigma_{Satellite,Cereal}$ = Standard deviation of Leaf Area Index estimated by the GEMI VGI model

$\sigma_{CropModel}$ = Standard deviation of Leaf Area Index estimated by the CropWatN model

Equation (8) $1/(\sigma_{Optimal})^2 = 1/(\sigma\ Satellite,Cereal)^2 + 1/(\sigma_{CropModel})^2$ [21]

$\sigma_{Optimal}$ = Standard deviation of Corrected Leaf Area Index estimated by the Kalman Filter

Baseline VGI (I-IV) linear (REG/Stepwise) and non-linear (RSREG) yield models for spring crops

Table 12. Optical VGI (I-IV) linear (REG/Stepwise) and non-linear (RSREG) yield models for spring cereals. Composite model VI (SAR/ASAR) used only in validation [37][(1),(2)].

Model Category	**Factor : Crop /Species [1)]**	**Model Equation (I-V)**	**R^2**	**RMSE kg/ha**	**Model equation**
I Optical [2)]	Swh	1.1 (I)	0.764	282.3	$y_b(swh)=4941.9-5455.9*\rho_{RED(ap)}-1351.4*\rho_{NIR(ap)}+957.1*\rho_{RED(bp)}+656.2*\rho_{NIR(bp)}+4742.1*\rho_{RED(cp)}-4983.5*\rho_{NIR(cp)}$
	Swh	1.2 (I)	0.794	242.5	$y_b(swh)=985.93+13337.46*\rho_{RED(ap)}+8355.88*\rho_{NIR(ap)}-387.19*\rho_{NIR(bp)}+255.58*\rho_{RED(cp)}$
	Swh	1.3 (II, NDVI)	0.737	297.6	$y_b(swh,NDVI)=4659.2+175.4*n_{ap}-25.6*n_{bp}-3215.5*n_{cp}+93.7*n_{ap}^2-19.1*n_{bp}*n_{ap}-178.5*n_{bp}^2-560.4*n_{cp}*n_{ap}+3250.4*n_{cp}*n_{bp}-864.7*ncp^2$
	Swh	1.4 (II, NDVI)	0.732	300.1	$y_b(swh,NDVI)=4692.90+109.84*n_{ap}-210.38*n_{bp}-969.22*n_{cp}$
	Swh	1.5 [5)] (III,GEMI)	0.704	316.1	$y(swh,GEMI)=5074.1-766.2*g_{ap}-143.1*g_{bp}-3378.2*g_{cp}+4254.1*g_{ap}^2+1079.8*g_{bp}*g_{ap}-1326.2*g_{bp}^2-7264.8*g_{cp}*g_{ap}+7717.2*g_{cp}*g_{bp}-2622.1*g_{cp}^2$
	Swh	1.6 [5)] (III,GEMI)	0.570	536.8	$y_b(swh,GEMI)=5506.31+7780.47*g_{ap}-12478.3*g_{bp}+761.96*g_{cp}$
	Swh	1.7 [5)] (IV,PARND)	0.712	311.6	$y_b(swh,PAR_{ND})=4397.9+2736.9*p_{ap}-379.4*p_{bp}-493.8*p_{cp}-4235.1*p_{ap}^2+2701.1*p_{bp}*p_{ap}+605.8*p_{bp}^2-2161.6*p_{cp}*p_{ap}+883.1*p_{cp}*p_{bp}+493.9p_{cp}^2$
	Swh	1.8 [5)] (IV,PARND)	0.509	406.3	$y_b(swh,PAR_{ND})=4502.31+529.36*p_{ap}+2377.05*p_{bp}-779.31*p_{cp}$
	Brl	2.1 (I)	0.615	449.3	$y_b(brl)=5348.8-600.8*\rho_{RED(ap)}-184.5*\rho_{NIR(ap)}-8562.4*\rho_{RED(bp)}-2105.6*\rho_{NIR(bp)}-2766.9*\rho_{RED(cp)}-1556.2*\rho_{NIR(cp)}$
	Brl	2.2 (II, NDVI)	0.611	449.6	$y_b(brl,NDVI)=3481.5-205.5*n_{ap}-312.1*n_{bp}+396.5*n_{cp}-60.5*n_{ap}^2-584.5*n_{bp}*n_{ap}+864.6*n_{bp}^2+1081.4*n_{cp}*n_{ap}-710.5*n_{cp}*n_{bp}-232.4*n_{cp}^2$
	Brl	2.3 [5)] (III, GEMI)	0.614	448.6	$y_b(brl,GEMI)=5184.0-2802.9*g_{ap}-187.4*g_{bp}-3457.9*g_{cp}-374.8*g_{ap}^2+91.5*g_{bp}*g_{ap}+1161.4*g_{bp}^2+4817.1*g_{cp}*g_{ap}-1932.1*g_{cp}*g_{bp}+2255.6*g_{cp}^2$
	Brl	2.4 [5)] (IV,PARND)	0.587	463.7	$y_b(brl,PAR_{ND})=4621.7+1852.8*p_{ap}-6418.5*p_{bp}-5850.4*p_{cp}+48.9*p_{ap}^2-5952.3*p_{bp}*p_{ap}+10853.0*p_{bp}^2-2040.4*p_{cp}*p_{ap}+12879.0*p_{cp}*p_{bp}+6002.9*p_{cp}^2$
	Oats	2.5 (I)	0.760	258.0	$y_b(oats)=3457.4-3762.5*\rho_{RED(ap)}-2135.8*\rho_{NIR(ap)}+6643.1*\rho_{RED(bp)}+1566.5*\rho_{NIR(bp)}+571.4*\rho_{RED(cp)}-179.1*\rho_{NIR(cp)}$
	Crop /Species [1)]	Model	R^2	RMSE	Model equation
II Optical Species*soil Covariance [2)]	Swh * sandy clay	2.6 (I)	0.764	282.3	$y_{b(swheat,clay)}=6765.5-38407.0*\rho_{RED(ap)}-14979.0*\rho_{NIR(ap}-23698.0*\rho_{RED(bp)}+9552.7*\rho_{NIR(bp)}+7261.4*\rho_{RED(cp)}-22022.0*\rho_{NIR(cp)}$
	Brl * sandy clay	2.7 (I)	0.166	1382	$y_{b(barley,clay)}=7141.4-3842.1*\rho_{RED(ap)}-2612.4*\rho_{NIR(ap)}-3032.1*\rho_{RED(bp)}-11708.0*\rho_{NIR(bp)}-28637.0*\rho_{RED(cp)}-1636.2*\rho_{NIR(cp)}$
III Optical Species* Cultivar Cov. [2)]	Swh* cv. Manu	3.1 (I)	0.089	1292	$y_{b\ (cv.\ Manu*clay)} = 5696.5+2293.8*\rho_{RED(bp)}+5387.9*\rho_{RED(cp)}-736396.0*(\rho_{RED(bp)})^2$
	Swh * cv. Satu	3.2 (I)	0.046	1031	$y_{b\ (cv.\ Satu*clay)} = -9798.2+736440.0*\rho_{RED(bp)}-9925014.0*(\rho_{RED(bp)})^2$
	Brl * cv. Inari	3.3 (I)	0.144	1220	$y_{b\ (cv.\ Inari*clay)} = 8336.8-71506.0*\rho_{RED(bp)}-45627.0*(\rho_{RED(bp)})^2$

Table 12. *Cont.*

	Sensor	Cereal specie	Model	R^2	RMSE	Model equation
IV Microwave SAR/ASAR [2,3]	ERS SAR	Brl	4.1(VI)	0.448	482.7	$y_{b\ (brl,\ ERS2)}$ =4345.7+109.4*$NDVI_{ap}$ -211.6*$NDVI_{bp}$ -983.3*$NDVI_{cp}$ -0.57*$VV_{(5GHz,cp)}$+5.61*$VV_{(5GHz,dp)}$
		Oats	4.2(VI)	0.417	584.2	$y_{b\ (oats,\ ERS2)}$ =3739.5+108.9*$NDVI_{ap}$-212.1*$NDVI_{bp}$-938.8*$NDVI_{cp}$ -0.47*$VV_{(5GHz,cp)}$+4.28*$VV_{(5GHz,dp)}$
	Radarsat SAR	Swh	5.1(VI)	0.731	300.8	$y_{b\ (swh,\ Radarsat)}$=4690.7+111.8*$NDVI_{ap}$- 213.4*$NDVI_{bp}$ -982.6*$NDVI_{cp}$- 2.69*$HH_{(5GHz,cp)}$ + 3.9*$HH_{(5GHz,dp)}$
		Brl	5.2(VI)	0.702	322.8	$y_{b(brl,Radarsat)}$=4430.1+109.4*$NDVI_{ap}$-211.6*$NDVI_{bp}$-983.3*$NDVI_{cp}$ - 0.52*$HH_{(5GHz,cp)}$ +5.07*$HH_{(5GHz,dp)}$
		Oats	5.3(VI)	0.624	483.6	$y_{b\ (oats,\ Radarsat)}$=3843.3+108.9*$NDVI_{ap}$- 212.1*$NDVI_{bp}$-983.8*$NDVI_{cp}$ -0.47*$HH_{(5GHz,cp)}$ +4.03*$HH_{(5GHz,dp)}$
	Envisat ASAR	Swh	6.1(VI)	0.723	302.1	$y_{b(swh,Envisat)}$=4701.1+108.2*$NDVI_{ap}$-208.8*$NDVI_{bp}$-983.1*$NDVI_{cp}$ - 3.9*$VH_{(5GHz,cp)}$+17.4*$VV_{(5GHz,cp)}$ -3.1*$VH_{(5GHz,dp)}$+5.2*$VV_{(5GHz,dp)}$
		Brl	6.2(VI)	0.694	349.8	$y_{b\ (brl,\ Envisat)}$ =4261.4+109.4*$NDVI_{ap}$-211.6*$NDVI_{bp}$-983.3*$NDVI_{cp}$ -4.59*$VH_{(5GHz,cp)}$+18.24*$VV_{(5GHz,cp)}$ -4.04*$VH_{(5GHz,dp)}$+6.15*$VV_{(5GHz,dp)}$
		Oats	6.3(VI)	0.617	389.7	$y_{b\ (oats,\ Envisat)}$ =3635.7+108.9*$NDVI_{ap}$-212.8*$NDVI_{bp}$-983.8*$NDVI_{cp}$ -2.59*$VH_{(5GHz,cp)}$+16.46*$VV_{(5GHz,cp)}$-2.03*$VH_{(5GHz,dp)}$+4.05*$VV_{(5GHz,dp)}$

[1)] For abbreviations refer to Table 9 [2)] Independent variables classified with SatPhenClass-algorithm [3)] SAR/ASAR used only in validation of the optical VGI models [37].

Table 13. Calibrated α_c, β_c crop specific regression coefficients for cereal LAI estimation using GEMI-index in Equation 6 [29].

Crop	**α_c**	**β_c**	**R^2**	**RMSE**
Spring wheat	−2.878	6.241	0.962	0.21
Barley	−3.201	6.750	0.847	0.42
Oats	−3.578	7.189	0.841	0.44
All crops mean	−2.573	5.732	0.749	0.51

Appendix C. SatPhenClass Classification Algorithm for Satellite Data

Appendix figures and tables can be downloaded from the link:
http://koti.armas.fi/~hlaurila/download/Pb4.
The SatPhenClass classification algorithm can be downloaded from the link:
http://koti.armas.fi/~hlaurila/download/Pb4 file: SatPhenClass-Appendix.pdf
Alternative mirror-site is http://cid-c669a6f402aa3b2b.skydrive.live.com/self.aspx/.Public.